ADVANCED TORQUE MEASUREMENT SYSTEMS TECHNIQUE FOR AIRCRAFT TURBOSHAFT ENGINES

Frank E. Scoppe

Avco Lycoming Division

Prepared for:

Army Air Mobility Research and Development Laboratory

June 1973

AD

USAAMRDL TECHNICAL REPORT 73-37

ADVANCED TORQUE MEASUREMENT SYSTEMS TECHNIQUE FOR AIRCRAFT TURBOSHAFT ENGINES

By

Frank E. Scoppe

June 1973

EUSTIS DIRECTORATE
U. S. ARMY AIR MOBILITY RESEARCH AND DEVELOPMENT LABORATORY
FORT EUSTIS, VIRGINIA

CONTRACT DAAJ02-72-C-0045
AVCO LYCOMING DIVISION
STRATFORD, CONNECTICUT

DISCLAIMERS

The findings in this report are not to be construed as an official Department of the Army position unless so designated by other authorized documents.

When Government drawings, specifications, or other data are used for any purpose other than in connection with a definitely related Government procurement operation, the United States Government thereby incurs no responsibility nor any obligation whatsoever; and the fact that the Government may have formulated, furnished, or in any way supplied the said drawings, specifications, or other data is not to be regarded by implication or otherwise as in any manner licensing the holder or any other person or corporation, or conveying any rights or permission, to manufacture, use, or sell any patented invention that may in any way be related thereto.

Trade names cited in this report do not constitute an official endorsement or approval of the use of such commercial hardware or software.

DISPOSITION INSTRUCTIONS

Destroy this report when no longer needed. Do not return it to the originator.

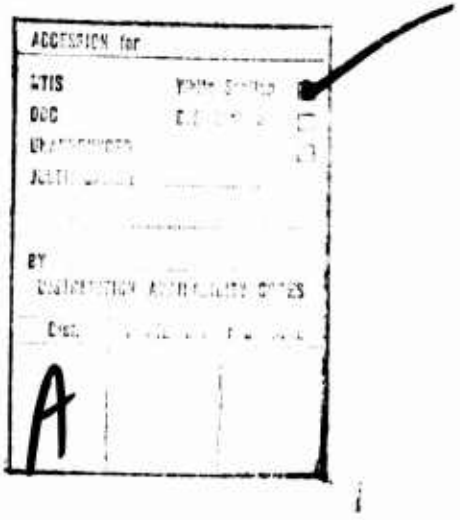

Unclassified

Security Classification

DOCUMENT CONTROL DATA - R & D

(Security classification of title, body of abstract and indexing annotation must be entered when the overall report is classified)

1. ORIGINATING ACTIVITY (Corporate author)	2a. REPORT SECURITY CLASSIFICATION
Avco Lycoming Division 550 South Main Street Stratford, Conn. 06497	Unclassified 2b. GROUP N/A

3. REPORT TITLE

ADVANCED TORQUE MEASUREMENT SYSTEMS TECHNIQUE FOR AIRCRAFT TURBOSHAFT ENGINES

4. DESCRIPTIVE NOTES (Type of report and inclusive dates)

Final Report 7 March 1972 through 7 February 1973

5. AUTHOR(S) (First name, middle initial, last name)

Frank E. Scoppe

6. REPORT DATE	7a. TOTAL NO. OF PAGES	7b. NO. OF REFS
June 1973	~~108~~ 11	7

8a. CONTRACT OR GRANT NO.	9a. ORIGINATOR'S REPORT NUMBER(S)
DAAJ02-72-C-0045	USAAMRDL Technical Report 73-37
8b. PROJECT NO. Task 1F162203A43405	
c.	9b. OTHER REPORT NO(S) (Any other numbers that may be assigned this report) LYC 73-4
d.	

10. DISTRIBUTION STATEMENT

Approved for public release; distribution unlimited.

11. SUPPLEMENTARY NOTES	12. SPONSORING MILITARY ACTIVITY
	Eustis Directorate U. S. Army Air Mobility R&D Laboratory Fort Eustis, Virginia

13. ABSTRACT

A torque measuring system based upon a transducer using the magnetostrictive effect of a ferromagnetic material has been evaluated. Required accuracy of the measurement system was ±1% of reading for a range from 30 to 100% of shaft torque. This accuracy was to be obtained on shafts with metal temperature to 500°F and with a system environmental temperature from -35° to +165°F. The evaluation was performed in three phases: analysis, design and fabrication, and test.

The evaluation showed that an SAE 9310 steel properly heat treated is required for generation of the torque transducer transfer curve. Optimum values for input parameters, i.e., excitation current frequency and an air gap, have been selected to provide minimal sensitivity variances. Metal temperature to 500°F is not a suitable environment for the transducer. Accuracy of ±1% can be obtained by the system in a 180°F temperature range. The system design is adaptable in minimal engine space allowances; therefore, it is felt that this limited temperature range is possible. Hardware for testing was fabricated to support the test phase and to demonstrate design concepts of adaptability.

DD FORM 1 NOV 68 1473 REPLACES DD FORM 1473, 1 JAN 64, WHICH IS OBSOLETE FOR ARMY USE.

Unclassified

Security Classification

14. KEY WORDS	LINK A		LINK B		LINK C	
	ROLE	WT	ROLE	WT	ROLE	WT
Magnetostrictive						
Torque Sensor						
Design and Fabrication						
Test of System to Performance Requirements						
Analysis						
Test of System to Establish Input						
Parameters						
Lamination Assembly						
Detector						

DEPARTMENT OF THE ARMY
U. S. ARMY AIR MOBILITY RESEARCH & DEVELOPMENT LABORATORY
EUSTIS DIRECTORATE
FORT EUSTIS, VIRGINIA 23604

This report was prepared by Avco Lycoming Division under the terms of Contract DAAJ02-72-C-0045. It presents the findings of a 12-month study that was undertaken to evaluate an aircraft turboshaft engine torque-measuring system using the magnetostrictive effect of a ferromagnetic material for the measurement transducer. The unique feature of this system is an increase in accuracy over existing systems. The increased accuracy is a requirement for engine diagnostic efforts.

The objective of this contractual effort was to design, fabricate and test an advanced concept torque measurement system to measure actual torque on Army aircraft gas turbine engines. The program resulted in an increase in accuracy to 1% of point or better, over a power range of 30% to maximum. The torque sensing technique investigated should also be capable of satisfactory operation on shafts having metal temperatures of up to 500^{o}F, and should be adaptable to a wide range of rotational speeds and torques.

The conclusions and recommendations contained herein are generally concurred in by this Directorate. The study is considered to have adequately fulfilled the major objectives.

Technical direction for this contractual effort was provided by Mr. Roger J. Hunthausen, Military Operations Technology Division.

Task 1F162203A43405
Contract DAAJ02-72-C-0045
USAAMRDL Technical Report 73-37
June 1973

ADVANCED TORQUE MEASUREMENT SYSTEMS TECHNIQUE FOR AIRCRAFT TURBOSHAFT ENGINES

Final Report

Avco Lycoming Report LYC 73-4

By

Frank E. Scoppe

Prepared by

Avco Lycoming Division
Stratford, Connecticut

for
EUSTIS DIRECTORATE
U.S. ARMY AIR MOBILITY RESEARCH
AND DEVELOPMENT LABORATORY
FORT EUSTIS, VIRGINIA

SUMMARY

The need for accurate and reliable measurement of shaft torque in Army gas turbine helicopters has been dictated by the requirements for engine diagnostic and control functions.

An accuracy of measurement within $\pm .5$ of reading throughout a torque range from 30 to 100 percent of engine power is considered as a design goal to satisfy this need.

This desired accuracy goal is to be obtained by the measurement system with no lessening of the severe environmental conditions imposed in the gas turbine environment. A study was undertaken to evaluate a torque measuring system using the magnetostrictive effect of a ferromagnetic material for the measurement transducer.

For evaluation of the system, two laminations assemblies were designed and fabricated predicated on an optimum shaft outside diameter of 2 inches. This shaft diameter was selected as nominal with the torque and speed ranges in the design specification. One specimen shaft was fabricated of the SAE 9310 material, and one shaft was sleeved of SAE 9310 material. The purpose of two shafts was to demonstrate the adaptability of the measurement system to shafts that could not be fabricated of the SAE 9310 steel.

A breadboard model of the detector circuit was fabricated and tested with the torque sensor.

Testing on the system was performed to determine nominal operating parameters; i.e., excitation current, frequency, and a maximum allowed clearance between the shaft and lamination assembly. After selection of the input parameters, the system was tested for conformance to the design specifications.

Evaluation of the test data showed that the temperature environment significantly restricted accuracy of the measurement. The tested system did not meet the design goal of $\pm .5$ percent of accuracy; however, the required goal of ± 1.0 percent could be obtained in a limited temperature range.

FOREWORD

The work was performed by Avco Lycoming for the Eustis Directorate, U.S. Army Air Mobility Research and Development Laboratory, under Contract DAAJ02-72-C-0045. The program was conducted to develop a new generation of torque measuring systems using the proven method of magnetostriction. The program monitor was Mr. Roger Hunthausen of the Eustis Directorate.

The report covers the performance of work during the period 7 March 1972 through 7 February 1973.

TABLE OF CONTENTS

LIST OF ILLUSTRATIONS

LIST OF TABLES

LIST OF SYMBOLS

LP	low pressure
HP	high pressure
V_T	voltage of secondary coils to sense tension stress
V_C	voltage of secondary coils to sense compression stress
R_c	Rockwell hardness
D. A.	double amplitude
K	constant of proportionality derived from test data
P. E.	percentage error
I_P	primary coil current
σ_T	tension stress, lb/in.^{2}
σ_C	compression stress, lb/in.^{2}
M	bending moment
I	area moment of inertia, in.^{4}
r_o	outside radius of shaft, in.
r_i	inside radius of shaft, in.
θ	angle between shaft radius in line with lamination pole and bending force, deg
τ	shear stress, lb/in.^{2}
T	torque, in.-lb
J	polar moment of inertia, in.^{4}

INTRODUCTION

Future U. S. Army aircraft will require gas turbine engine torque measuring systems that must provide considerably improved accuracies over presently available systems. This immediate need for a more precise shaft torque signal is an outgrowth from the rapid development of engine diagnostic and control instrumentation, which utilizes the torque signal.

Avco Lycoming has been involved in gas turbine diagnostic development programs, both hardware and software concepts, for several years and fully appreciates the need for a more accurate shaft torque signal. The following partial list of diagnostics systems and concepts, either introduced or developed by Avco Lycoming, further substantiates the requirement for gas turbine output shaft torque accuracy:

1. Engine performance is evaluated by determining engine torque, engine fuel flow, and low-pressure (LP) compressor inlet temperature at a fixed speed. The sensed engine torque value is compared with a referenced value. When the sensed value exceeds the referenced value, engine fuel flow and LP compressor inlet temperature are sensed to allow for computation of referred fuel flow. Should the referred fuel flow exceed a preset value, an output signal is generated.

2. Gas generator performance is evaluated by sensing four engine parameters. These are LP compressor inlet temperature, inlet pressure, inlet speed, and engine torque. A referred speed is computed from the sensed LP compressor inlet temperature and speed and compared with a preset value. When the computed value equals the preset value for a prescribed length of time, engine torque and LP compressor inlet pressure are sensed to allow for computation of referred torque. The computed value of referred torque is compared with a referenced value. When the referred value of torque is equal to or less than the referenced value, an output signal is generated.

3. A "power remaining" accessory provides an automatic computation of the percentage of engine horsepower remaining

compared with the maximum horsepower available from the engine at any instant. The "power remaining" accessory uses three engine parameters to generate a signal. These are LP compressor inlet temperature, high-pressure (HP) compressor speed, and engine torque.

Accuracies of the transducers available to sense the necessary parameters required to evaluate engine performance, gas producer performance, and power remaining are given in Table I.

TABLE I. PRESENT TRANSDUCER ACCURACIES

Parameter	Range	Transducer Accuracy
LP Compressor Inlet Temperature	-54° to 85°C	$\pm 1^{\circ}$C
Engine Torque	0-394 ft-lb	$\pm 2\%$
Fuel Flow	0-1000 lb/hr	
LP Compressor Inlet Pressure	10-17 psia	$\pm 0.1\%$
LP Compressor Speed	0-110%	Exact
HP Compressor Speed	50-100%	Exact

In all cases it can be seen that a limiting factor to providing improved diagnostic measurements is the limitation in accuracy of available torque measuring systems. Avco Lycoming has pursued a vigorous research effort to provide a satisfactory torque system. As a consequence of this effort, the magnetostrictive effect of a ferromagnetic material has been determined as the principle of measurement that can most satisfactorily meet the requirements for torque measurement in a gas turbine engine.

Accordingly, a program was conducted to investigate the problem areas and to develop a new generation of the proven magnetostrictive torque measuring system. The objective of this program was to develop a complete torque system that would make a significant advancement over present technology. This report presents the results of this program.

EVOLUTION OF THE MAGNETOSTRICTIVE METHOD FOR TORQUE MEASUREMENT

Essential to any measurement system principle is the ability of the sensing transducer to differentiate between torsional forces and those forces which provide a false information signal. Included as false information signals would be transducer sensitivity to bending or thrust loads on the shaft and the effects of temperature on transducer sensitivity.

Differentiation of the true torsional force from biasing forces may be an inherent trait of the measurement principle or can be provided through compensation techniques employed in the application of the measuring system. Additionally, the gas turbine and its environment impose design constraints of: available space allowances; measurements from high-speed rotating parts; lack of accessibility to the shaft of measure, making replacements and/or required installation adjustments of the transducer difficult. The gas turbine engine application demands long-term reliability and stability of calibration of the torque measurement. High rotational speeds and limited space allowances restrict the selection of a measurement principle to one that can readily be adapted to transmission methods from high-speed shafts and that is not dependent on engine available space for system gain and/or resolution.

Requirement for accurately measuring the output shaft torque in gas turbine engines was realized by Avco Lycoming in the early 1960's. In the mid-1960's, a development program was initiated to demonstrate the practicality of a transducer employing the magnetostrictive effect for measuring the output shaft torque of gas turbine engines. This principle of shaft torque measurement through a stress-related magnetostrictive effect in a ferromagnetic material was described in published works as early as 1953 (Reference 1). A practical system for industrial use was described as early as 1954 (Reference 2). In both of the described systems, the measurement principle is that of detecting the change in permeability of a ferromagnetic material as a function of torsionally induced stress. The apparent advantages of temperature independence of the measured parameter and the capability of measurement without mechanical contact to the shaft of measurement (since magnetic field coupling through transformer action can be used for the measurement effect) make the magnetostriction effect a suitable principle for the measurement of output shaft torque in gas turbine engines.

The torque transducer developed by Avco Lycoming for the T55-L-11 and T53-L-701 engines under this early program operated on the principle of magnetostriction and had an accuracy of ± 2 percent. This particular transducer relied upon a unique procedure for linearizing the torque sensor transfer curve. The procedure was required since the transfer curves generated for the material of the shaft were markedly nonlinear at shear stresses above 4000 psi (Reference 3). The object of this recently completed development program was to design a completely new torque measuring system, not just a transducer, to fulfill the more demanding requirements of gas turbine engine diagnostic and control equipment for an accurate torque signal. The new torque system differs from the present operational system in the following respects:

1. Use of a shaft material with inherent properties of linearity suitable to the magnetic sensing circuit and also having mechanical properties required for a mechanically loaded shaft

2. Ease of installation and maintainability by making a split sensor which can be installed without shaft removal

3. Major improvement in accuracy by developing a closed-loop measuring system which minimizes the need for a closely regulated power supply

4. Design of a sensor which can tolerate large relative motions between the rotating shaft and the stationary sensor

5. Application of the torque measuring sensor in a system concept with the power amplifier and indicator in a single aircraft package

The selection of a four-pole sensor configuration was based upon a comparative trade-off in the stress-averaging capability of the system and loss of system performance or sensor reliability. From prior experience with the three-pole sensor, an increase in the number of poles was considered necessary in order to increase the total stress sensed around the shaft circumference. This would minimize the effects of nonconcentric shaft and sensor alignments. These effects on the three-pole sensor were apparent as changes in signal sensitivity, when the torque sensor electrical output, as determined by a static calibration, was compared to the electrical

output of a dynamic calibration. In some instances, these changes in signal sensitivity were as high as 4 percent on the existing system.

Since the split concept of sensor design was proposed for benefits of system adaptability and maintainability, the pole number was to be of an even integer to allow for symmetrical design of the lamination halves. A six-pole sensor was considered as imposing too severe a restriction in allowable space for coil placements around the pole structures. That is, the reduced clearance between pole structures would require either fewer turns per coil or reduction in the wire size. Depending on the method selected, this would result in either a reduced core flux or a decrease in system reliability. Based upon these considerations, the four-pole sensor was selected as optimal since it increased the stress averaging by one-third and did not require a reduced number of coil turns or a reduced size in diameter of the coil wiring.

EXECUTION OF THE PROGRAM

The program for evaluation of the more advanced torque measuring system was organized into the following three major phases:

Phase I: Analysis

An evaluation of the complete system based upon the design specifications.

Phase II: Design and Fabrication

Design and fabrication of a laboratory or breadboard model of the torque measuring system which could be tested to the specifications stated in the contract.

Phase III: Test

Test the designed system to the stated specifications.

TERMINOLOGY

The torque sensor, as defined for this report, will be considered as the lamination assembly (sensor) and the specimen shaft used for test or engine shafts when magnetically coupled for torque measurement by the magnetostrictive effect.

The lamination assembly refers to that portion of the torque sensor which is stationary and contains the pole structures for coil mounting.

Air gap refers to the dimensional clearance measured radially between the pole structures on the lamination assembly and the shaft.

The detector is that portion of the indicator electronics used to extract an information signal from the secondary coil voltages of the torque sensor.

The information signal is that portion of the electrical voltage from the torque sensor or detector circuit which is proportional to the applied torque.

The inverter is that portion of the indicator electronics used to supply the magnetizing force for the torque sensor.

REPORT ORGANIZATION

The organization of this report is not in order of the program phases. The Analysis presentation follows the Design and Test presentations. This is necessary to maintain logical sequence since the analysis phase was performed simultaneously with the other two phases. This requirement is imposed by the transducer principle of magnetostriction which does not lend itself to analytical evaluation. Rather, empirical data are used from test for the predictions of performance of the torque sensor.

DESCRIPTION OF THE TORQUE MEASURING SYSTEM OF THIS STUDY

The torque measuring system uses the principle of magnetostriction for the transducer effect of converting torsional mechanical force to a directly related electrical information signal. The mechanical force of shaft torsional shear stress is related to the magnetic reluctance of a shaft material. It is known that shaft material magnetic reluctance changes with torsionally caused stresses. The reluctance in the principal tension plane decreases with applied torque; the reluctance in the principal compression plane increases with applied torque. This relationship of reluctance change as a function of shaft torque is the concept of measurement.

To apply the concept, a transformer is used which includes as a portion of its core flux path the stress-oriented planes of shaft magnetic reluctance. Secondary induced voltages of the transformer are functions of the reluctance. The secondary induced voltages, one from each plane of principal stress, are combined in a self-balancing bridge detector. The null position of a servomechanism actuated by a null-sensing bridge is used as a measure of the shaft torque. An electrical output signal proportional to shaft torque is generated.

The system includes the following three elemental sections:

1. The torque sensor, consisting of the lamination assembly when magnetically coupled to the shaft for torque measurement through coils installed on radial pole structures of the lamination assembly.

2. A power supply for providing the excitation to the torque sensor.

3. An indicator circuit for determination of an information signal and display of same on a dial indicator. Since the dial display would not provide adequate resolution for accuracy within the design specification requirements, the indicator will also provide a DC output voltage in proportion to the displayed torque.

Figure 1 is a block diagram showing the elemental concepts for the system of this program.

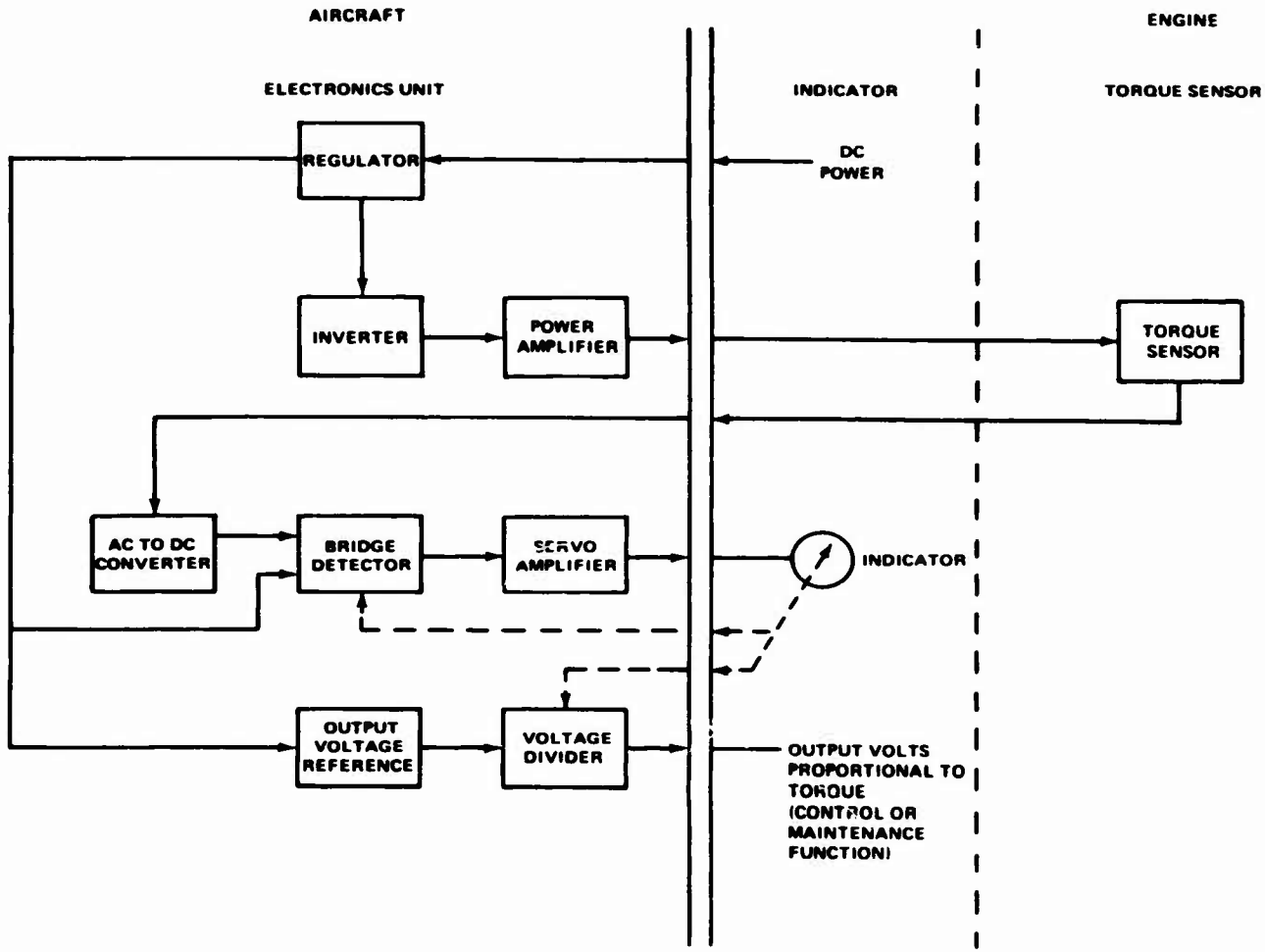

Figure 1. Block Diagram of the Proposed System.

DESIGN SPECIFICATIONS

The requirements for the system are: (1) accuracy of ± 1.0 percent of reading from 30 to 100 percent torque ratings, (2) a design goal of $\pm .5$ percent accuracy, which is considered desirable, and (3) shaft metal temperatures of up to $500^{\circ}F$.

TABLE II. ROTATIONAL SPEED AND TORQUE RANGES

Shaft Speed (rpm)	Torque Ranges (ft-lb)
6000	75-250
6600	250-725
26,000	100-300

The designed system is to demonstrate concepts for reliability, accuracy, repeatability, tolerance to operating environments, long life, low weight, maintainability, and adaptability to Army gas turbine engines.

A laboratory test of the designed system is to be performed. The performance of the system is to be evaluated as operational under the following environmental and load conditions:

1. Ambient temperature range from -35° to $+165^{\circ}F$
2. Shaft metal temperature range from -35° to $+200^{\circ}F$
3. Torque range from 100 to 1500 ft-lb
4. Vibration from 10 to 30 Hz at .2 inch double-amplitude displacement and 31 Hz to 10 kHz at 10g acceleration
5. Speed of shaft rotation from 7500 to 15,000 rpm

DESIGN

TORQUE SENSOR DESIGN

A 2-inch shaft diameter was selected for fabrication of shaft test specimens. The 2-inch diameter was chosen from gas turbine engine experience and is considered as a nominal size based upon the torque ranges from the design specification. With the 2-inch OD established, the derived inside diameter was based upon providing an 8 psi/ft-lb shear stress to torque ratio. Therefore, the shear stress is 5800 psi when computed from a torque of 725 ft-lb (the maximum value from the torque ranges in the design specifications). The value of 5800 psi was selected as a maximum based upon prior experience with transfer curves of SAE 9310 steels.

Two specimen shafts were designed for the program evaluation. One shaft was fabricated entirely of the SAE 9310 steel. The other was made from a Nitralloy 135 material with a sleeve of SAE 9310 attached in the area used for torque measurement. The design concept of two shafts is to demonstrate the ability of adapting the system to gas turbine engine installations which do not use the SAE 9310 steel as a shaft material. Nitralloy 135 was selected for a shaft base material since it is used for engine shafts which require nitriding for surface hardening. This allows the shaft to be used in higher temperature environments than would be permitted with the SAE 9310 steel carburized for surface hardness. The sleeve was attached to the shaft by circumferential electron-beam welding. This constrains the sleeve to sense the applied shaft torque. Cross-sectional views of the two specimen shafts are shown in Figures 2 and 3. The tapped holes seen in Figure 2 were added for the flow of temperature-controlled fluids used for tests on metal temperature effects.

It should be noted that although an SAE 9310 carburizing grade steel is used for the torque sensor, the material in the area of torque sensing is not to be carburized. Carburization is used for surface hardening of the shaft as required by mechanical strength characteristics. SAE 9310 steel is selected for the shaft material since its inherent transfer curve linearity observed during development of Lycoming in-service torquemeters is considered as mandatory in obtaining the design accuracy.

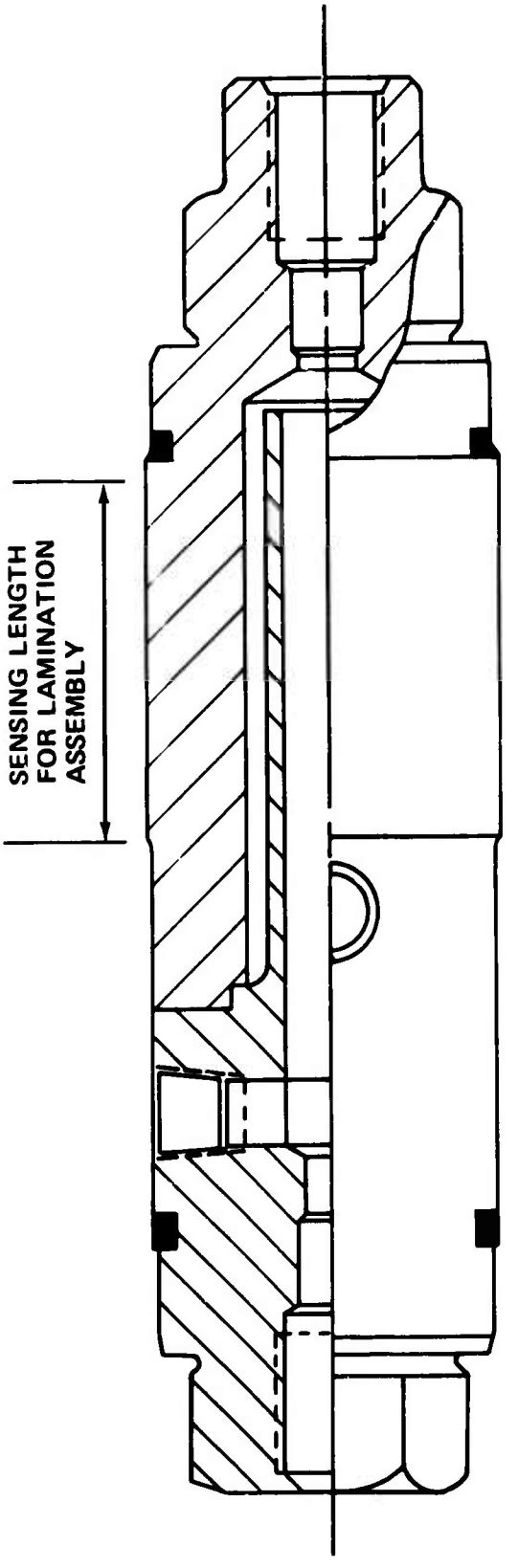

Figure 2. Cross Section of the Nonsleeved Specimen Shaft.

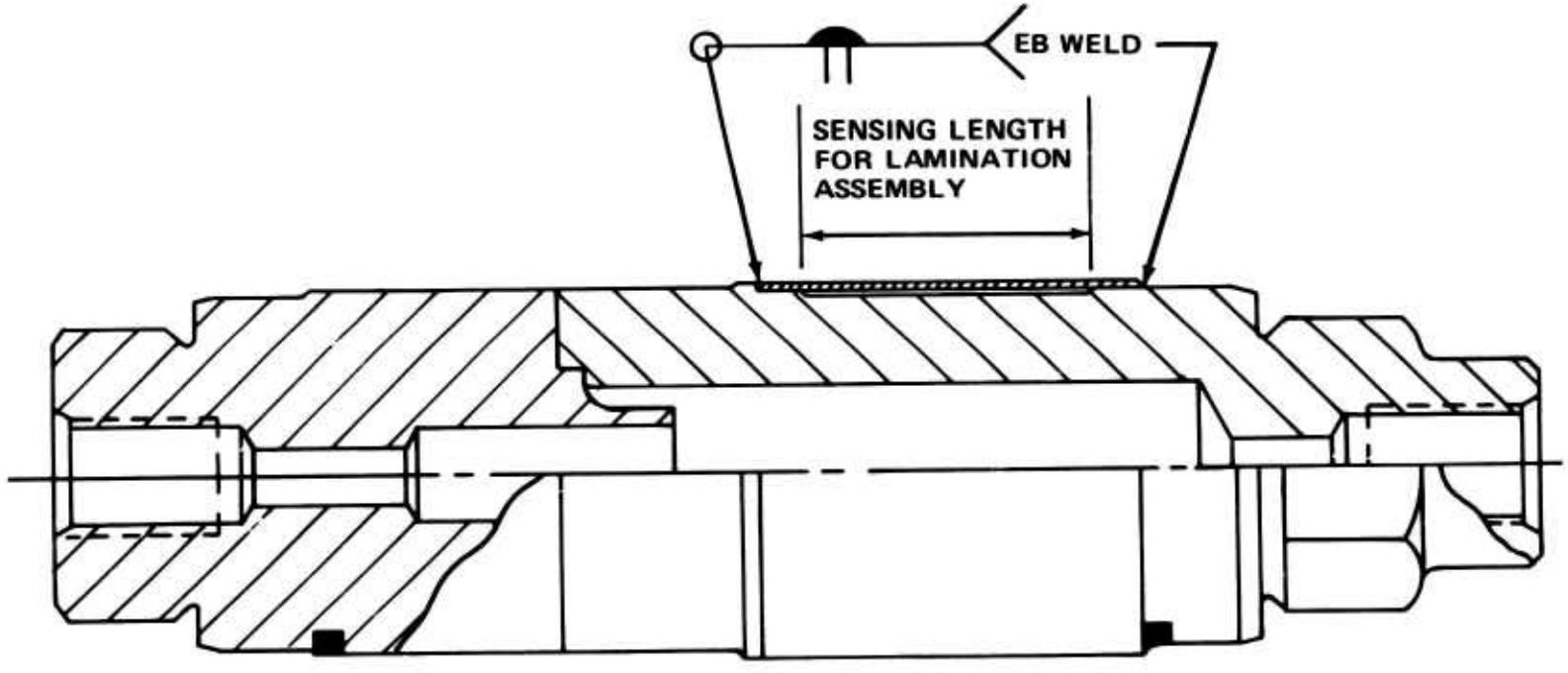

Figure 3. Cross Section of the Sleeved Specimen Shaft.

The lamination assembly is designed as a five-ring structure axially split to provide symmetrical halves. To provide a spacing between the outer pole rings used for attachment of the secondary coils, two inner rings are used without pole structures. Figure 4 shows a cross section of the ring assemblies installed around a shaft. The lamination assembly is designed as two axially split sections to facilitate installation around in-place shafting shown in Figure 5. The sections are symmetrically designed and need not be indexed for proper installation. Figures 6 and 7 are photographs of the fabricated assembly. Figure 6 shows the two halves prior to installation of coils. Figure 7 shows a lamination half with coils prior to completion.

The center ring assembly contains the pole structures for attachment of the primary coils. Four primary poles are used (two per half assembly) radially located at 90 degrees to one another.

The outer rings contain the pole structures for attachment of the secondary coils. These rings are spaced axially from the center ring to maintain a 45-degree relationship between the primary and secondary coils when the flux path is considered as being projected on the surface of the shaft. The angular orientation of the secondary poles is determined by allowance of space for the coil windings. For symmetrical design and maximum space allowance, a 30-degree angular length is required for secondary poles when measured from a primary pole.

With a 30-degree angular length determined for the pole spacing, the axial length for spacer rings was computed. For a shaft of 2-inch OD, the arc length of shaft surface for a 30-degree angle is .52 inch. Therefore, the spacer rings are used to obtain .52-inch axial spacing between each of the secondary pole rings fore and aft of the primary ring. The total axial length of the assembly becomes 1.29 inches as shown in Figure 8.

Figure 9 shows the projected pole images relative to the planes of stress in a torsionally loaded shaft. Figure 10 shows the internal wiring for the pole structure coils. The radial orientation of the pole structures is shown in Figure 11.

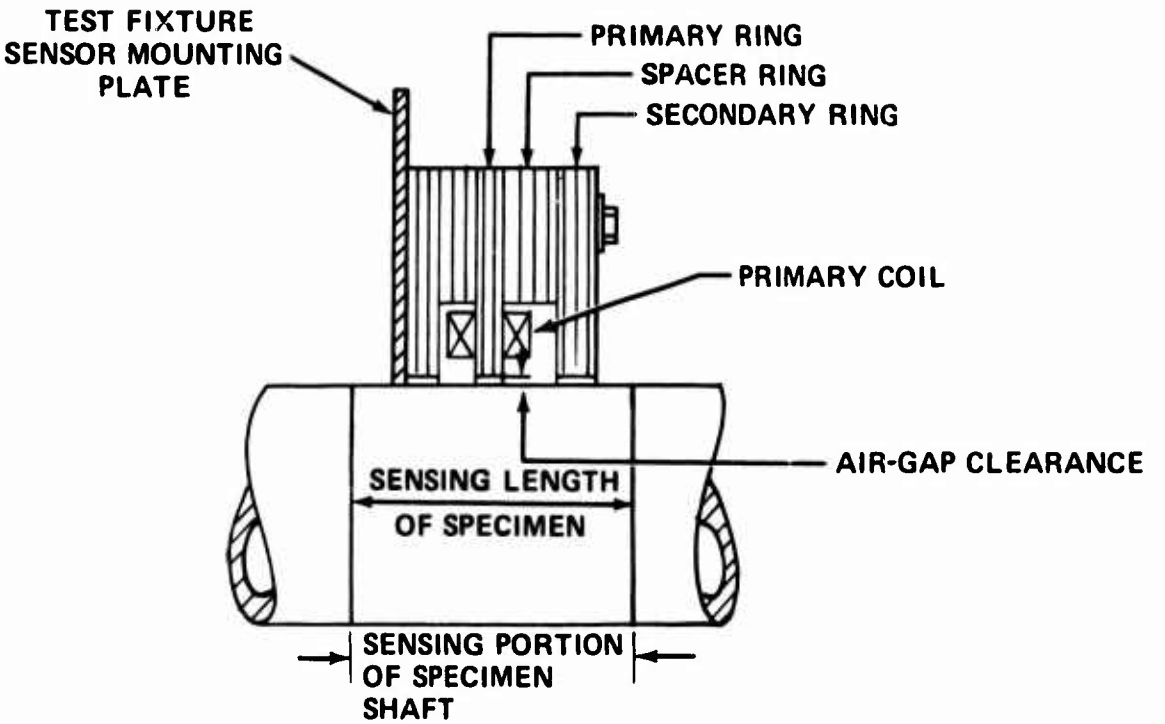

Figure 4. Cross Section of the Lamination Ring.

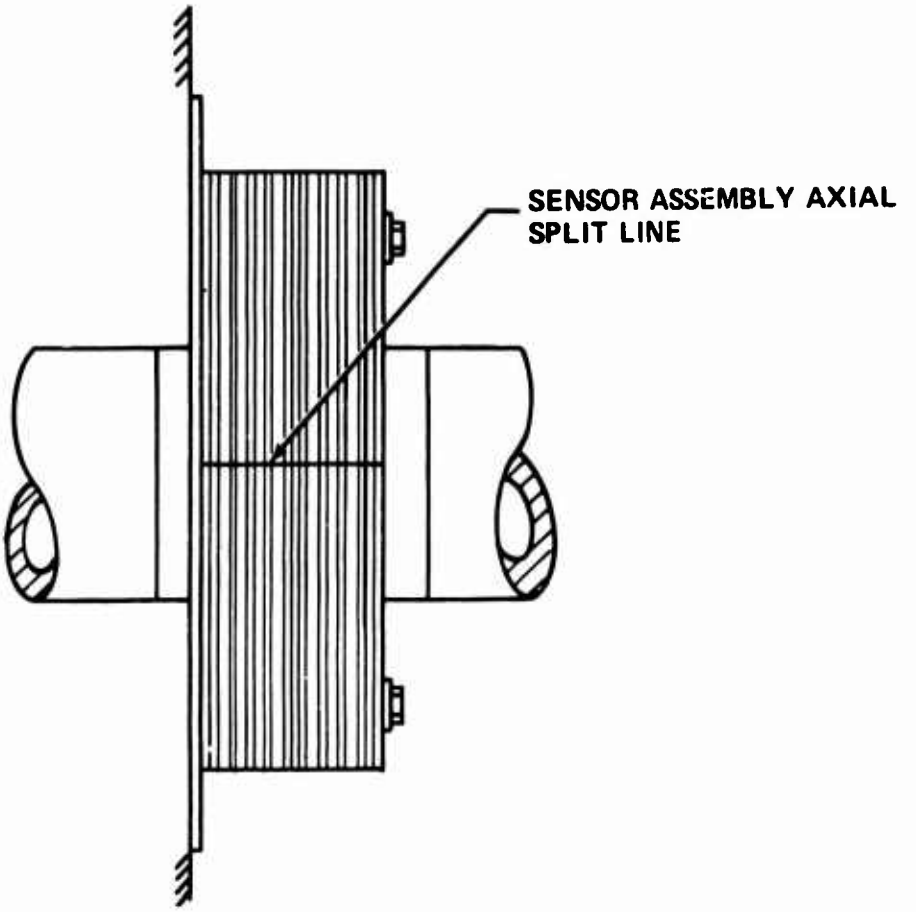

Figure 5. Axially Split Lamination Placed Around Shafting.

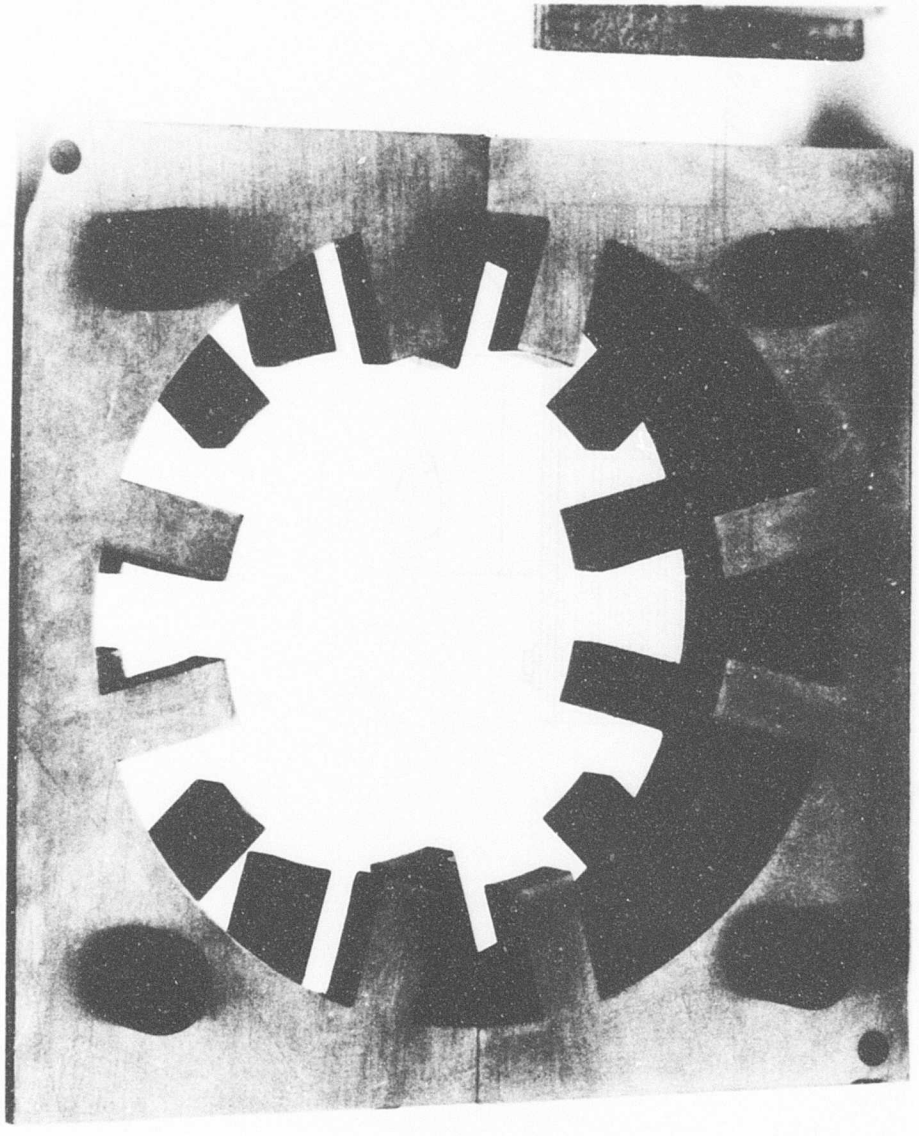

Figure 6. The Lamination Assembly Fabricated in Two Halves for Program.

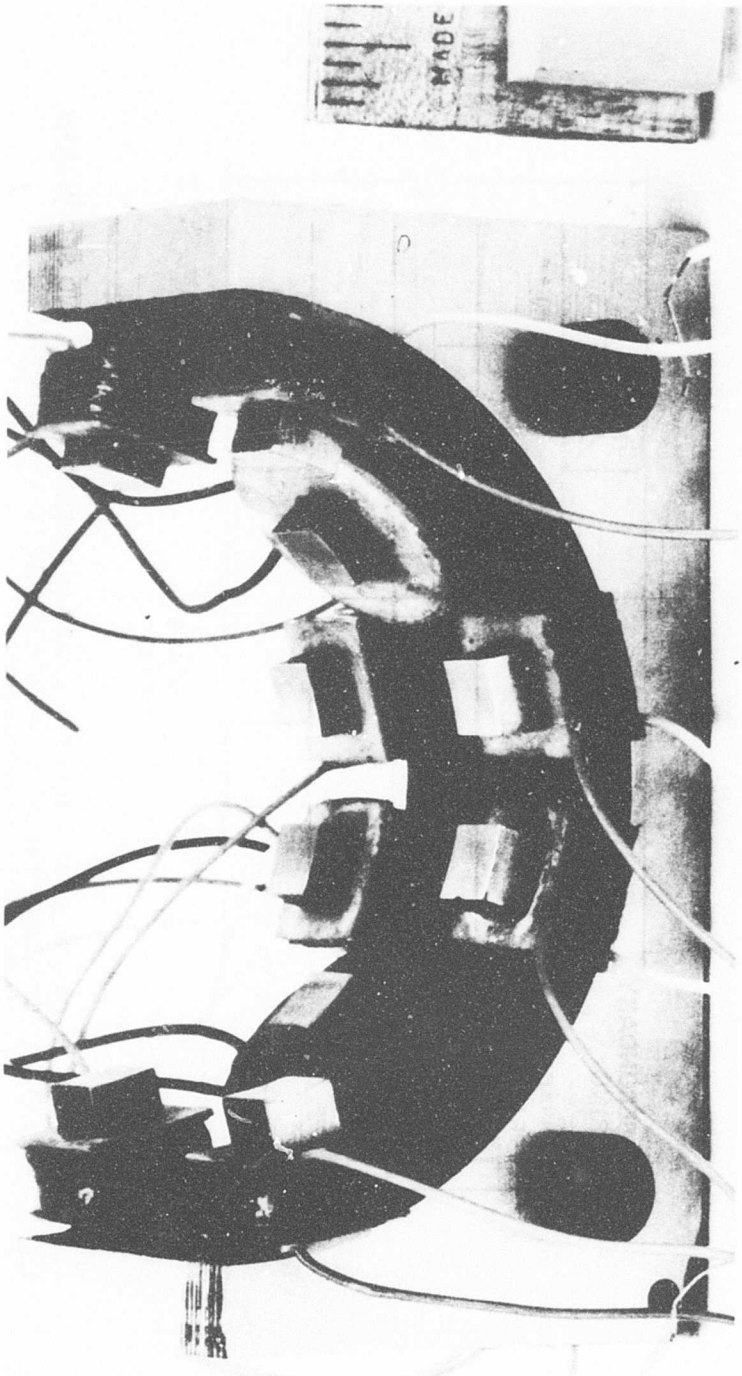

Figure 7. The Lamination Assembly With Coils Prior to Wiring.

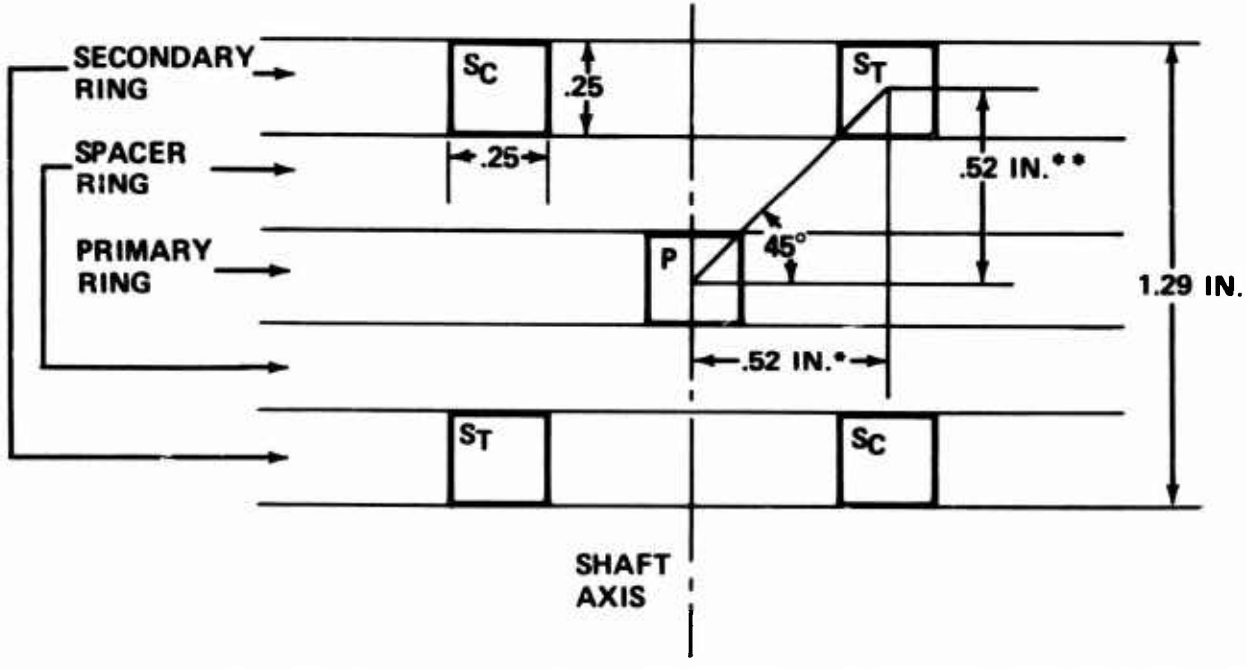

* CALCULATED FROM THE SHAFT OUTSIDE DIAMETER AND SECONDARY ORIENTATION OF 30° WITH RESPECT TO THE PRIMARY.
** MADE EQUAL TO DIMENSION *

Figure 8. Axial Length of the Lamination Assembly.

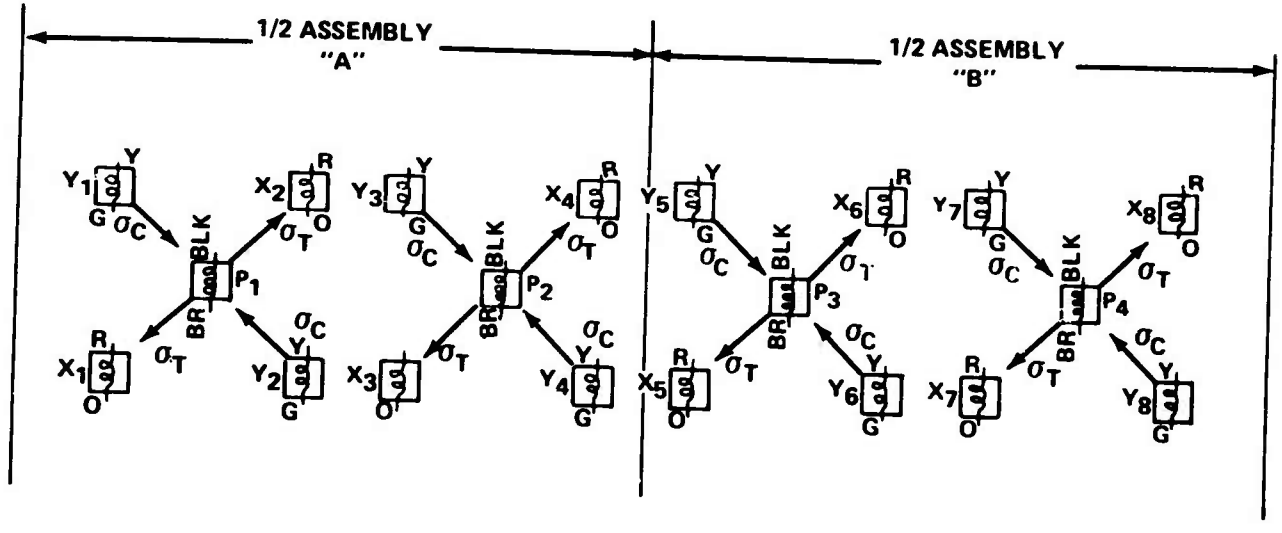

Figure 9. Projected Pole Images Relative to Planes of Stress.

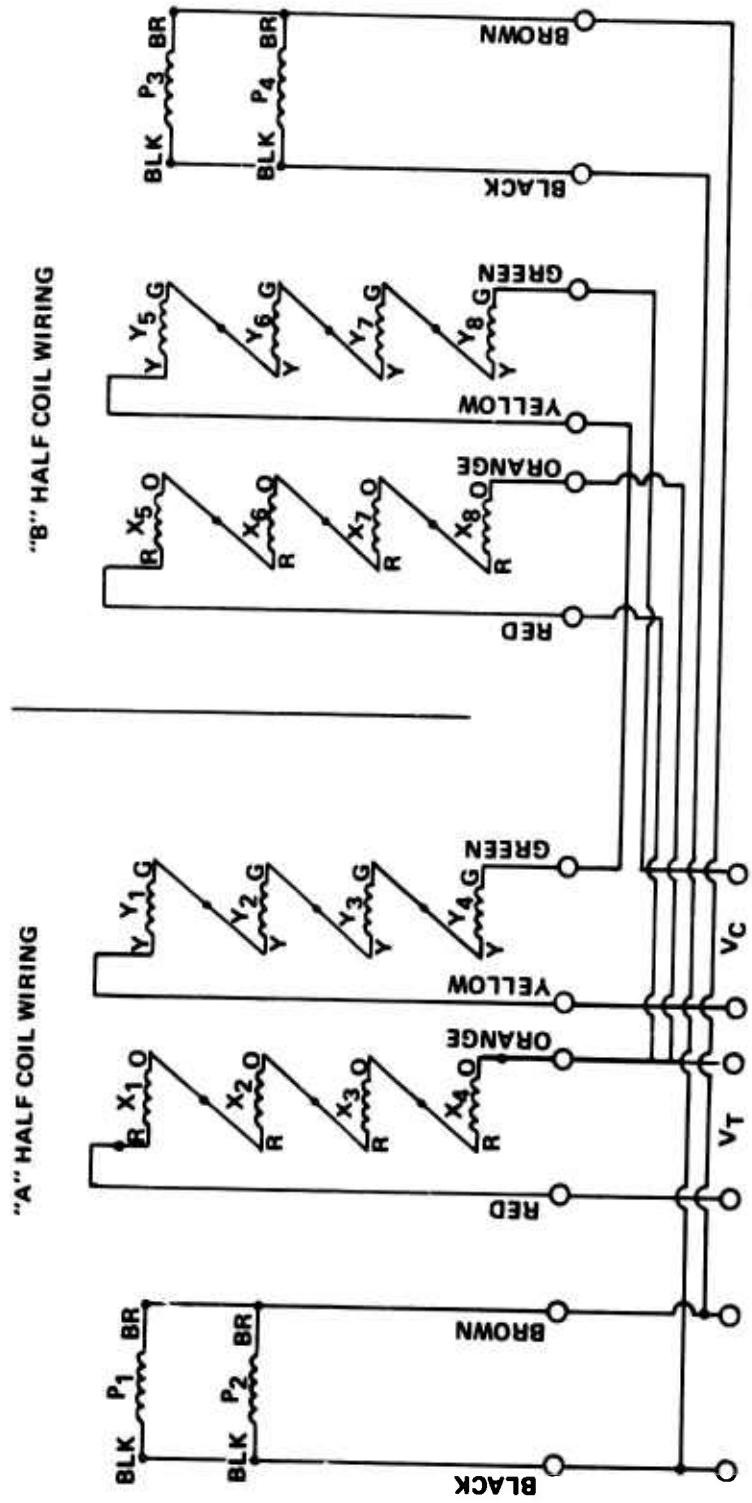

Figure 10. Internal Wiring of the Coils.

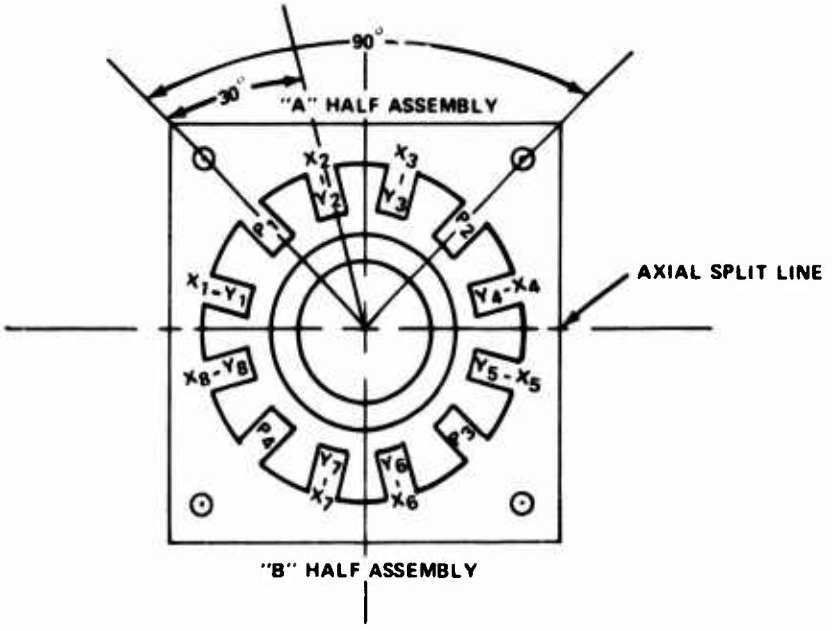

Figure 11. Radial Orientation of Poles.

Although the lamination assembly design is predicated on a 2-inch OD shaft, the same concept for pole orientation and requirement for axial length can be applied to shafts of different dimensions.

The two secondary coils on poles, oriented to lie in the plane of compression associated with each primary, are electrically connected in a series-aiding voltage configuration. The coils in the tension plane are also wired in the series-aiding configuration and are electrically independent from the compression coils. The effect of this wiring configuration is to provide independent terminal secondary voltages as the sum of eight core flux paths. The voltage summing, done by the wiring, provides for inherent system gain and allows for the effects of shaft-to-sensor concentricity variations to self-cancel. The gain effect is provided by the additive effect on voltage change as a result of the stress dependent reluctance change in each of the core flux paths. The self-cancelling of concentricity variations is best explained by the functional operation of the transformer.

The core flux path is through three areas of magnetic reluctance: the ring assemblies of the sensor, the air gap (clearance between the sensor and shaft), and the shaft material. Only the path through the shaft material provides a reluctance value for determining an information signal. The other paths are dependent on the transformer construction and are required to remain stable in operating characteristics to avoid producing an error signal (noise). The sensor ring assemblies are designed for stability of magnetic properties in selection of the material used and in construction. The air gap is, however, an uncontrollable variable since it is dependent on the dynamic behavior of the shaft.

The following description demonstrates the system design concepts for minimizing the effect of air gap variations. Air gap variation effects may be divided into two main categories:

1. Those due to nominal or uniform concentric variations.

2. Those resulting from eccentric location of the shaft with respect to the lamination assembly.

The former effects will be caused by manufacturing tolerances and temperature coefficient of expansion differences, while the latter will be the result of misalignment or radial play.

The expected effect of increasing air nominal gap is principally reduced operating flux, which would correspond in effect to reduced excitation. The basic relationship in the magnetic circuit may be seen in Figure 12, which shows the superimposed shaft magnetic material and air-gap characteristic. For simplification, the lamination assembly magnetic characteristic is not included because its magnetic potential drop is very low by comparison to the shaft. Figure 12 shows several important points: (1) the steel shaft is operating at low flux density, (2) most of the magnetic potential is consumed across the air gap, and (3) the effect of air gap and excitation ampere turns is linear and proportional largely because of (1) and (2). The large air gap linearizes the transfer curve of the magnetic material. Operating at high flux densities would require either an air gap too small mechanically to be practical, or more excitation current which would require a larger power supply inverter. The bridge detection scheme used should minimize the effects of air-gap and excitation variations; however, it cannot offset the effect of excitation on the magnetostrictive sensitivity.

Air-gap variations, due to eccentricity of the shaft with respect to the lamination assembly or eccentricity in the shaft section or motion, result in a once-per-revolution modulation or variation in output which repeats itself with each revolution.

During static calibration, this effect can be overcome by averaging the calibration obtained at multiple shaft positions.

The dynamic effect of this gap variation is a high-frequency (300 cps for 18,000 rpm) modulation. The effect on accuracy is dependent upon the detector. If the detector is truly averaging, responding linearly, and filtering the high-frequency component, there should be no effect on accuracy. Obviously, the larger the air gap is, the less this effect will be present. Therefore, it is desirable to use as large an air gap as possible.

Two lamination assemblies were fabricated to this design. Figure 13 shows an assembly partially installed around a specimen shaft in a static torque loading fixture. Figure 14 shows the installed assembly which when magnetically coupled to the specimen shaft is the torque

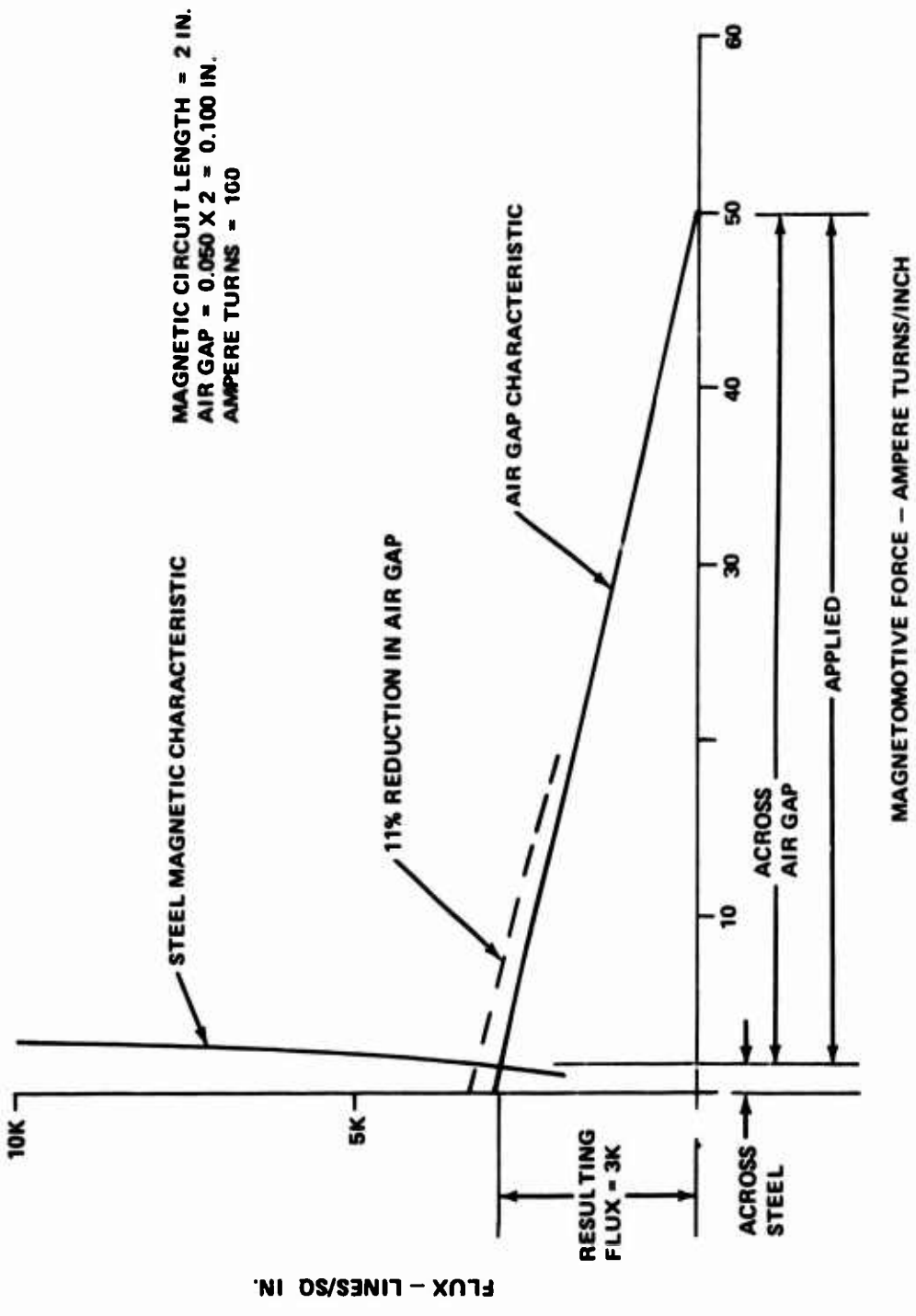

Figure 12. System Magnetic Characteristics.

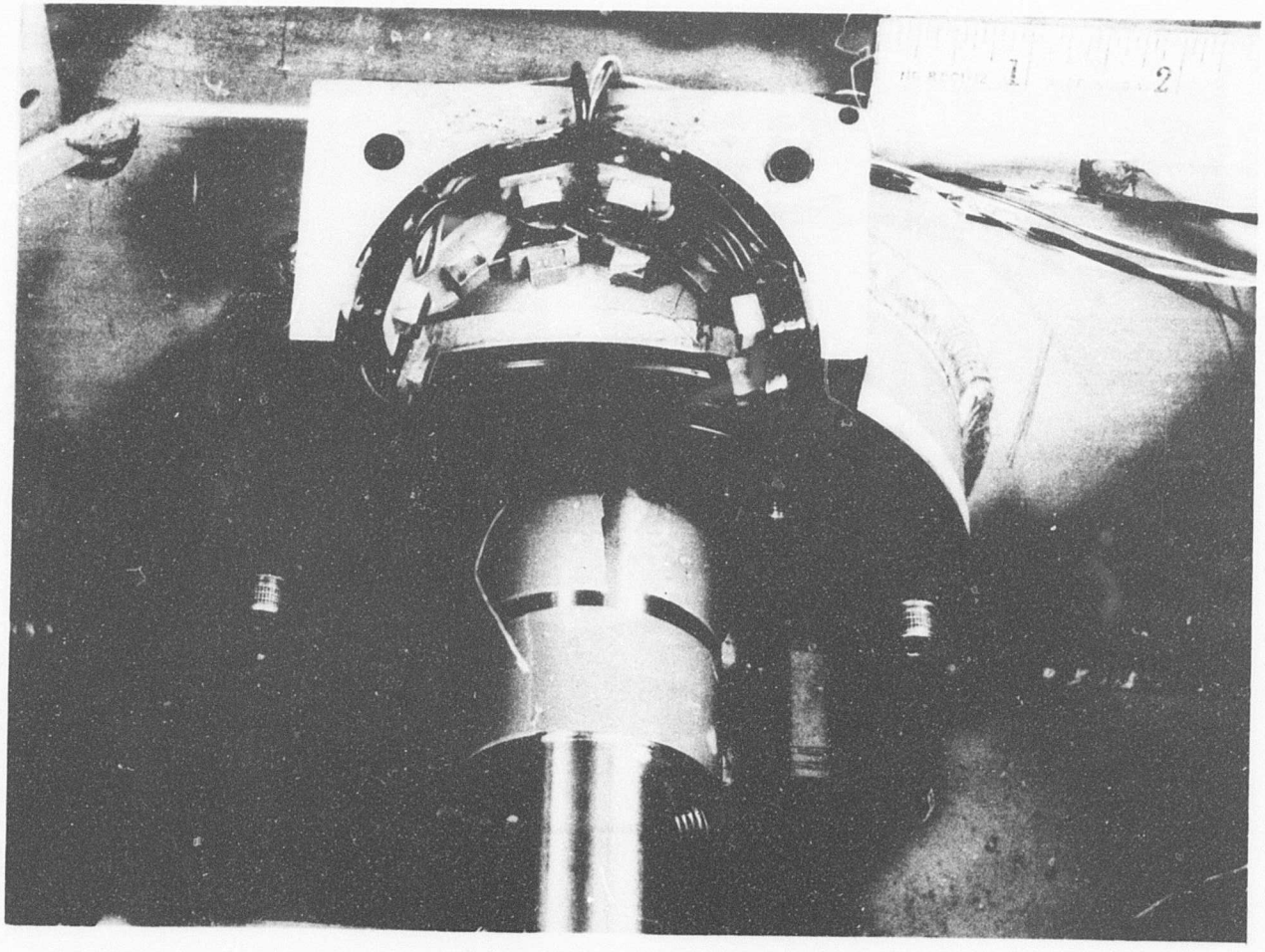

Figure 13. Lamination Assembly Partially Installed.

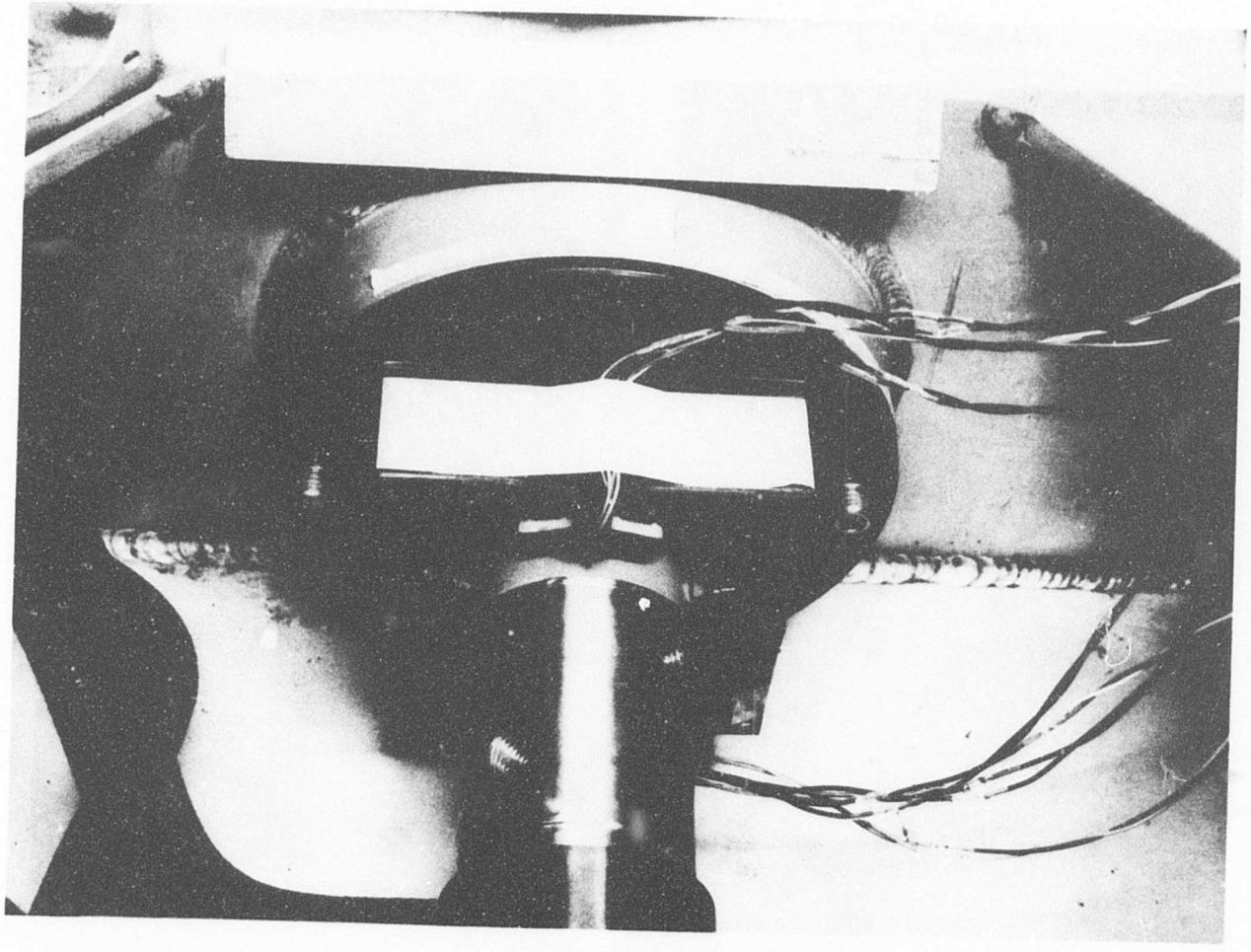

Figure 14. Lamination Assembly Installed for Testing.

sensor used for the test phase of the program. The rectangular perimeter of the test assemblies is not mandatory. This configuration was selected for test since no definition was provided on the envelope shape.

POWER SUPPLY DESIGN

During operation of the torque sensor, a controlled level of core flux is to be maintained throughout the operational environment. Since a design concept for the system is to package the power supply and the indicator electronics into a single package, the description of design is presented for a packaging concept. Figure 15 is a drawing of the indicator electronics package for an operationally designed system.

The electronic portion of the torque measurement system shown in Figure 16 consists of the following units:

1. Power Supply
2. Detector
3. Indicator

The power supply is required to provide an accurately controlled excitation current to excite the torque sensor. Constant current excitation is required because the magnetic excitation level and the resulting sensor output are dependent upon the ampere turns in the primary coils. The excitation with constant current makes the torque sensor independent of error effects due to changing of the coil resistance with temperature. Square-wave-form current excitation was chosen because of its advantages in comparison with previously used sinusoidal excitation. These advantages apply both to generating the excitation current and to processing for an information signal.

One advantage of using the square-wave excitation current is to increase the efficiency of the power supply and consequently its reliability. This benefit is due to the more efficient on-off mode in operation of the output transistors which results in less heat dissipation.

A second advantage is the ease of generating a square wave rather than a sine wave. Also, with the square-wave excitation current,

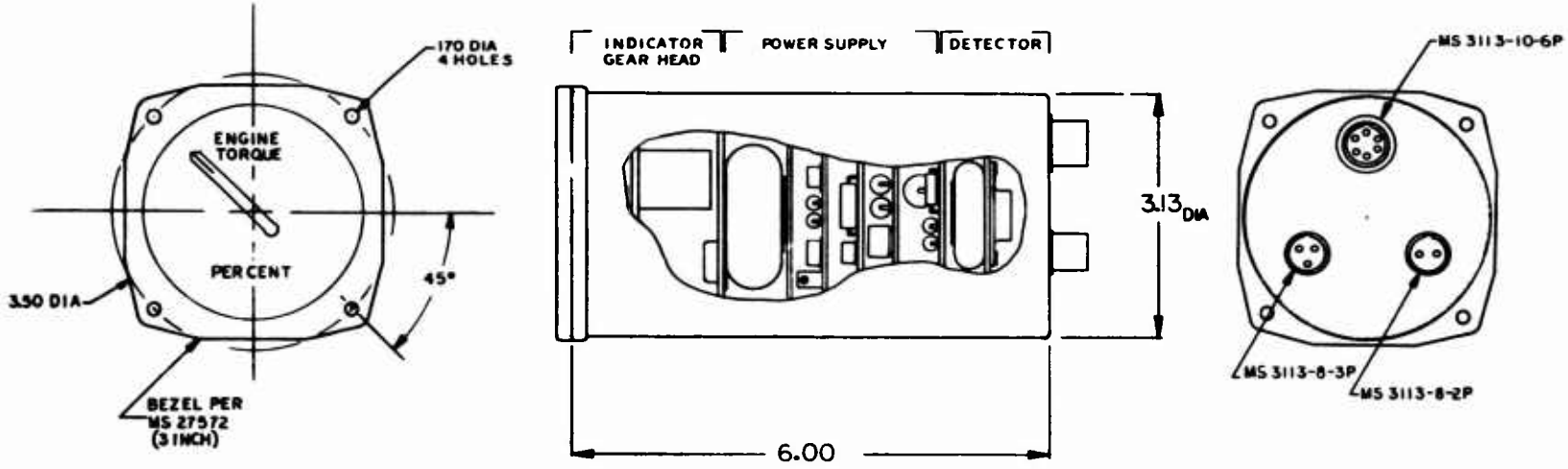

Figure 15. The Indicator Electronics Package.

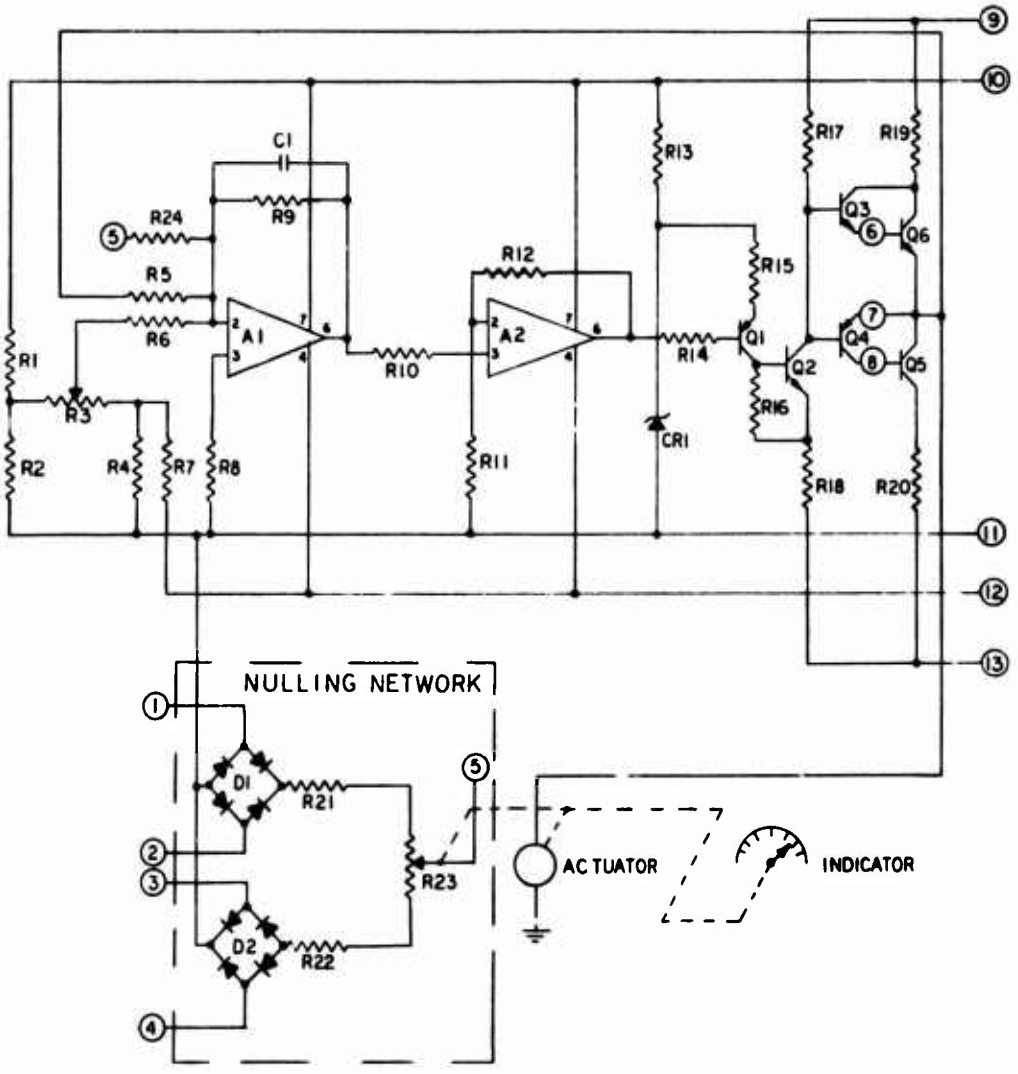

Figure 16. Schematic of the Indicator Electronics.

the output signal from the sensor assembly is not susceptible to power supply waveform distortion as was observed with sinusoidal excitation. The square-wave harmonic content is large, and small variations are not apparent.

Torque sensor signal detection and conditioning are performed by a closed-loop DC servo system as shown in Figure 16. The secondary sensor coils associated with each plane of tension and compression stresses are connected in a ratio mode rather than differential. In a differential mode, two output voltages across the tension and compression coils are subtracted from each other to produce a signal proportional to torque. A change in the excitation frequency or excitation current changes the output of both coils proportionally, and consequently the output voltage related to torque is changed.

Considerable improvements have been made with the secondary coils connected in a ratio mode and arranged with a potentiometer in a bridge. The position of the potentiometer that nulls the bridge corresponds to the imbalance of the secondary coil voltages. With this null-balance measuring system, the ratio of coil voltages is measured, and the effect of change of the excitation frequency or current on the information signal is minimized.

The electronic detector system is illustrated in Figure 16. In this system, the signal conditioning unit fully rectifies each secondary voltage and performs a comparison through use of a nulling network. The nulling network is constructed with voltage scaling resistors and a single-turn precision potentiometer, which nulls the bridge. The potentiometer is driven by a servomotor actuator, which is operated by a null-sensing detector circuit. This circuit senses a signal between the wiper and the common of both coils and provides sufficient amplification to drive the DC servomotor. As a consequence, the mechanically coupled DC servomotor drives the wiper in the direction to nullify the error signal. Since the error signal is ordinarily in the range of millivolts, amplification is required to raise the voltage and power levels required to drive the DC motor.

The breadboard used in the servo amplifier contains a preamplifier with high voltage gain followed by a power amplifier with low voltage gain but with high power gain. In operation, the power amplifier has two drivers which act as On-Off switches to channel the supply current through the motor-armature resistance in forward or

reversed directions, depending upon the presence of a driving signal. The gain of the servo amplifier is made sufficiently high so that small error signals will initiate a corrective action. Also, the servo amplifier has its own closed loop with negative feedback for greater stability.

The DC servomotor is capable of following a 500 ft-lb/sec change in torque.

Since the resulting potentiometer position is indicated by a pointer, which is attached to the potentiometer shaft, the electrical output signal proportional to torque is generated by coupling a reference voltage divider to the pointer.

The advantages of using a closed-loop detection control system are: high accuracy; better stability; relative insensitivity to environmental conditions such as temperature, vibration, shock, line voltage variations, noise, aging, and loading; and fast speed of response to changing input command signal.

To provide a reference voltage proportional to the indicator position, a ganged potentiometer configuration is used. The second potentiometer is driven coincidentally with the null-balancing potentiometer. By using this second unit as a voltage divider supplied from a stable DC voltage supply, an output voltage proportional to the indicator position is provided. This arrangement, although not shown in Figure 16, was used in the test phase of the program and is a design concept for an operational system to provide an electrical signal proportional to shaft torque.

SUMMARY OF DESIGN

The system designed for the program evaluations contains concepts for the practical application of the measurement system in an Army gas turbine engine. These concepts include:

1. A split-ring lamination assembly for ease of installation around installed shafting and around shafting with portions of the OD greater than the lamination assembly bore.

2. Packaging of the electronics and indicator into a single unit. This would simplify logistics but will require further consideration based upon system reliability.

3. Use of SAE 9310 carburizing steel for the magnetostrictive transfer curve generation. This material when properly processed has suitable linearity for obtaining the measurement accuracy.

4. A method for attachment of the SAE 9310 steel on shafts fabricated from other materials.

The test phase of the program, which is discussed in the following section, used a torque sensor and a breadboard electronic circuit fabrication as described in this section.

TEST

The test phase of the program was divided into two parts. In the first part, the optimal operating levels for the torque sensor were established; in the second part, the optimum designed system was evaluated within the parameters of the design specification.

TESTING TO ESTABLISH THE SYSTEM OPERATING LEVELS

The first series of tests determined the magnetostrictive transfer curves of the SAE 9310 steel as dependent functions of the input parameters, i.e., excitation current and frequency. These tests were performed on both specimen shafts to obtain comparative information for a sleeved and a nonsleeved specimen. Figure 17 shows the test assembly. Static torque loads to 1500 foot-pounds were used. The data plotted in Figures 18 through 25 were used to establish the nominal values for the excitation current and frequency. Figures 18 through 21 are the transfer curves generated for the sleeved test specimen at input frequencies of 2, 3, 4, and 6 kHz and at input currents ranging from .400 to .800 ampere. Figures 22 through 25 show the same information for the nonsleeved test specimen. Data was obtained as measured V_T and V_C voltages. The difference was computed and is plotted as the transfer curves. From this data, the displayed nonlinearity of the transfer curves was an unexpected condition. Prior testing on this material had shown good linearity. It was felt that the annealed condition of the SAE 9310 steel used in this program was responsible for the now-observed nonlinearity.

The program schedule of testing was continued with the concept of hardening the material following additional tests.

For comparison of the transfer curves generated by the sleeved and nonsleeved specimens, the data from each specimen operating at the same input parameter level is plotted in Figure 26. Although no appreciable change of sensitivity was noted, the sleeved specimen was slightly more linear. This was a probable effect of surface hardening of the sleeve which received a final machining operation after attachment to the shaft. To determine the optimum levels of excitation current, the data taken at 6400 psi was replotted in a format to determine signal sensitivity versus input parameter at a constant value of shear stress. Figure 27 depicts the stress

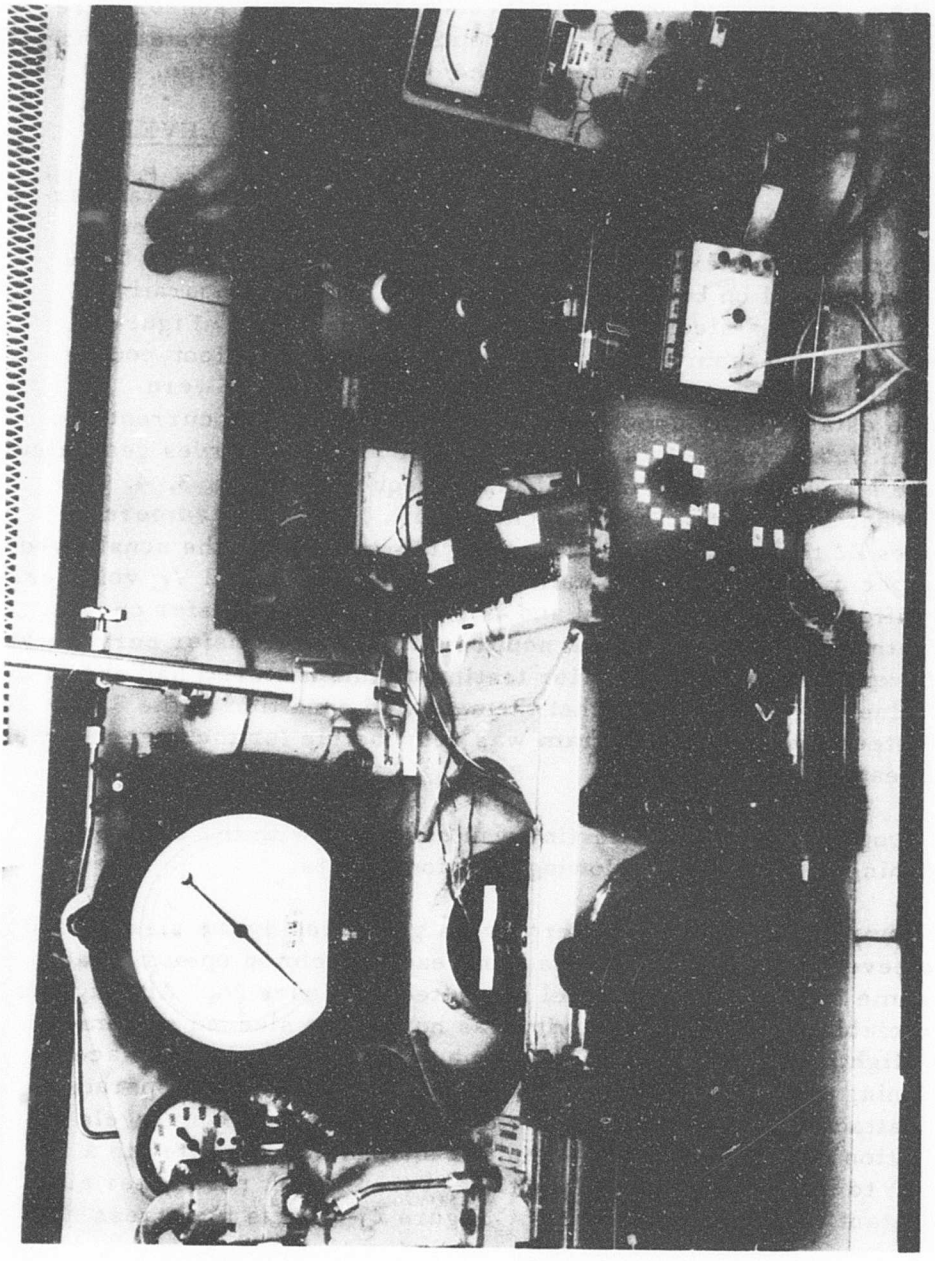

Figure 17. The Static Loading Fixture.

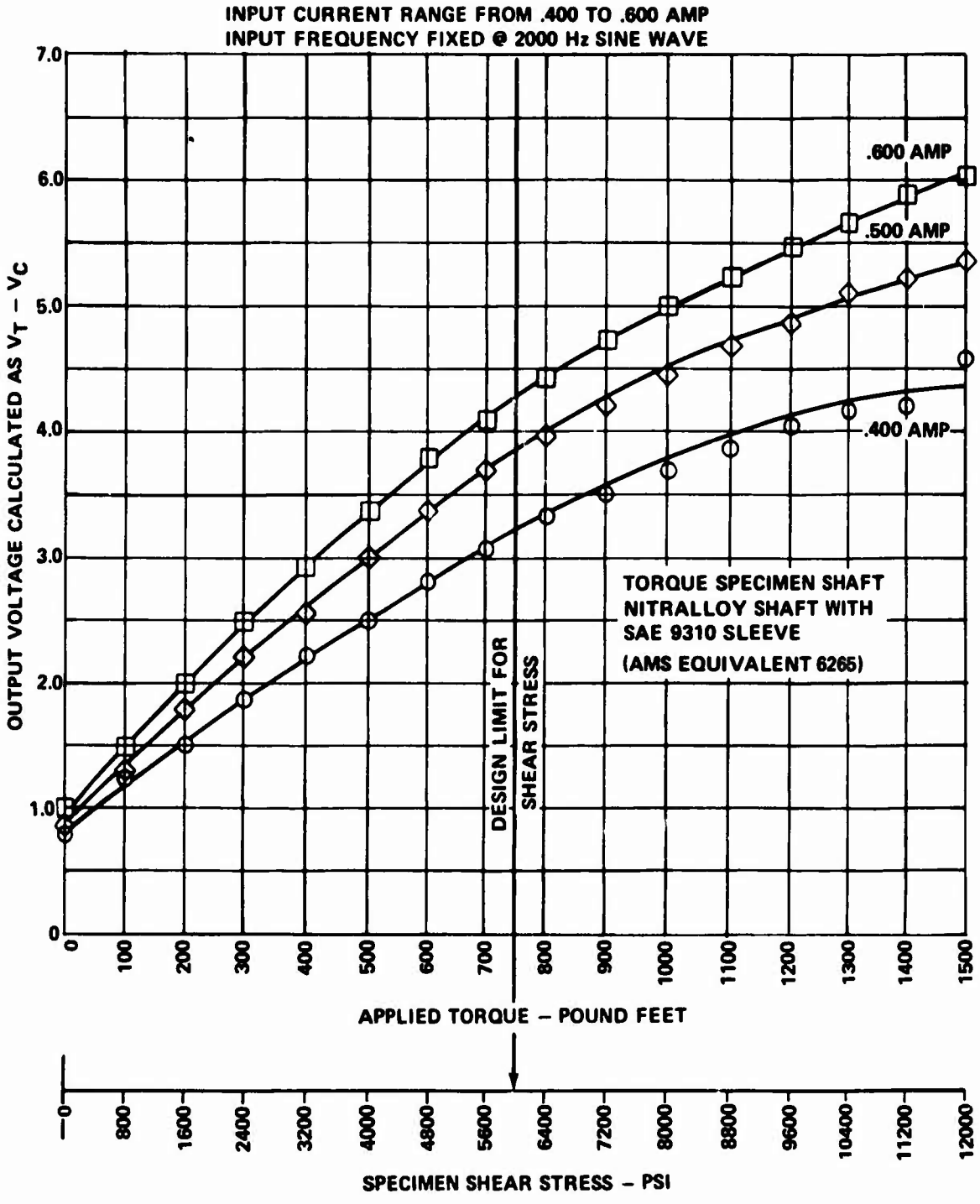

Figure 18. Data Obtained on Sleeved Specimen at 2 kHz.

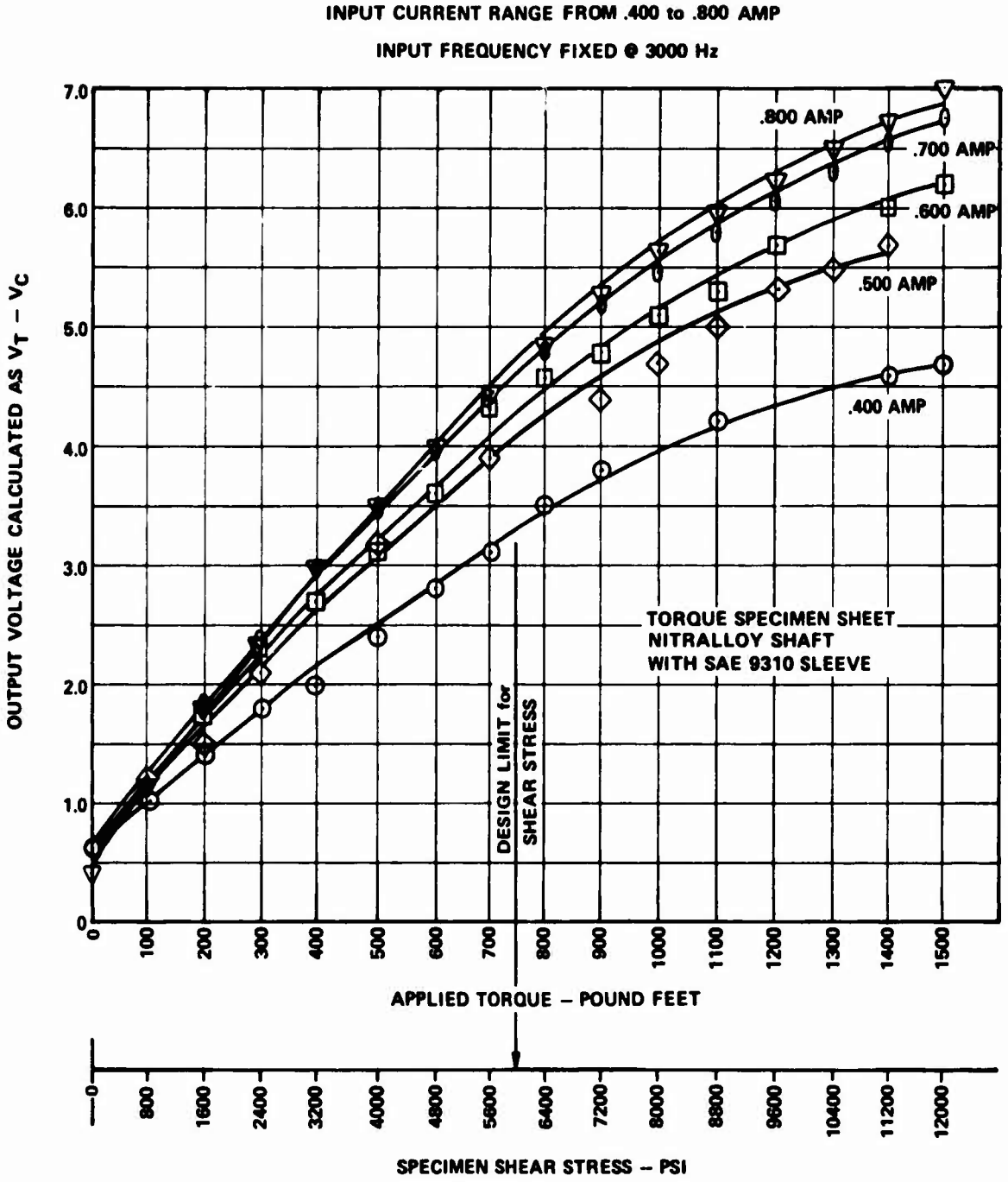

Figure 19. Data Obtained on Sleeved Specimen at 3 kHz.

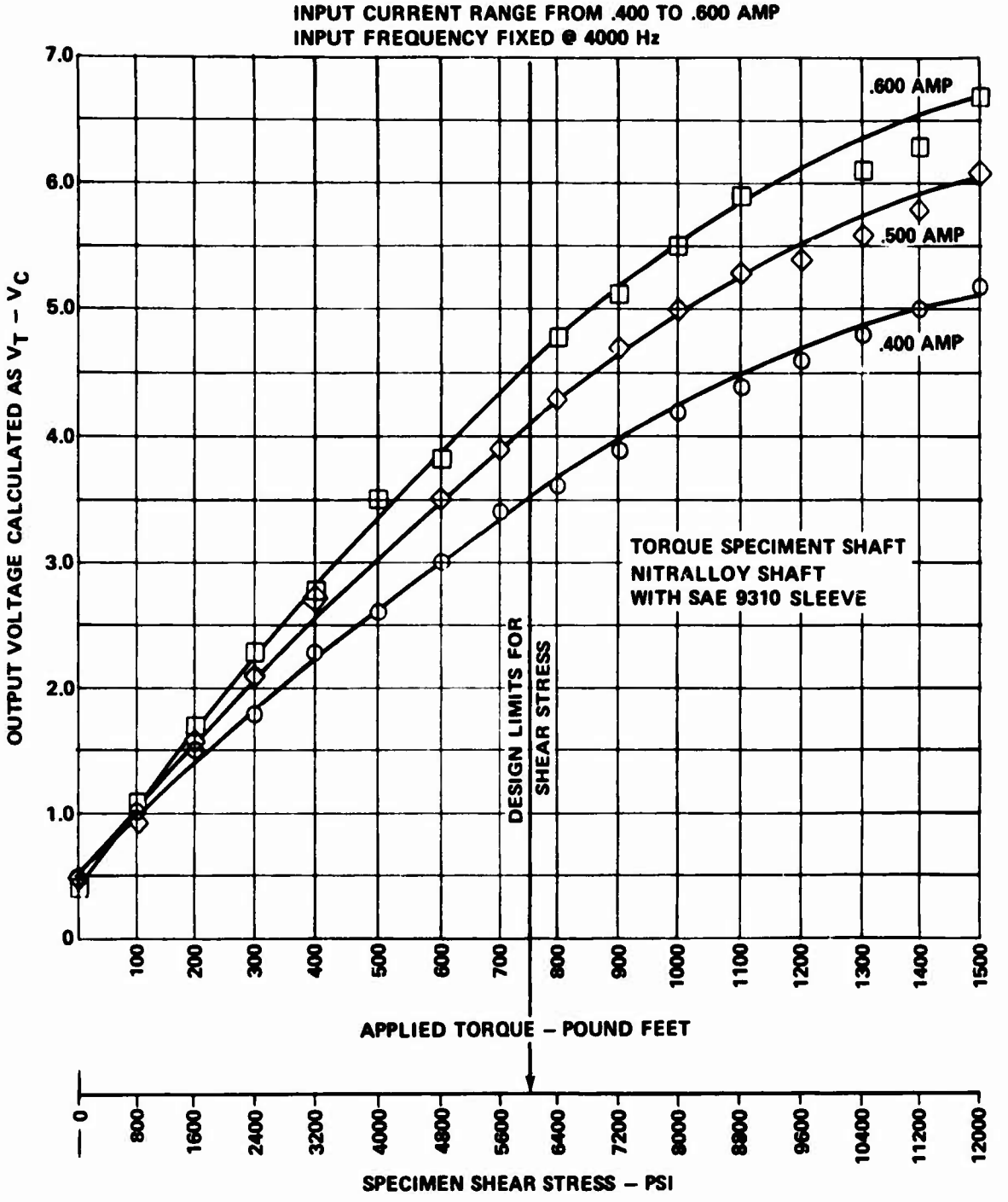

Figure 20. Data Obtained on Sleeved Specimen at 4 kHz.

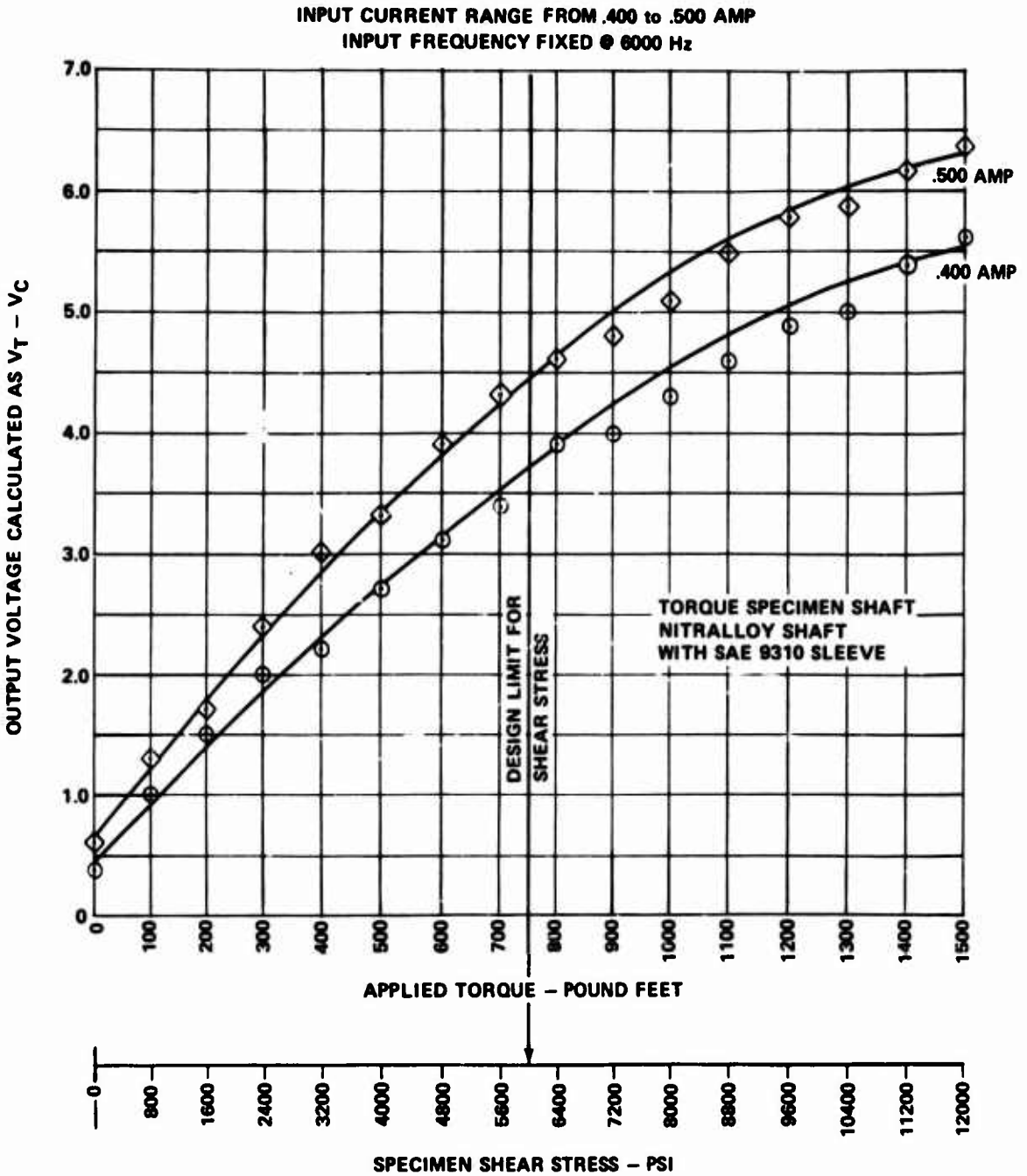

Figure 21. Data Obtained on Sleeved Specimen at 6 kHz.

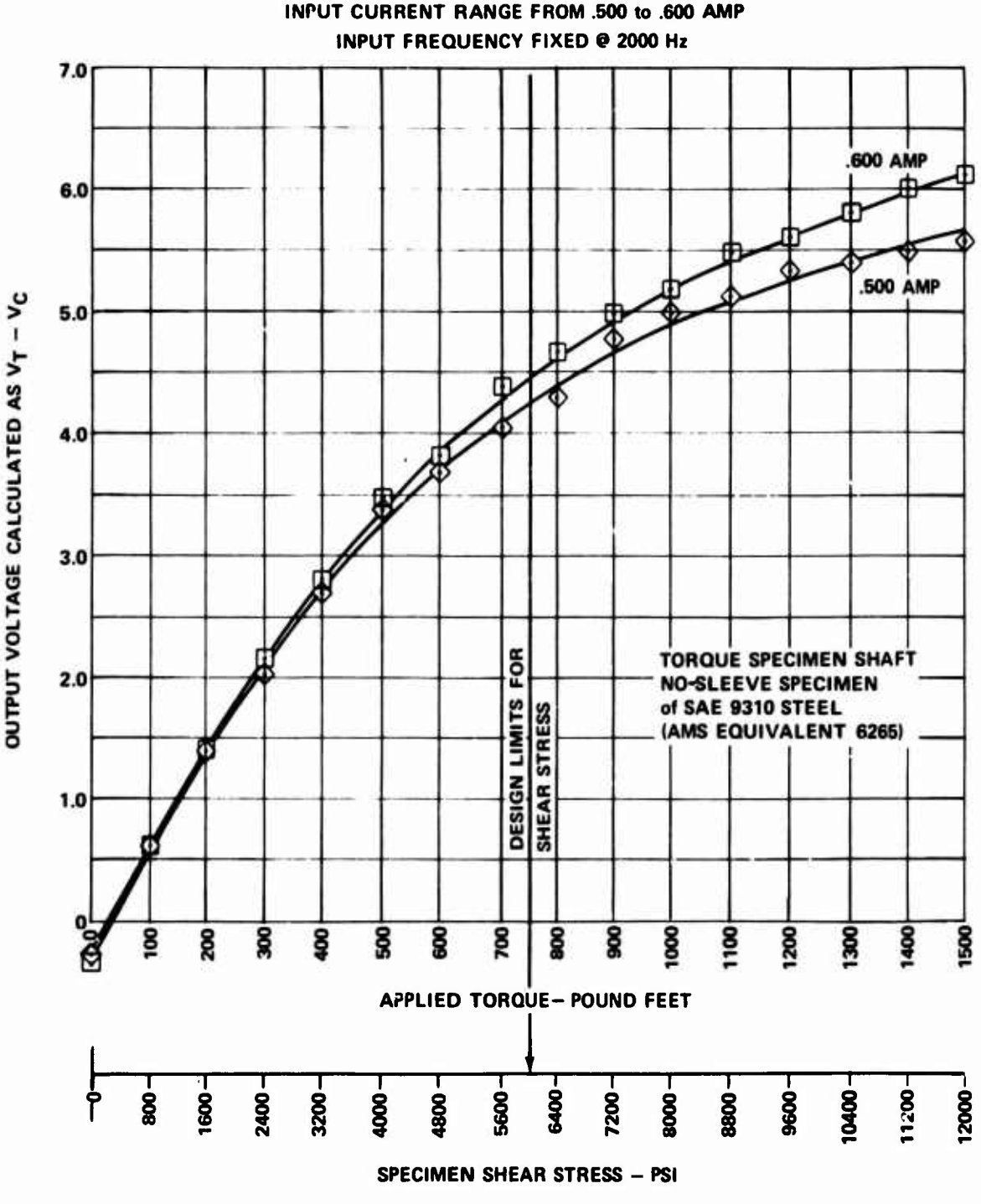

Figure 22. Data Obtained on Nonsleeved Specimen at 2 kHz.

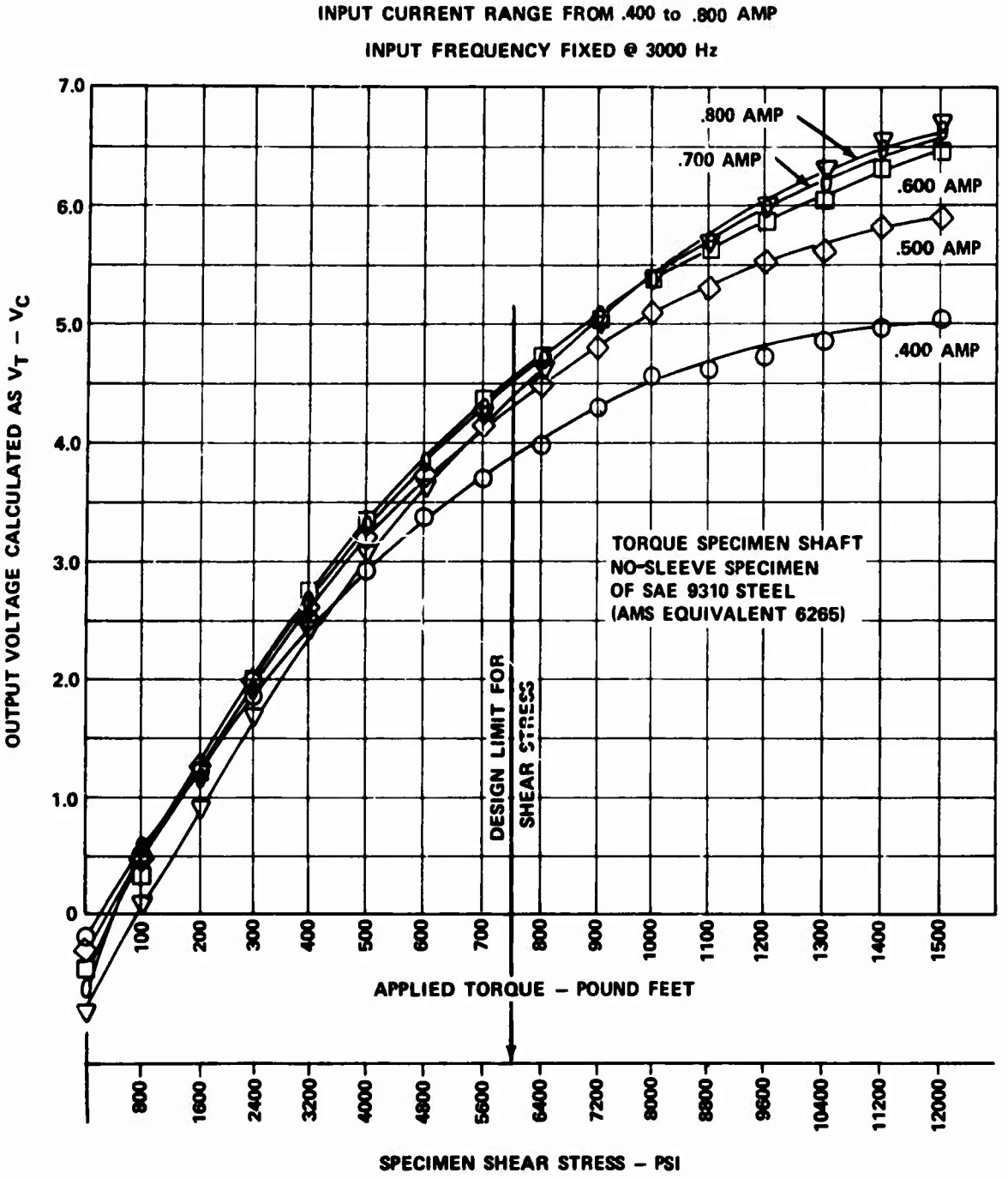

Figure 23. Data Obtained on Nonsleeved Specimen at 3 kHz.

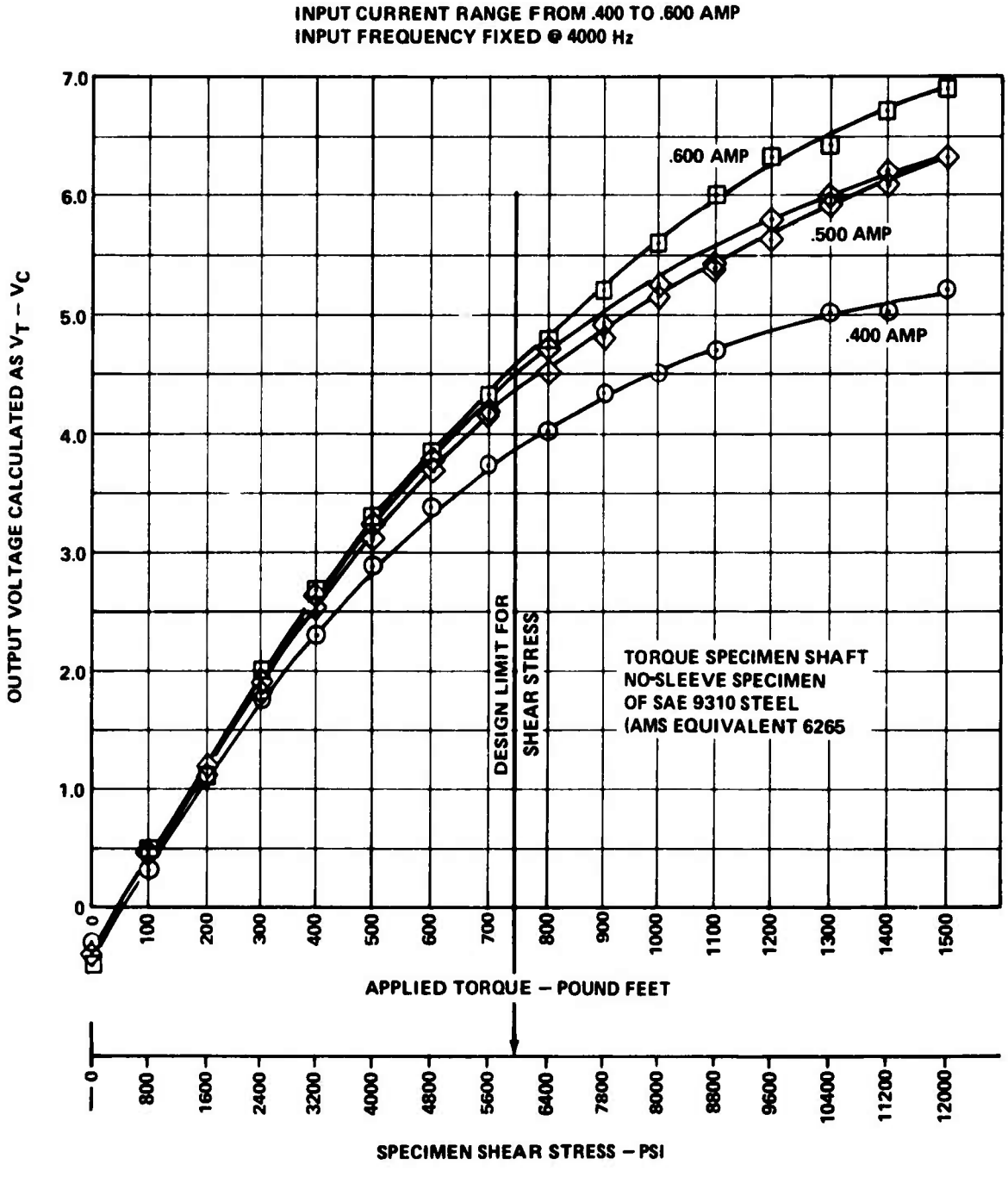

Figure 24. Data Obtained on Nonsleeved Specimen at 4 kHz.

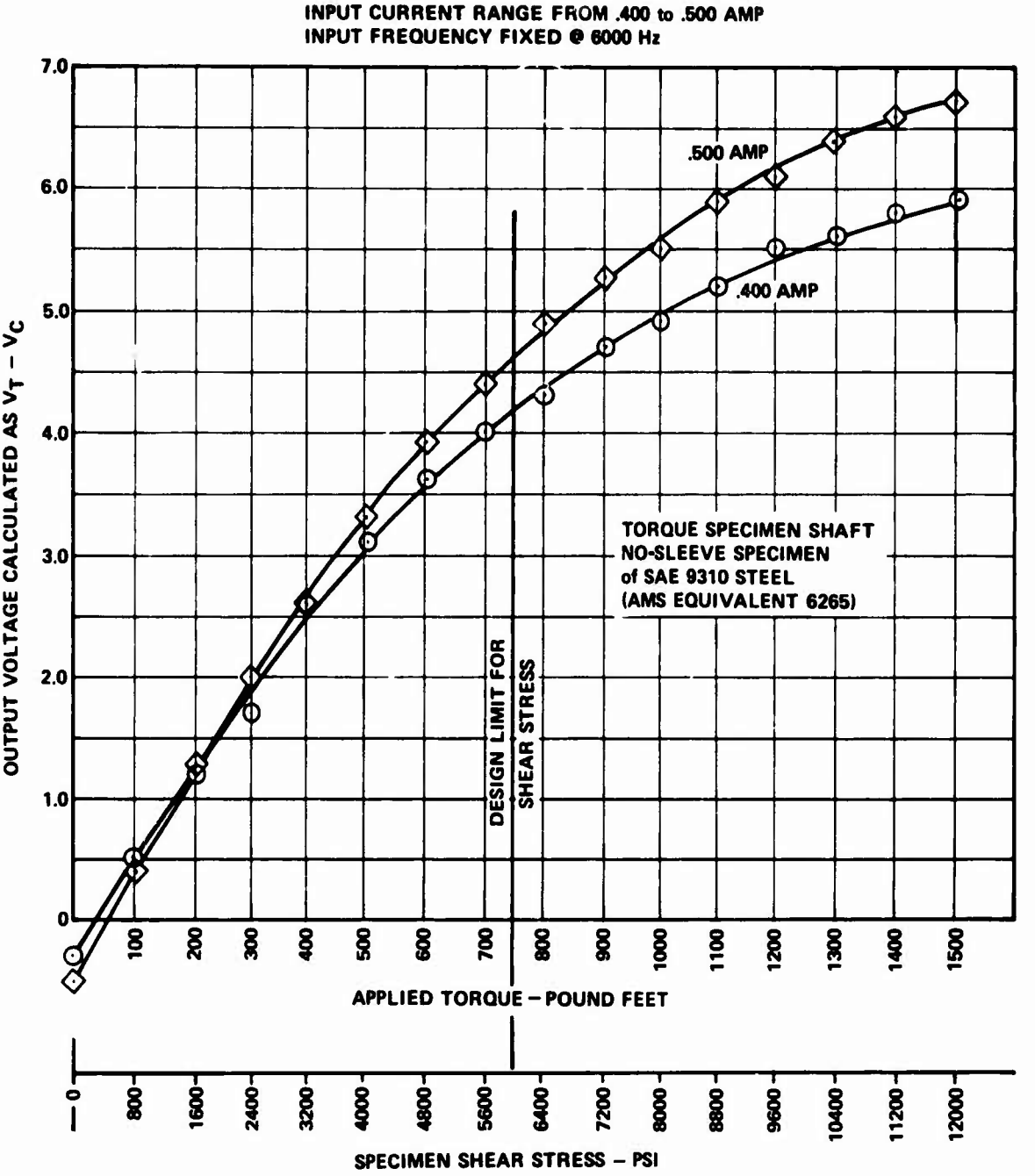

Figure 25. Data Obtained on Nonsleeved Specimen at 6 kHz.

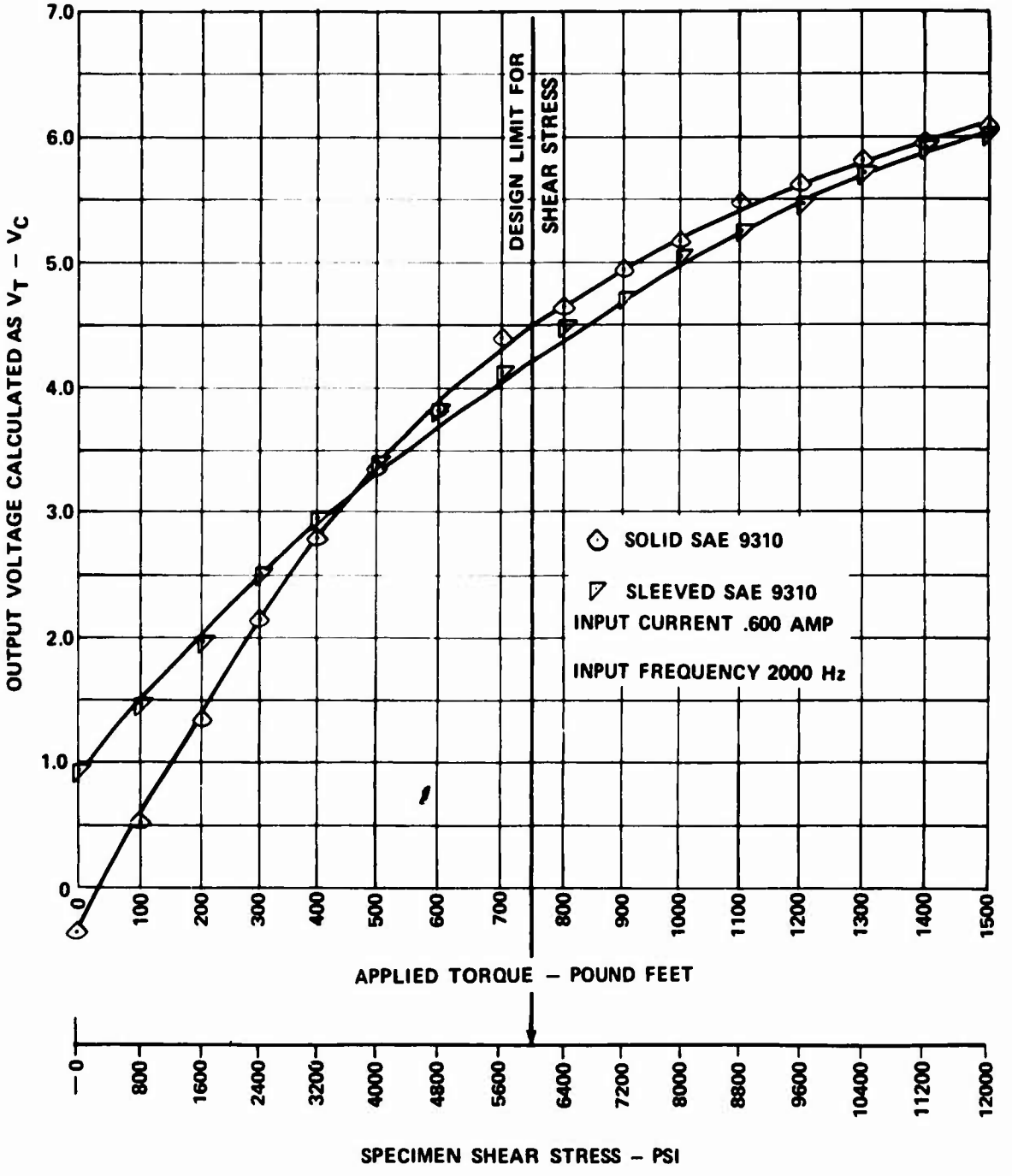

Figure 26. Comparison of Sleeved to Nonsleeved Specimen Linearity.

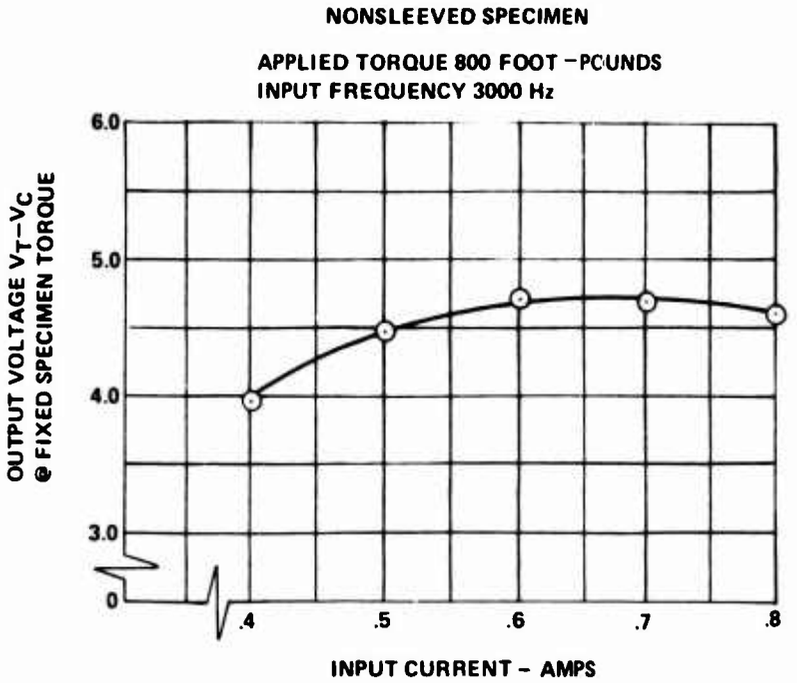

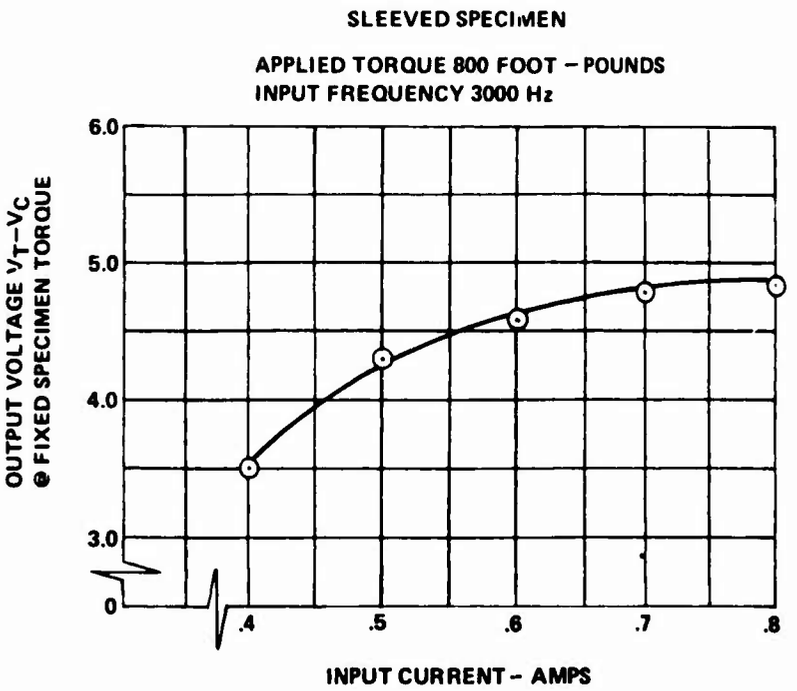

Figure 27. Stress Sensitivity Due to Excitation Current.

sensitivity to excitation current, and Figure 28 depicts the stress sensitivity to excitation frequency.

From this data, the signal sensitivity is derived. The selection of input parameters that would minimize signal sensitivity change with input parameter variations was important. The concept of the detector circuit is dependent on the stress sensitivity of the input voltages; i.e., if both the V_T and V_C voltages increase proportionally with the input, no change in the established null is observed. However, the magnetostrictive sensitivity alters the V_T and V_C voltages of opposite sense. This could be apparent as a false information signal by operating the magnetizing force at a point that displays a high value of magnetostrictive sensitivity.

To minimize the requirements on input regulation consistent with obtaining a useful information signal, the nominal operating levels were established at .670 ampere and 3000 Hz. The nonsleeved specimen shaft was used for selection of the input parameters, since it was scheduled for the tests on air gap variation. Tests of the air gap were made with the nonsleeved test specimen and lamination assembly as shown for the configurations in Figure 29. The baseline configuration was used to determine the signal sensitivity as a function of increased symmetrical air gap with the same level of magnetizing force applied to the magnetic circuit. The axial, radial, and angular displaced sensor configurations were used to determine the effect of gap variation at each increment of nominal radial gap clearance. From this, an optimum value of air gap was established that maintained a maximum clearance between the rotating shaft and the lamination assembly pole structures consistent with obtaining a useful information signal without increasing the adverse effects of shaft misalignment.

Figure 30 shows the effective change in signal sensitivity at each of the nominal values of air gap; i.e. .015, .030, and .045 inch. Testing was terminated at the .045-inch nominal gap since an extrapolation of data indicated a loss of signal with the gap increased above .055 inch.

For the axial and angularly displaced sensor, no significant change of signal sensitivity about the nominal gap sensitivity was noted. Figures 31 through 33 show the data obtained for each gap position tested. The small changes of sensitivity noted for the axial and angularly displaced sensor are thought to be changes of radial positioning incurred while changing the specimen in the fixture.

sensitivity to excitation current, and Figure 28 depicts the stress sensitivity to excitation frequency.

From this data, the signal sensitivity is derived. The selection of input parameters that would minimize signal sensitivity change with input parameter variations was important. The concept of the detector circuit is dependent on the stress sensitivity of the input voltages; i.e., if both the V_T and V_C voltages increase proportionally with the input, no change in the established null is observed. However, the magnetostrictive sensitivity alters the V_T and V_C voltages of opposite sense. This could be apparent as a false information signal by operating the magnetizing force at a point that displays a high value of magnetostrictive sensitivity.

To minimize the requirements on input regulation consistent with obtaining a useful information signal, the nominal operating levels were established at .670 ampere and 3000 Hz. The nonsleeved specimen shaft was used for selection of the input parameters, since it was scheduled for the tests on air gap variation. Tests of the air gap were made with the nonsleeved test specimen and lamination assembly as shown for the configurations in Figure 29. The baseline configuration was used to determine the signal sensitivity as a function of increased symmetrical air gap with the same level of magnetizing force applied to the magnetic circuit. The axial, radial, and angular displaced sensor configurations were used to determine the effect of gap variation at each increment of nominal radial gap clearance. From this, an optimum value of air gap was established that maintained a maximum clearance between the rotating shaft and the lamination assembly pole structures consistent with obtaining a useful information signal without increasing the adverse effects of shaft misalignment.

Figure 30 shows the effective change in signal sensitivity at each of the nominal values of air gap; i.e. .015, .030, and .045 inch. Testing was terminated at the .045-inch nominal gap since an extrapolation of data indicated a loss of signal with the gap increased above .055 inch.

For the axial and angularly displaced sensor, no significant change of signal sensitivity about the nominal gap sensitivity was noted. Figures 31 through 33 show the data obtained for each gap position tested. The small changes of sensitivity noted for the axial and angularly displaced sensor are thought to be changes of radial positioning incurred while changing the specimen in the fixture.

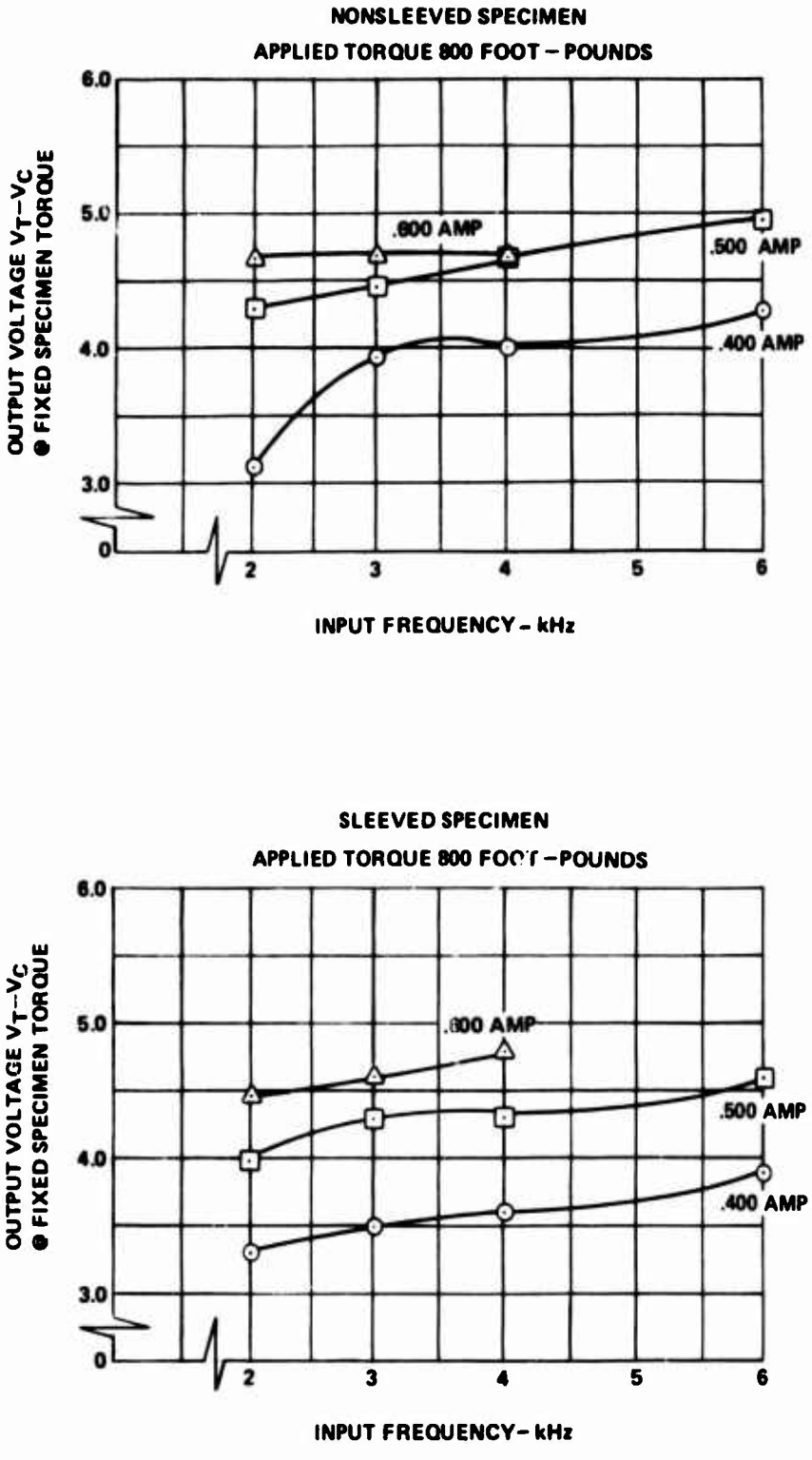

Figure 28. Stress Sensitivity Due to Excitation Frequency.

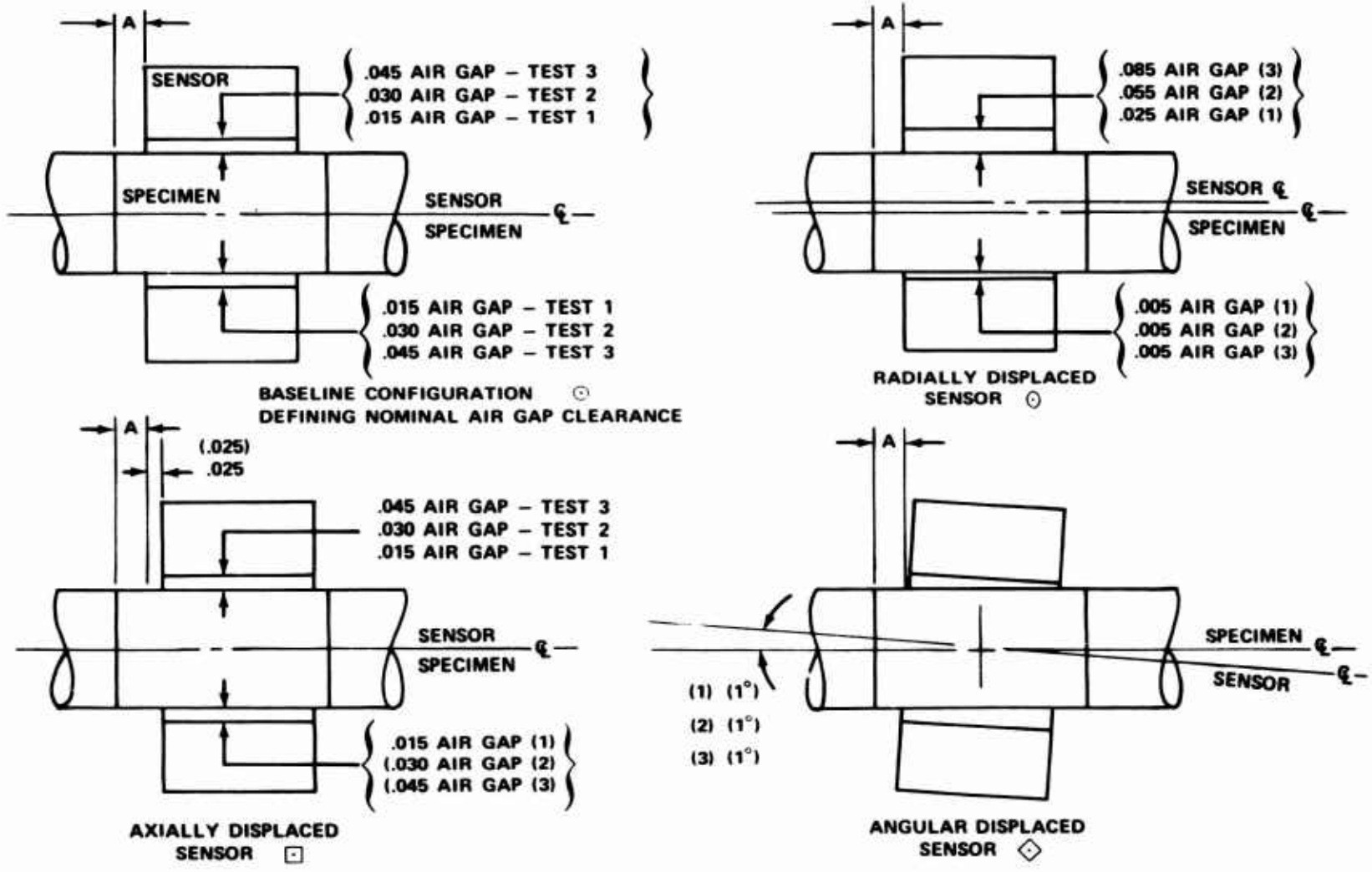

Figure 29. Air Gap Test Configurations.

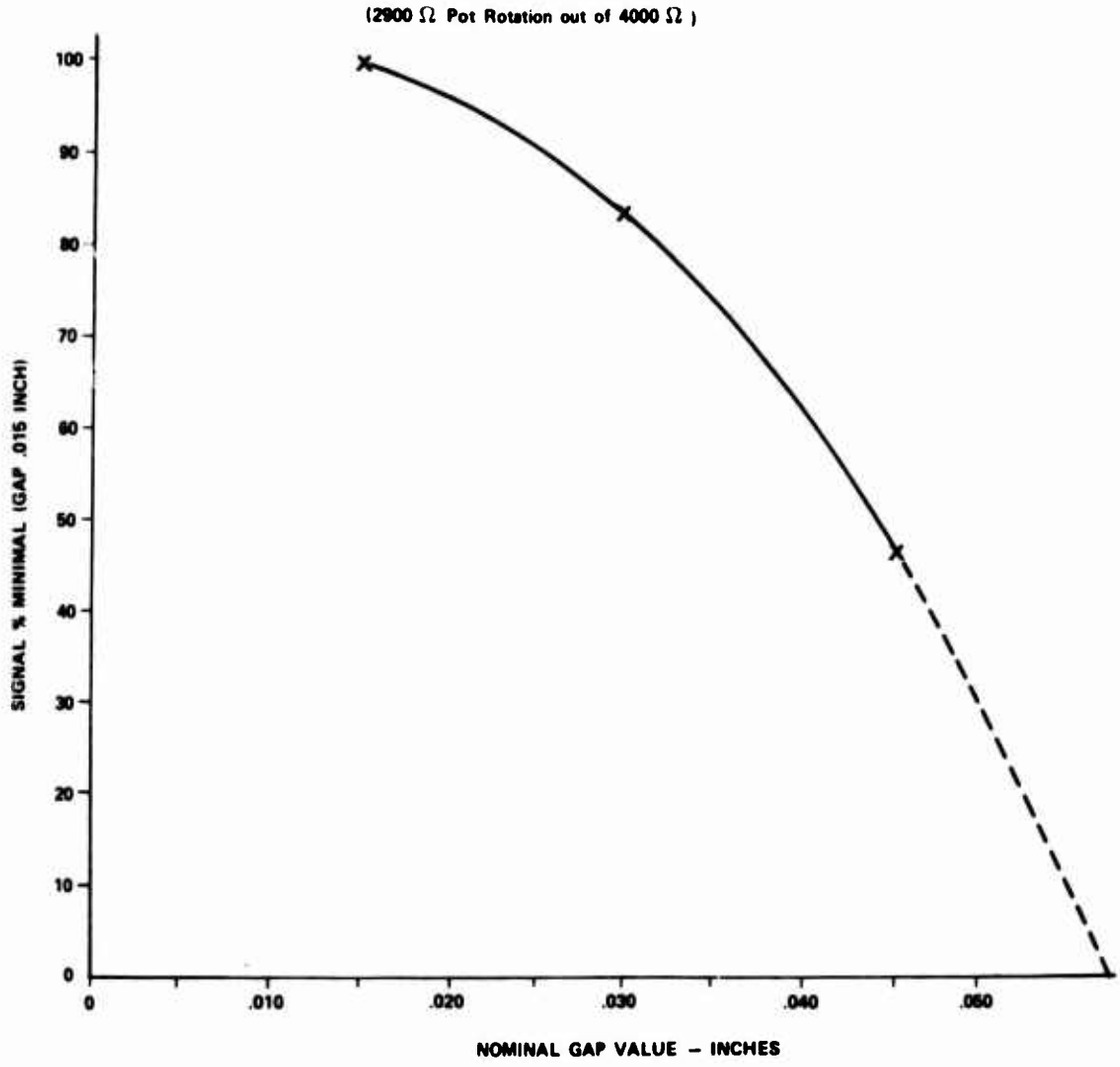

Figure 30. Signal Sensitivity Change Due to Increased Values of Nominal Air Gap.

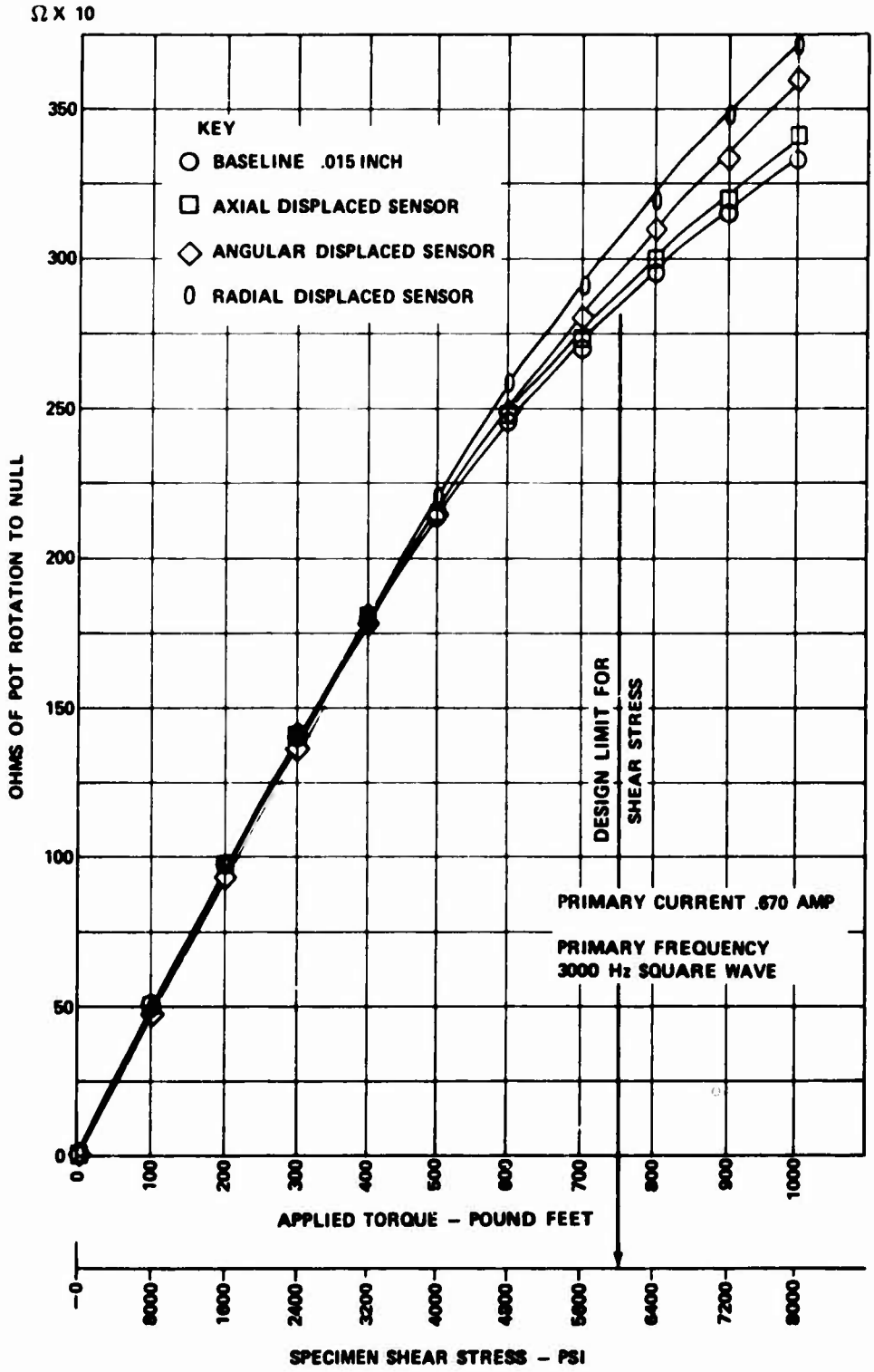

Figure 31. Data Obtained at a Nominal Air Gap of .015 Inch.

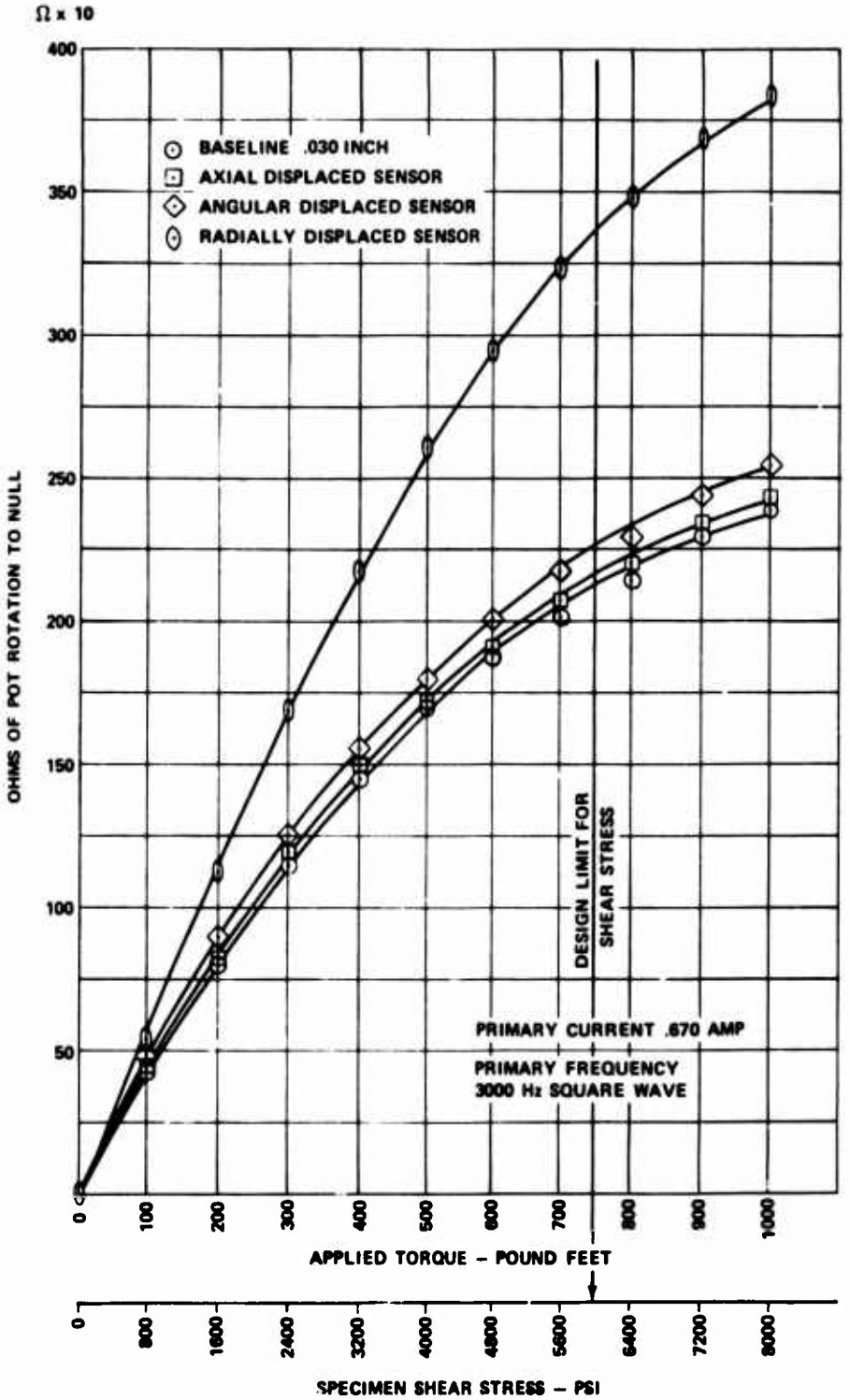

Figure 32. Data Obtained at a Nominal Air Gap of .030 Inch.

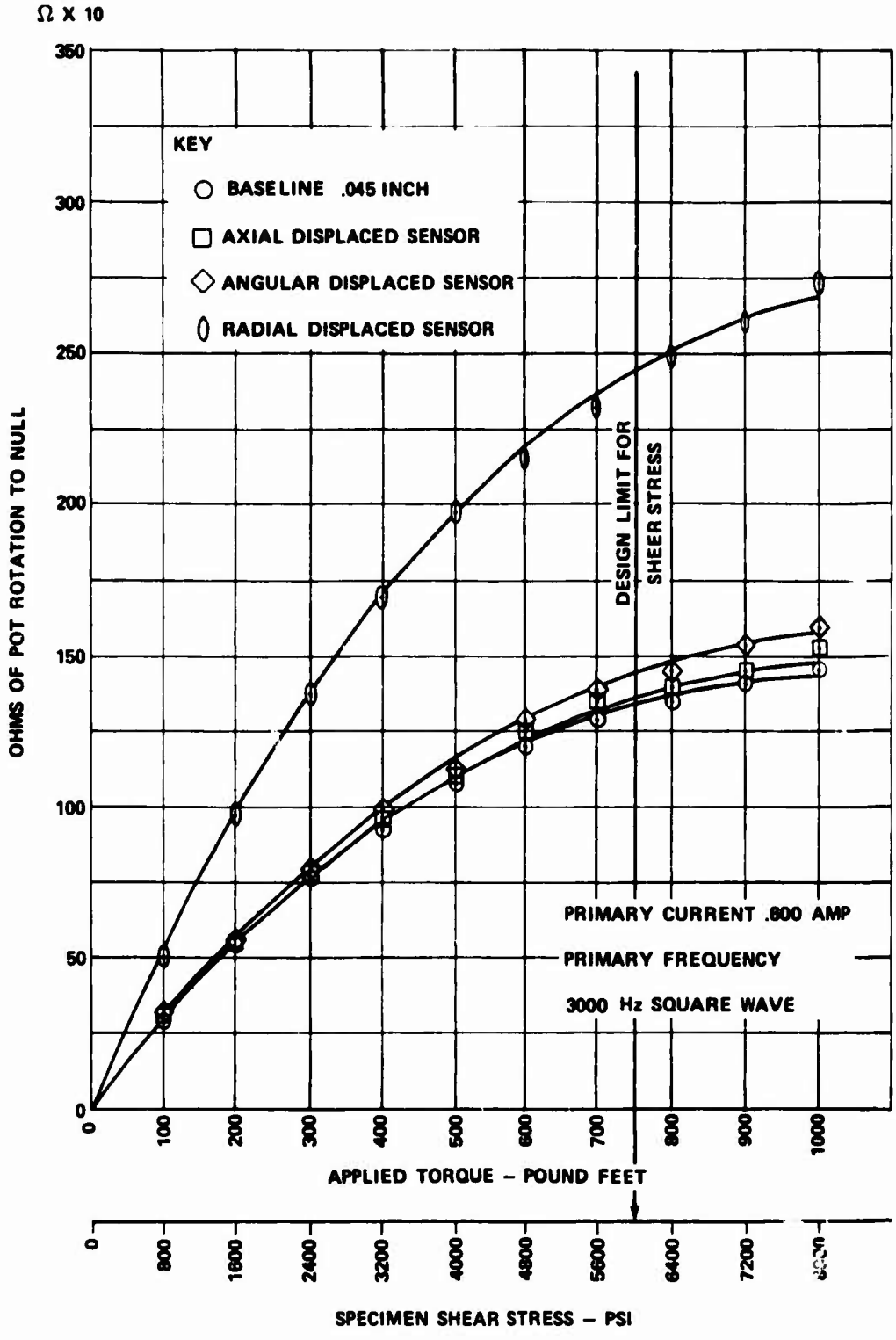

Figure 33. Data Obtained at a Nominal Air Gap of .045 Inch.

The change of sensitivity associated with radial displacement of the sensor was further evaluated to determine if the sensitivity change was in proportion to the value of nominal air gap. This would show if an increased air gap caused more of a sensitivity change for small shaft eccentric motion or if the percentage change in signal was dependent only on the amount of eccentric motion.

For this test, the test specimen with a nominal gap of .045 inch was used as a baseline. The sensitivity change of signal is plotted in Figure 34 for .005-inch radial shaft increments from the shaft centerline. The same information was plotted from data on the shaft with a .015-inch nominal gap and for a .030-inch nominal gap. The plotted data were obtained at a shaft shear stress of 6400 psi. From this curve, it is apparent that the signal sensitivity change is dependent only on the eccentric shaft motion and is not dependent on the nominal gap dimension.

It should be noted that these tests were performed in a static torsional loading fixture. The torque sensor is a device which with the shaft in rotation averages the shear stress around the shaft circumference. The signal sensitivity change as measured during these tests would in effect be cancelled in a dynamic test fixture. The testing was used to establish the optimum value for the air gap, i.e., maximum allowed with good signal sensitivity, and to determine if effects of increased gap dimensions would alter the averaging capability of the system.

From the test data, a nominal .035-inch radial gap was considered as optimum for the system operation. It provided adequate radial clearance between the shaft and pole structures, thereby minimizing the possibility of rub, and retained approximately 90 percent of the signal derived with a gap of .015 inch. The initial .015-inch radial gap was considered to be an absolute minimum for installation around a rotating shaft.

During formulation of the test program, it was initially intended to fabricate a sleeve for attachment to the nonsleeved specimen after the air gap testing. The sleeve was to be fabricated with the air gap clearance determined as nominal at this time. However, because of the nonlinearity, the specimen was heat treated to harden in lieu of the sleeve attachment. It was more significant for the program to determine the cause of nonlinearity, since a sleeved specimen was available, and the air gap tests showed that except for loss of signal,

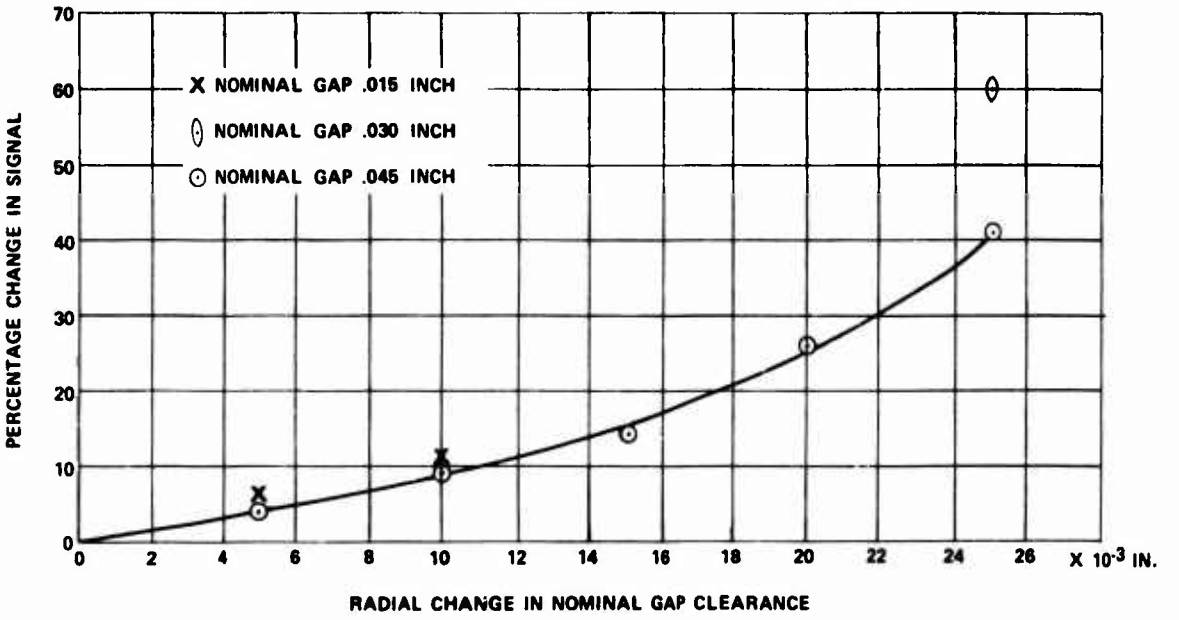

Figure 34. Incremental Air Gap Change Effect on Signal Sensitivity.

no adverse effects occurred with a large air gap.

After the air gap evaluation, the nonsleeved specimen shaft was heat treated to harden the material (heat to 1500°F and quench in oil). After the hardening, the piece was tempered at 300°F and air cooled. The resultant improvement of transfer curve linearity is shown in Figure 35. This figure shows the transfer curve generated on the nonsleeved specimen shaft with a .045-inch radial sensor shaft gap after hardening. The output or signal was obtained from the detector circuit. For comparison, the transfer curve of the sleeved specimen is shown with a .015-inch radial gap and the SAE 9310 material in an annealed condition.

This test demonstrated the effect of hardening the material on linearity correction. For specification of the SAE 9310 material as a magnetostrictive transducer, the surface hardness obtained by the heat treating process was R_c 32-40.

Summary of Testing for Input Parameter Specifications

- The optimum value of input current for the system is established at .670 ampere.
- The optimum frequency of input current is established at 3000 Hz.
- The radial clearance between the shaft and pole structures is determined as nominal at .035 inch.
- The annealed SAE 9310 material displayed a nonlinear transfer curve. After heat treatment to harden the material, the expected linearity of the material was restored.
- Based upon test with the hardened SAE 9310 material, the value of shear stress selected initially in the design of the specimens as a maximum of 5,800 psi is no longer considered as a limiting value.

TESTING TO DESIGN SPECIFICATIONS

To determine the fabricated system performance within the operating environment and load conditions of the design specifications, the following tests were performed:

1. Metal Temperature Evaluation
2. System Temperature Evaluation

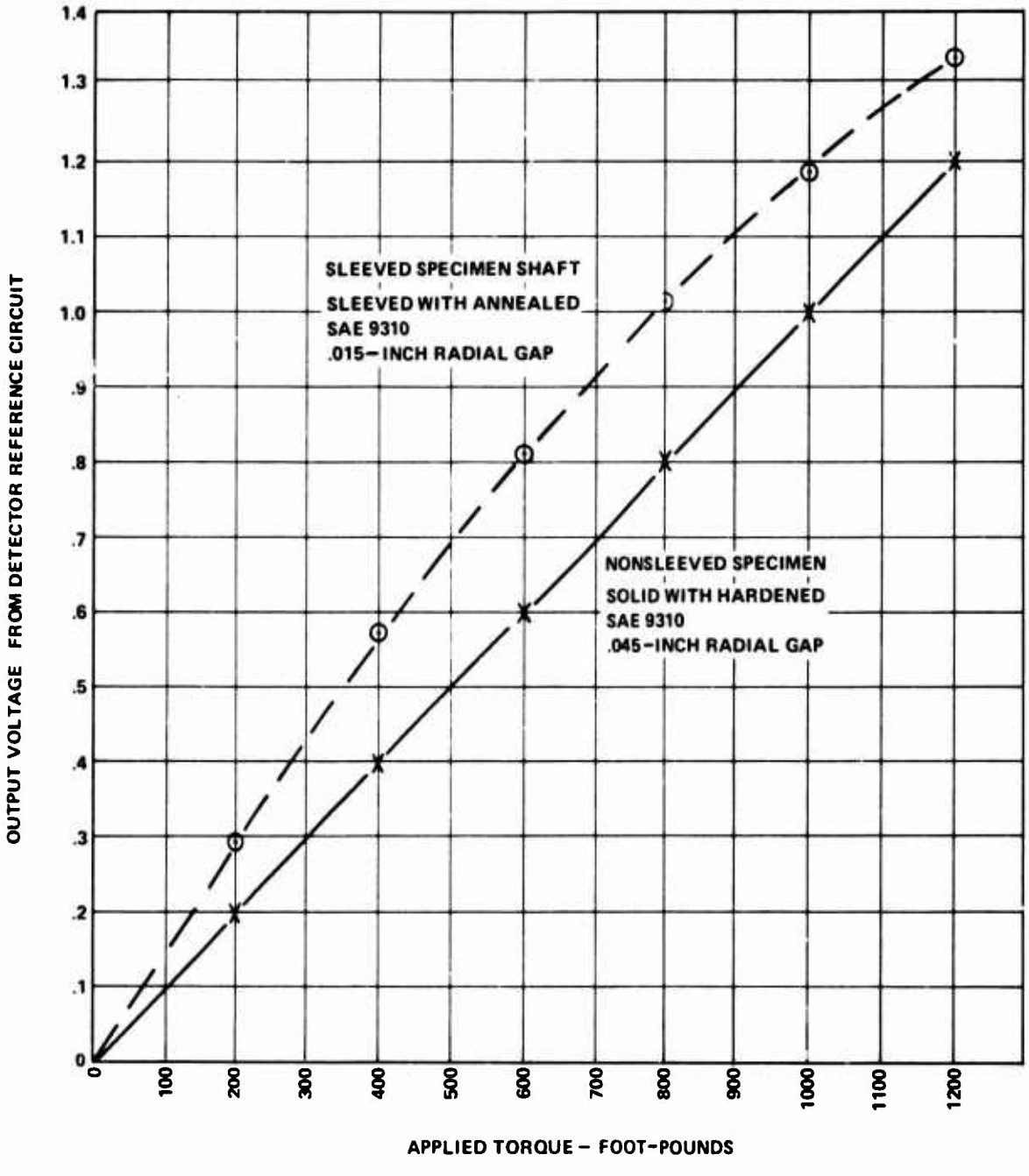

Figure 35. Transfer Curve Linearity Improvement Due to Hardening of the SAE 9310 Steel.

3. Vibration Testing

4. Rotational Testing

Metal Temperature Evaluation

The design specifications require satisfactory torque sensing techniques on shafts having metal temperatures up to 500°F. Testing was to be performed from -35° to +200°F for the evaluation.

Testing on the program system was performed with shaft metal temperature in the range from -35° to +250°F. The 250°F limit was imposed by the test fixture. The test was performed on the nonsleeved specimen shaft and a lamination assembly. No difference in the test results are expected by using either the sleeved or nonsleeved test specimen. This is based upon the depth of magnetic field penetration being limited to approximately .035 inch into the shaft material. The sleeve thickness is .055 inch which assures full penetration of the magnetic field.

Test data was derived as the computed difference of V_T and V_C secondary voltages. Comparison of this data at the ambient temperature condition with the data of Figure 23 shows the improvement in transfer curve linearity obtained by the hardening process.

For control of metal temperature, a temperature-regulated silicon fluid was flowed through the bore of the specimen shaft. This approach was used to minimize the heat transfer to the lamination assembly which encircled the specimen shaft.

The material was in a hardened condition, and the lamination assembly specimen air gap was at .045 inch as measured radially.

Transfer curves on the specimen were generated to 1200 ft-lb of applied torque with the specimen nominal metal temperature at -31°, +70°, and +249°F. The metal temperature was determined by thermocouples placed fore and aft, adjacent to the sensing length, and located at 180 degrees from one another.

Data from the test are shown plotted in Figure 36. To derive the transfer curve sensitivity to metal temperature, the percentage change in signal sensitivity was computed. A torque level of 1200 ft-lb was

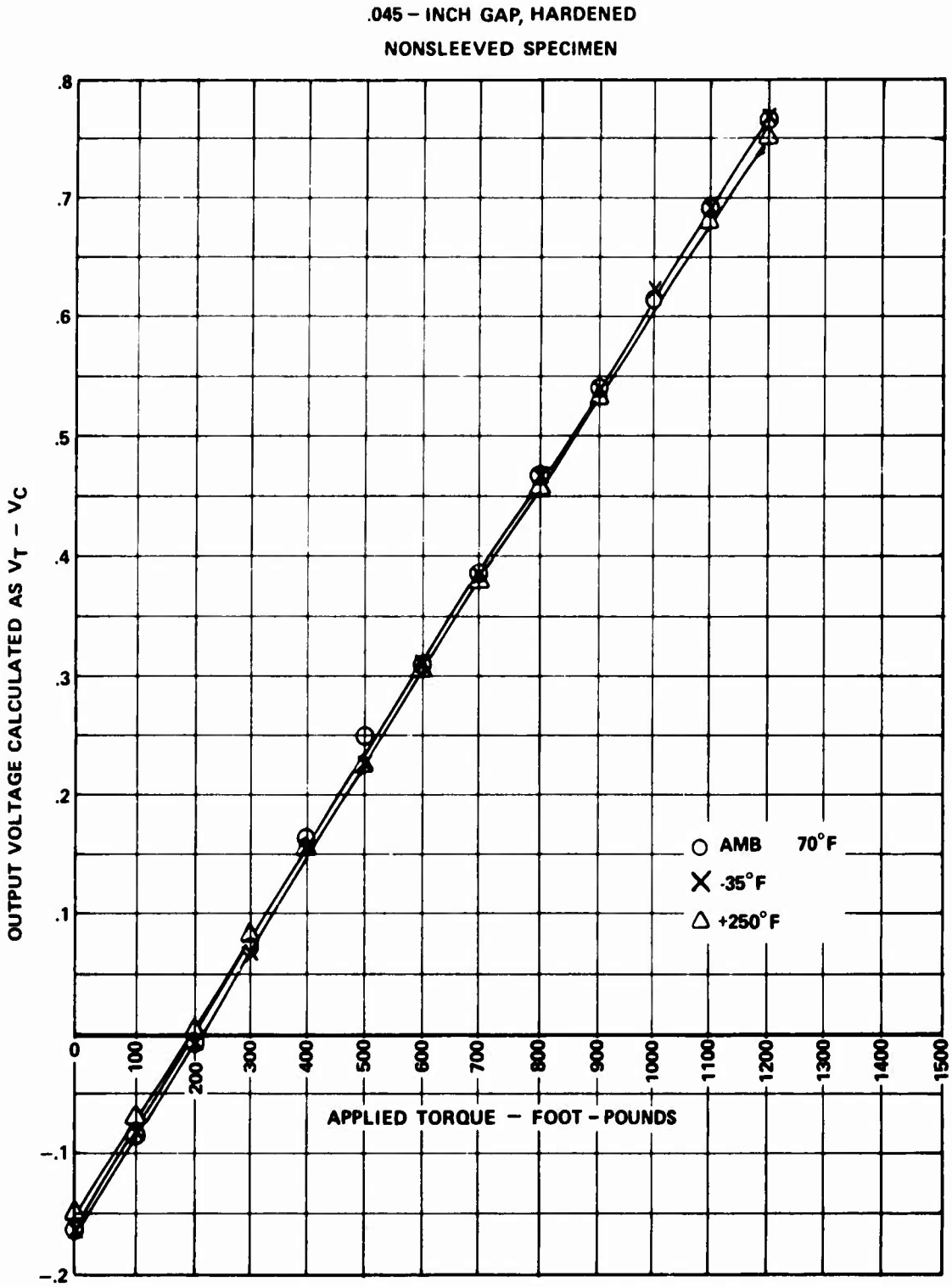

Figure 36. Transfer Curves Generated With Controlled Metal Temperature.

used to determine the sensitivity change at that point. These data are plotted and shown in Figure 37.

System Temperature Evaluation

The design specification requires testing of the torque sensor in an environmental temperature range from -35° to +165°F. Testing for the program system was performed in the range of temperatures from -35° to +250°F.

The test was performed on the sleeved specimen of shaft material, The torque sensor was coupled to the detector circuit, and the output was derived from the reference voltage driven by the servo balance motor. Figure 38 shows the breadboard detector circuit fabricated for this program. The dial indicator (degrees) was used for reference purposes.

Since the resolution of this indicator is not adequate to demonstrate the system accuracy, the ganged potentiometer concept coupled directly to the nulling potentiometer is used. This method has been described in the design section of this report. Figure 39 shows the complete electronics assembly used in the performance test phase. In place of a specifically designed power supply, a square wave generator and power amplifier were used to supply the input excitation parameters. Digital voltmeter readouts were used for accuracy and resolution capabilities for determining the information signal and maintaining a monitor on the input current.

The input parameters were maintained as constant at .670 ampere and 3000 Hz.

The data obtained from this test were taken with the torque sensor temperature points of -35°, 70°, 165°, and at 260°F. Temperature was maintained by encasing the torque sensor in dry ice for the low-temperature tests. High temperatures were obtained by induction heating. The power was disconnected from the heating element when measurements were made.

The change in signal sensitivity at the four temperature points is shown plotted in Figure 40.

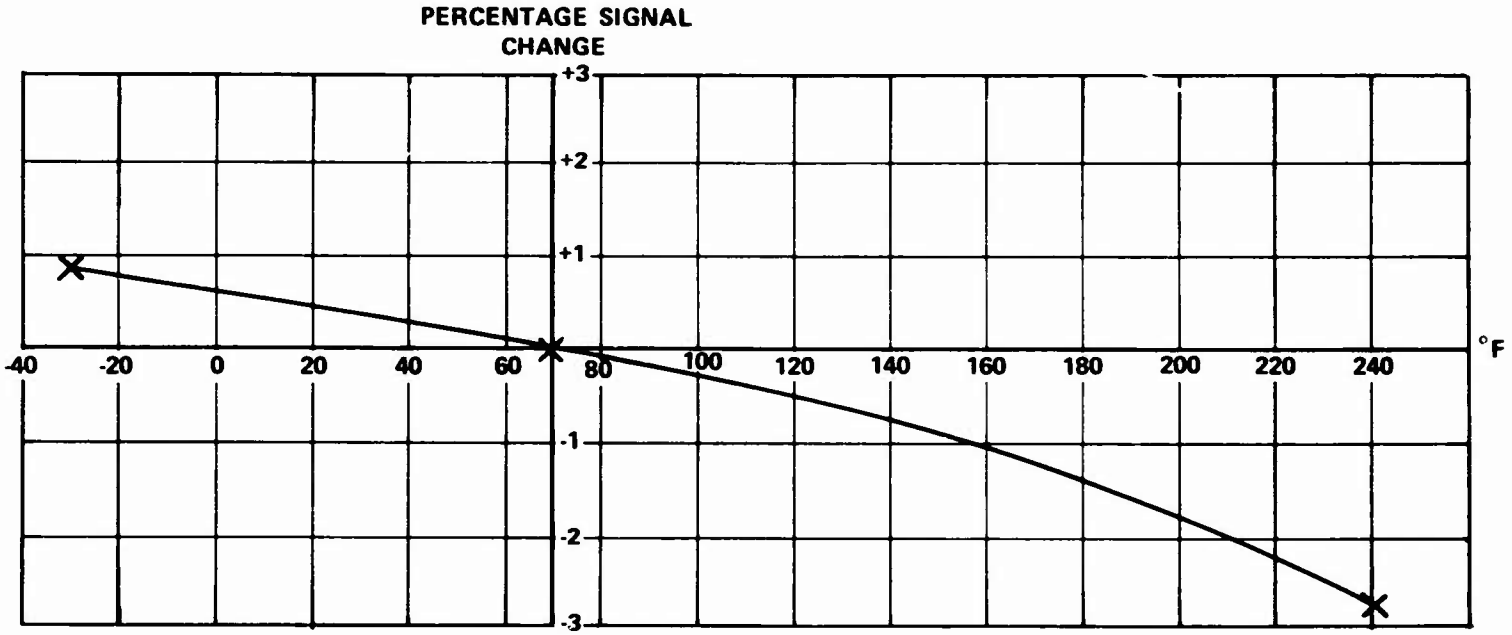

Figure 37. Sensitivity Change Due to Shaft Metal Temperature.

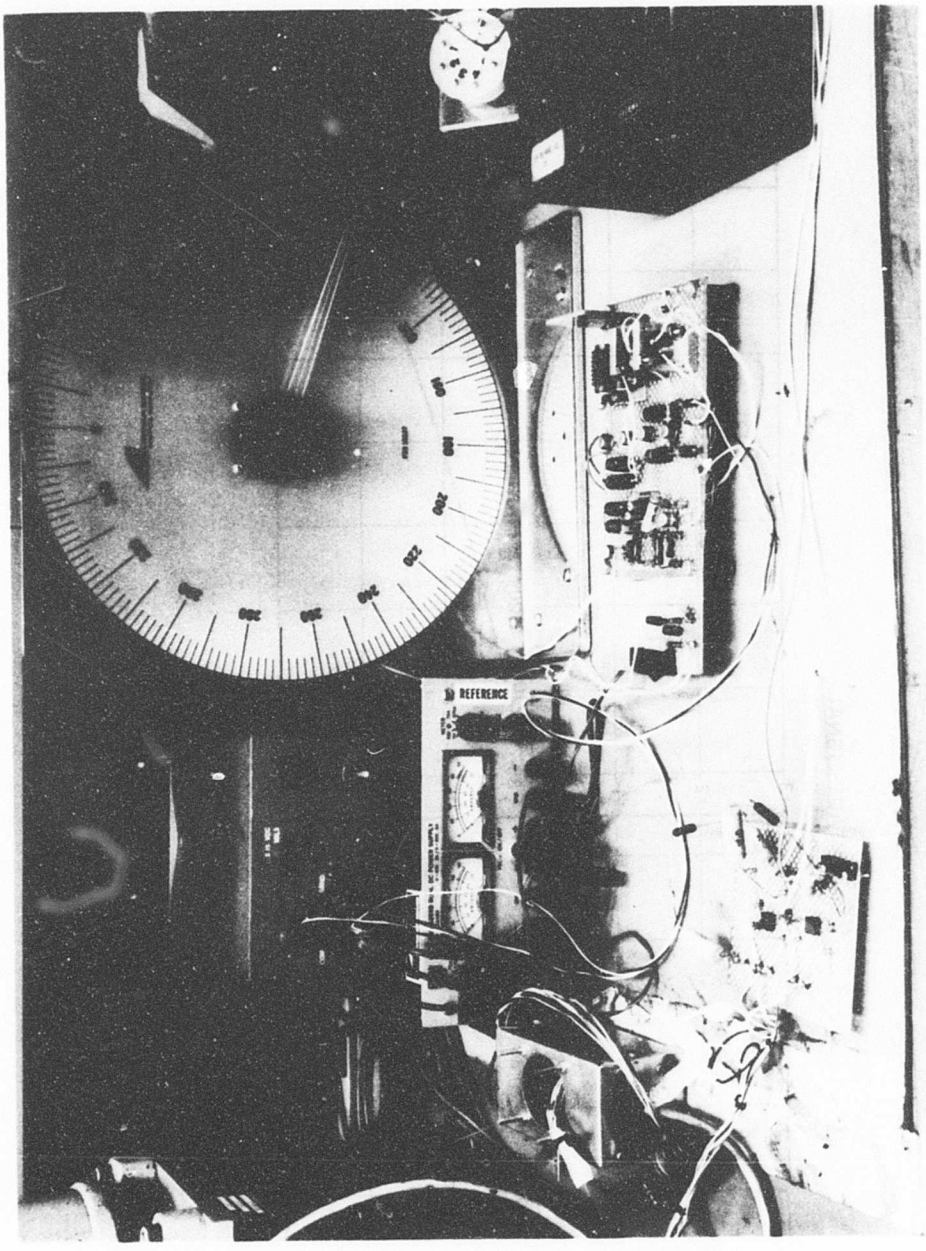

Figure 38. Breadboard Circuit Fabricated for Test Phase of Program.

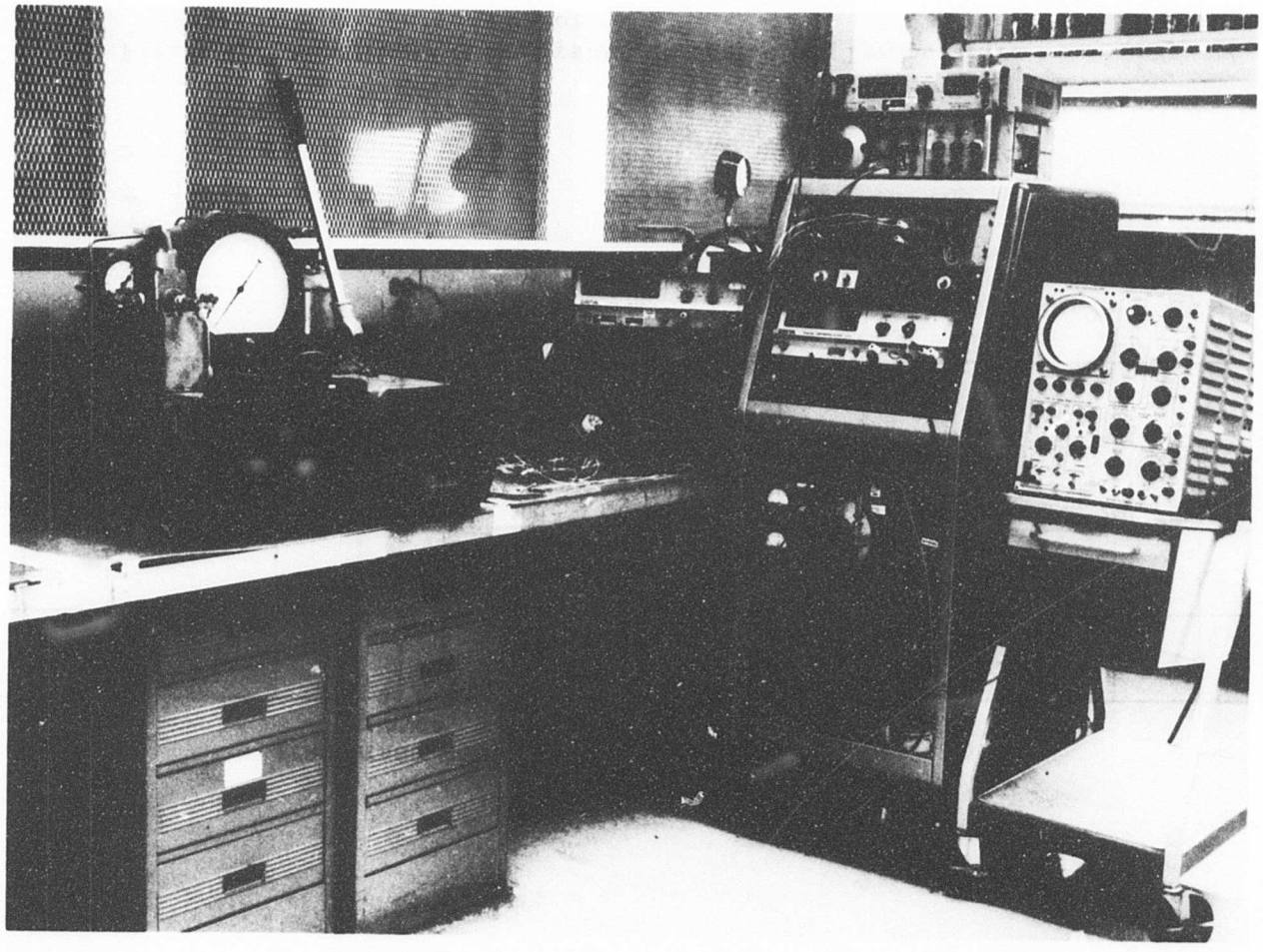

Figure 39. Electronics Assembly for Performance Evaluation.

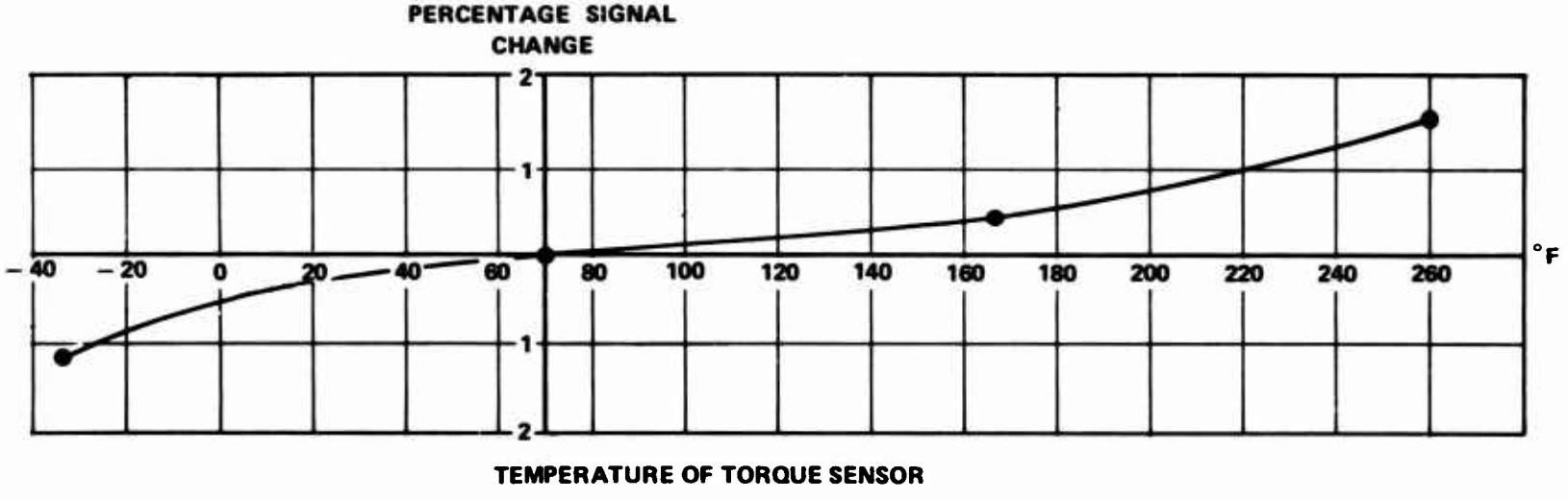

Figure 40. Sensitivity of the System at Controlled Temperature of the Torque Sensor.

Vibration Testing

The design specification requires the torque sensor to be tested in a vibratory environment of 10 to 30 Hz at .2-inch double amplitude displacement and from 31 to 10 kHz at a 10 g acceleration. Testing on the program torque sensor was performed at .2-inch double amplitude displacement from 10 to 31 Hz and between 31 to 3000 Hz at $\pm$10 g acceleration. The load capability of the vibration table did not allow the test to be performed throughout the entire frequency range of the design specification.

The torque sensor, consisting of the sleeved specimen shaft and a lamination assembly, was affixed to a vibration table as shown in Figure 41. Four 15-minute scanning cycles were made between 10 and 3000 Hz for a total of 1 hour vibration time in each plane.

The torque sensor was energized during the vibration scanning cycles. The secondary V_T and V_C coil voltages were monitored continuously to detect malfunction. No malfunction of the torque sensor occurred during the test program.

The lamination assembly from this test was used in a following test in a dynamic torsional loading fixture.

Rotational Testing

The design specification requires satisfactory torque sensor operation in a rotational environment from 7500 to 15000 rpm. Testing on the program system was performed in this speed range. A torque range from 100 to 1000 ft-lb was evaluated.

The test was performed on the nonsleeved specimen of shaft material. The material was in a hardened condition, and the air gap between lamination assembly and shaft was .045 inch measured radially. The torque sensor was coupled to the detector circuit shown in Figure 39. Prior to the start of rotational tests, the torque sensor had been calibrated by use of static torque loads. Calibration accuracy of the static torque system is $\pm$.3 percent. After this calibration, the intact detector circuit was moved to the rotational test site. No changes were made to the electronics which would affect the established sensitivity or balance point of the calibrated torque sensor.

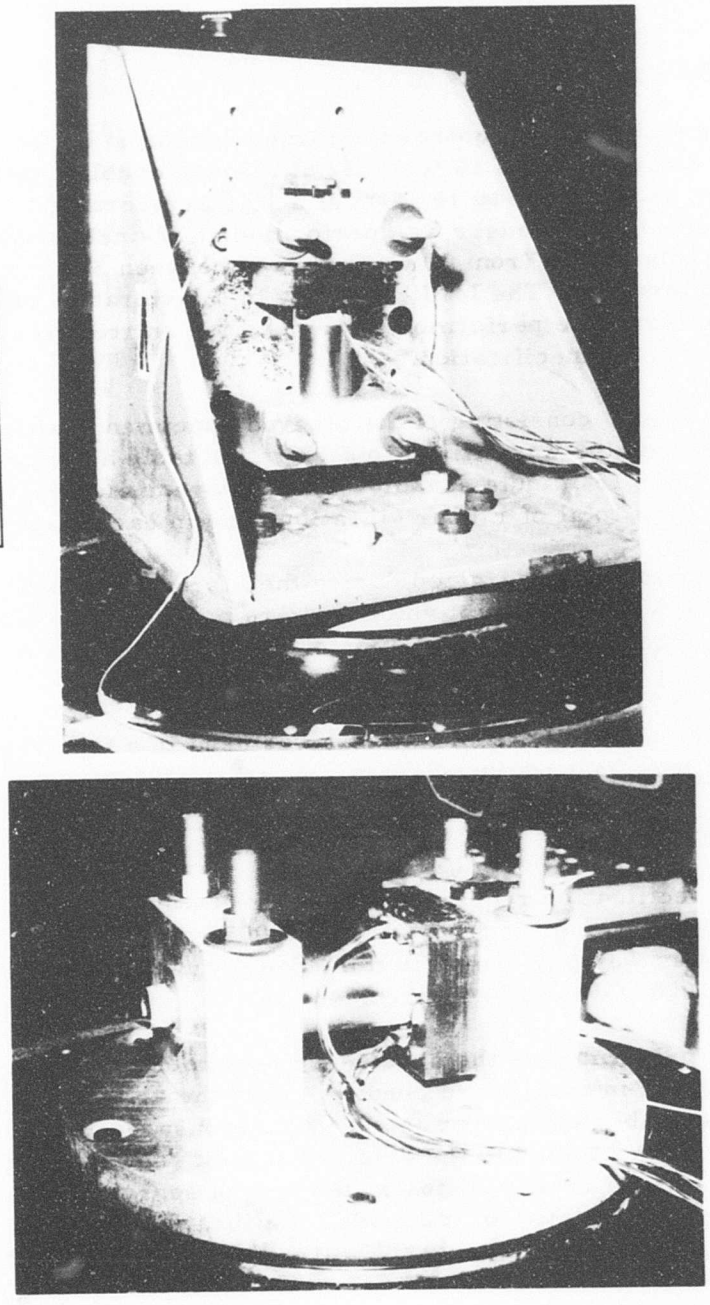

Figure 41. Vibration Test Rig.

For dynamic rotational tests, the torque sensor was coupled between a T55-L-11 engine used as the prime mover and a test cell reference torque system. The reference torque system is interposed between the specimen shaft and a water brake used for power absorption. The reference system has a calibration accuracy of $\pm$. 5 percent of reading in the range of torque tested. The following three objectives were planned from the rotational testing:

1. Determine the calibration coincidence from a nonrotating to a rotational torque sensor

2. Determine the speed sensitivity of the output signal (i. e., does rotational speed induce an error signal)

3. Modify the input parameters if necessary from the optimum values selected during the static tests

The first testing was done to evaluate the calibration coincidence. An incremental ascending and descending torque run was made with the torque sensor and system electronics in the as-received condition from static calibration. The electrical signal from the reference potentiometer was recorded at each point along with the engine torque derived from the test cell reference torque system and the specimen shaft speed. The data from this test are summarized in Table III.

Figure 42 is a plot of the data. For comparison of calibration coincidence, the static calibration of the system is shown as the solid line. The static balance (origin) was deliberately offset to a positive value of reference output voltage. This was done to anticipate a possible shift in calibration that would have caused the dynamic sensitivity to shift below the static value obtained.

The calibration data show no change in calibration sensitivity; i. e., the slopes of static and dynamic calibration lines are the same. The offset of zero (origin) noted for the dynamic system is most probably an effect of alignment differences for the torque sensor as installed in either the static or dynamic loading fixture. Reference to Figures 31 through 34 shows that along with the sensitivity changes for radial gap variations, a shift of origin also occurred. This in effect changed the null position of the detector at the point of zero torque established by the scaling resistors used in the detector for balance. The torque sensor sensitivity is not affected since the torque sensor is an averaging device, and the effect of alignment would not alter the average value of measured stress.

TABLE III. CALIBRATION OF TORQUE SENSOR WITH ROTATING SHAFT

Reference Torque (ft-lb)		Torque Sensor Voltage	Shaft (%)	Speed (rpm)
1*	100	.2561	27.0	4,200
2	360	.5093	73.3	11,300
3	487	.6346	89.4	13,900
4	629	.7649	92.4	14,300
5	767	.8915	93.1	14,300
6	885	1.004	88.0	13,600
7	1035	1.154	101.5	15,700
8	885	1.004	88.0	13,600
9	747	.885	78	12,300
10	484	.639	54	8,350
11	368	.529	49	7,600
12	252	.421	37	5,750

*The number index of data point specifies the sequence of applied torque. This is to identify either ascending or descending runs to determine hysteresis.

To evaluate the speed sensitivity of the torque sensor, the system was retained in the same condition as in the preceding test. A selected value of reference torque was maintained, and the output voltage from the detector circuit was recorded with the specimen shaft at different rotational speeds. The data for three reference torque conditions are summarized in Table IV.

TABLE IV. SPEED DEPENDENCE OF TORQUE SENSOR

Reference Torque (ft-lb)		Torque Sensor Voltage		Shaft Speed (%)	(rpm)
Measured	Standardized*	Measured	Corrected**		
368	375	.529	.536	49.0	7,600
375		.537		67.5	10,400
375		.534		87	13,500
479	488	.636	.645	51.1	7,900
488		.646		105.0	16,300
1039	1047	1.163	1.171	90.0	13,900
1047		1.176		100.0	15,500

*Because of the instability of torque over the speed range, a standardized value is used to calculate a corrected value of torque sensor voltage.

**The corrected value of torque sensor voltage is computed by multiplying the difference in "Measured" torque and "Standardized" torque by the sensitivity of the torque sensor determined from the static calibration as .00097 volt per foot-pound. The value of computed voltage is added to the measured value for the corrected torque sensor voltage. These data (i.e., corrected torque sensor voltage) are used for the plot of speed dependency in Figure 43.

Since the stability of the reference torque system is dependent on the engine operating point, it was not always possible to maintain a fixed value of reference torque. To standardize the data for torque change, the sensitivity derived during the static calibration of the system is used to correct the detector output voltage.

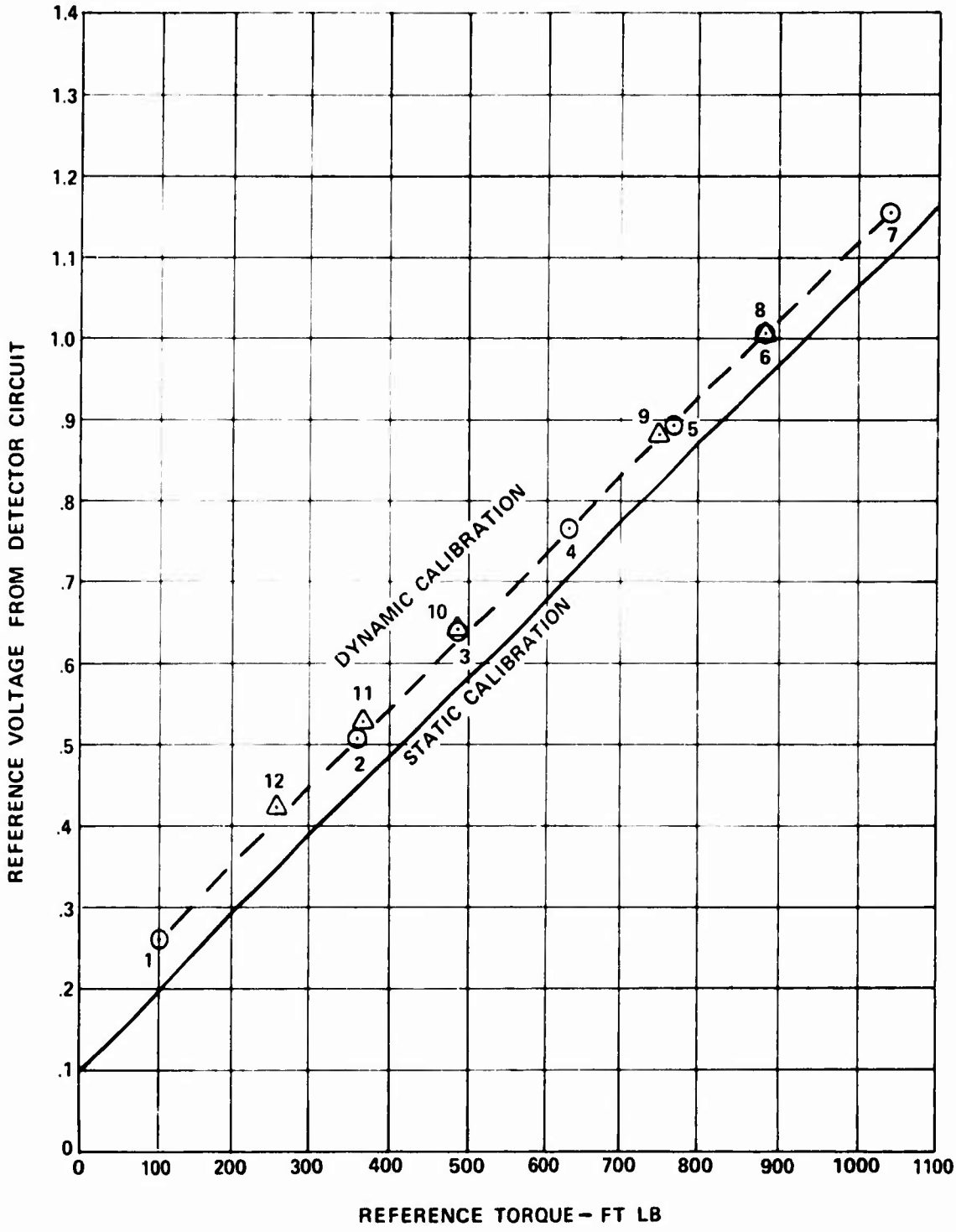

Figure 42. Dynamic to Static Calibration Coincidence.

The correction of .00097 volt per ft-lb was used to standardize the data. The corrected values of output are plotted on Figure 43. From the corrected data at 488 ft-lb, a calculated change in signal sensitivity of less than .2 percent is determined for a range in shaft speed of from 7,900 to 16,300 rpm.

The final test in the dynamic fixture was used to substantiate the choice of input parameter. A selected torque point was held, and the change in signal sensitivity was noted at an increased value of excitation frequency. This data showed no apparent difference in the amount of signal as calculated above.

No further testing was performed on the system, and the statically derived input parameters were considered as optimal for the system operation.

The dynamic testing completed the test phase of the program. The following is a summary of the test results and a discussion of the system concept for an operational system.

Summary of Testing to Design Specifications

The following is a summary from testing of the system in accordance with the design specifications:

1. Increasing the shaft metal temperature reduces the magnetostrictive sensitivity of the torque sensor.

2. A compensatory effect on the reduced sensitivity is provided by an inherent reduction of the air gap when both the shaft and lamination assembly are maintained at the same temperature. The torque sensor did not maintain a calibration accuracy of $\pm$.5 percent in the tested range from -35° to +165°F.

3. The vibratory environment did not adversely affect the mechanical structure of the torque sensor.

4. Static-to-dynamic calibration coincidence was not maintained. The effect noted was that of a change in the null established for the system with no torque on the shaft. Sensitivity of the torque sensor remained coincident. The effect of null shift is felt to be the result of alignment differences in the fixtures. A correction for this would be to devise a procedure by which

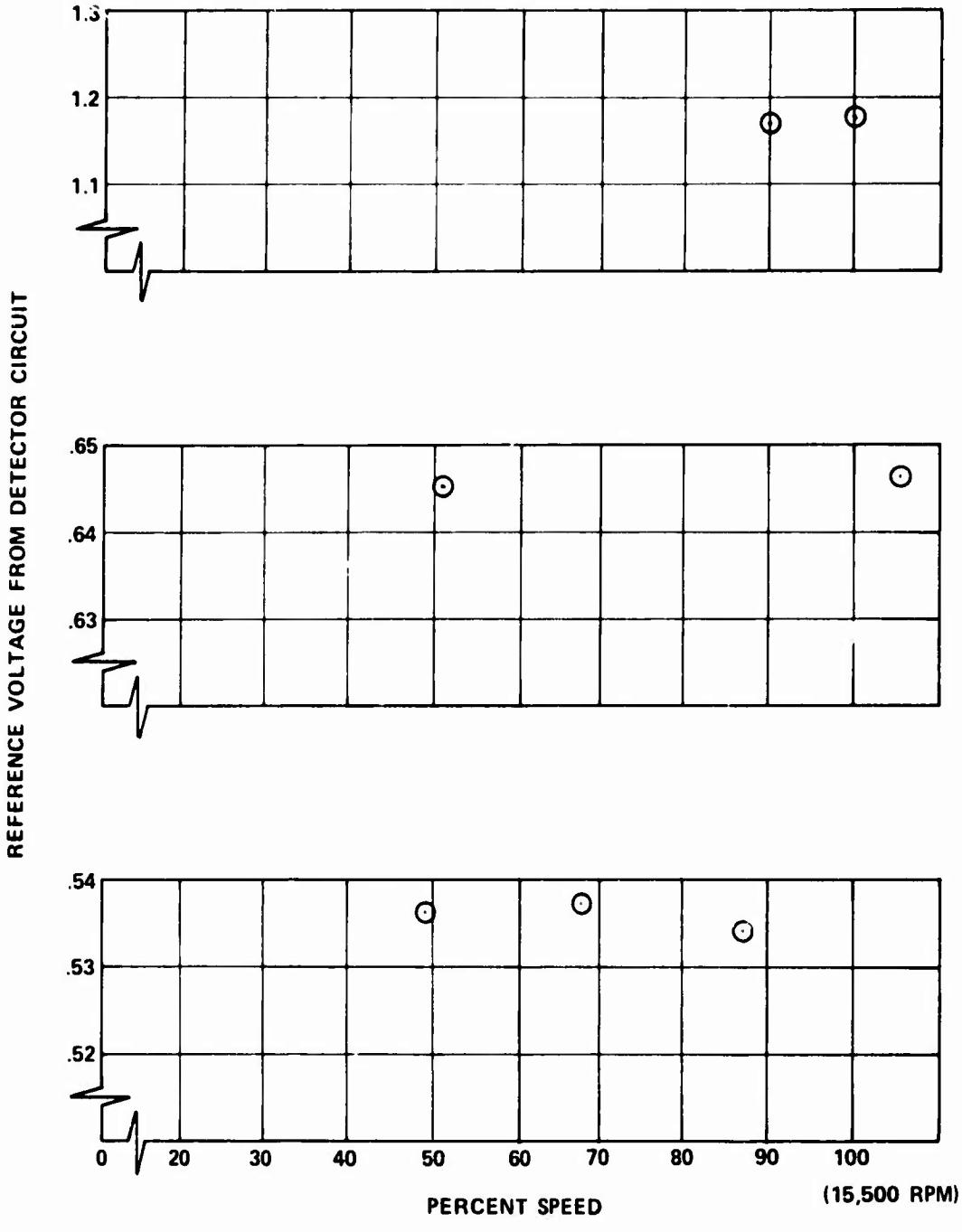

Figure 43. Corrected Data To Determine Speed Dependency of Signal.

the null or no-torque position could be established if the torque sensor were changed from the installation in which it was calibrated. The procedure would require the shaft to be rotated with no torque in the operational installation in which it is to be used.

During this test program, the controls for balancing the detector circuit and the control for establishing the sensitivity were interrelated. This would not be the case in a detector circuit used for an operational system.

5. Speed dependency on the designed system has been established. The range of shaft speed of from 7,900 to 16,300 rpm displayed a change in signal sensitivity of only .2 percent. Since this shaft surface velocity change is excessive for a helicopter engine, the effect of speed sensitivity is considered as minimal.

6. The input parameters derived from static testing of .670 ampere at 3000 Hz for excitation of the torque sensor are considered as optimal.

DISCUSSION OF TESTS

The torque sensor was initially tested in a static loading fixture to determine the SAE 9310 material transfer curve characteristics and an optimum level for operation of the system.

Data were obtained during most of the initial testing with the torque sensor operating in an open-loop system. This was to preclude the possibility of the detector's influencing the torque sensor. Transfer curves generated on both the sleeved and nonsleeved specimen shaft displayed a nonlinearity which was unexpected. It was assumed that the nonlinearity was due to the specimens' being in an annealed condition. One specimen shaft was linearized through a heat treating process to harden the material. This verified the assumption, and a specification on hardness was obtained.

It was also established during this testing that the effect of air gap variations was not a function of the nominal gap value. This allowed the air gap selection to be based only upon the sensitivity of the signal considered for input to the detector circuit.

Data on the system tested in accordance with the design specification were mostly obtained with the torque sensor coupled to the detector circuit. The performance characteristics of the system did not meet the design requirement for all tests. The summation of errors for a temperature range from -35° to +165°F along with the rotational speed error exceeds the allowable error for obtaining a system goal accuracy of ±.5 percent. However, it is felt that the required accuracy of ±1 percent can be obtained with the torque sensor operating in a limited temperature range.

Operation of the torque sensor in an environment with metal temperature to 500°F is not considered desirable. No data was obtained in the test program to fully explore the effect on magnetostrictive sensitivity at this temperature. Further, the requirement for adapting the lamination assembly and coils to temperature is considered detrimental to the system operation. However, it should be noted that the magnetostrictive torque sensor requires a minimum space envelope for installation. This makes it readily adaptable to environmental areas either internal or external to the engine more suited to its operation.

To provide a torque measurement system adaptable to existing gas turbine engines, a test was made to determine static to dynamic calibration coincidence of the system. This test disclosed a shift in the origin of the system from static to dynamic calibration. The problem may be resolved by procedures used when installing the system and in design of the detector electronics.

ANALYSIS

The analysis portion of the program was performed in conjunction with the design and test phases. This approach was necessary since the magnetostrictive torque sensor does not lend itself to analytical evaluation. Data from testing were used to provide empirical evaluation of the system and were also used to provide data for prediction of the system performance when operating in the environment as stated in the design specifications. Where data from testing of the program are used, a reference is made to the test from which they were obtained.

ACCURACY

For performance analysis of the measurement system, the following factors are considered as contributing a percentage of inaccuracy to the total.

1. Shaft metal temperature effect on magnetostrictive sensitivity

2. System operating temperature effect on the sensitivity of the magnetizing force

3. Biasing voltages induced by rotation of the measurement shaft

Therefore, compensation for these effects must be provided by the measurement system. The magnitude of compensation required is derived from the design goal for the system of ± .5 percent accuracy of reading for a torque range of from 30 to 100 percent of the rated value. The following analysis specified the contribution of measurement error attributable to each of the listed factors. The method for compensation is stated, and the summed total of the measurement accuracy when operating in a specified environment is derived.

Shaft Metal Temperature Effect on Magnetostrictive Sensitivity

The effect of temperature on magnetostrictive sensitivity is not predictable from analytical evaluation. From data obtained on metal temperature tests for the SAE 9310 steel, the signal sensitivity decreased by -3.6 percent for the temperature range from -35° to +250° F. Figure 37 shows the data obtained as percentage of signal change versus total temperature. The negative sign indicates the sensitivity decrease. These data are in good agreement with published data (Reference 4) on magnetostrictive temperature sensitivity, which explains an inherent compensatory effect provided by increased magnetic field penetration with increasing temperature.

An extrapolation from the measured results to a metal temperature of 500°F, as stated in the design parameters, places the sensitivity change to approximately -13 percent for a temperature range from -35° to +500°F. Therefore, it is apparent that the inherent compensation provided is not adequate to provide a signal accuracy of ±.5 percent with the metal temperature range in the design specifications.

Further compensation is provided by an unexplained effect with the lamination assembly and shaft at the same environmental temperature. The small package size of the lamination assembly permits mounting of this unit in the same engine location as the shaft. This maintains a minimal temperature gradient between the components to allow full use of the inherent compensatory effect. Test data showed a +1.5 percent change of signal sensitivity for a temperature range from -35° to +165°F. The positive sign indicates a sensitivity increase. Figure 44 shows the percentage change in signal for the two conditions; i.e., shaft metal temperature altering the magnetostrictive sensitivity and a compensatory effect occurring when the torque sensor is at the same temperature. The data are plotted in Figure 44 with a room temperature ambient of 70°F as the origin. The addition of temperature compensation from an external source, such as a resistance element to sense the temperature and control the excitation current, could be used to further reduce temperature-induced error of the system. By assuming a straight-line relationship, the error would be reduced to +.3 percent of reading in the temperature range of from -10° to +210°F.

In the range from room temperature ambient (70°F) to a system operating temperature of +165°F, the signal sensitivity is .0042 percent per °F. Therefore, a significant improvement of temperature compensation can be effected by maintaining the torque sensor in a controlled environment. Such an installation is possible if the torque sensor is in an environment of oil bathing. This is possible with the magnetostrictive sensor because its inherent design requires a limited axial length and minimal diametral clearance surrounding the shaft of measurement.

System Operating Temperature Effect on Sensitivity of the Magnetizing Force

By utilizing the magnetostrictive principle for torque measurement, the requirement for temperature compensation of the primary measurement parameter is eliminated. This results from measured shear stress being an independent function of the temperature environment. However, a secondary effect of temperature, such as change in the magnetic core

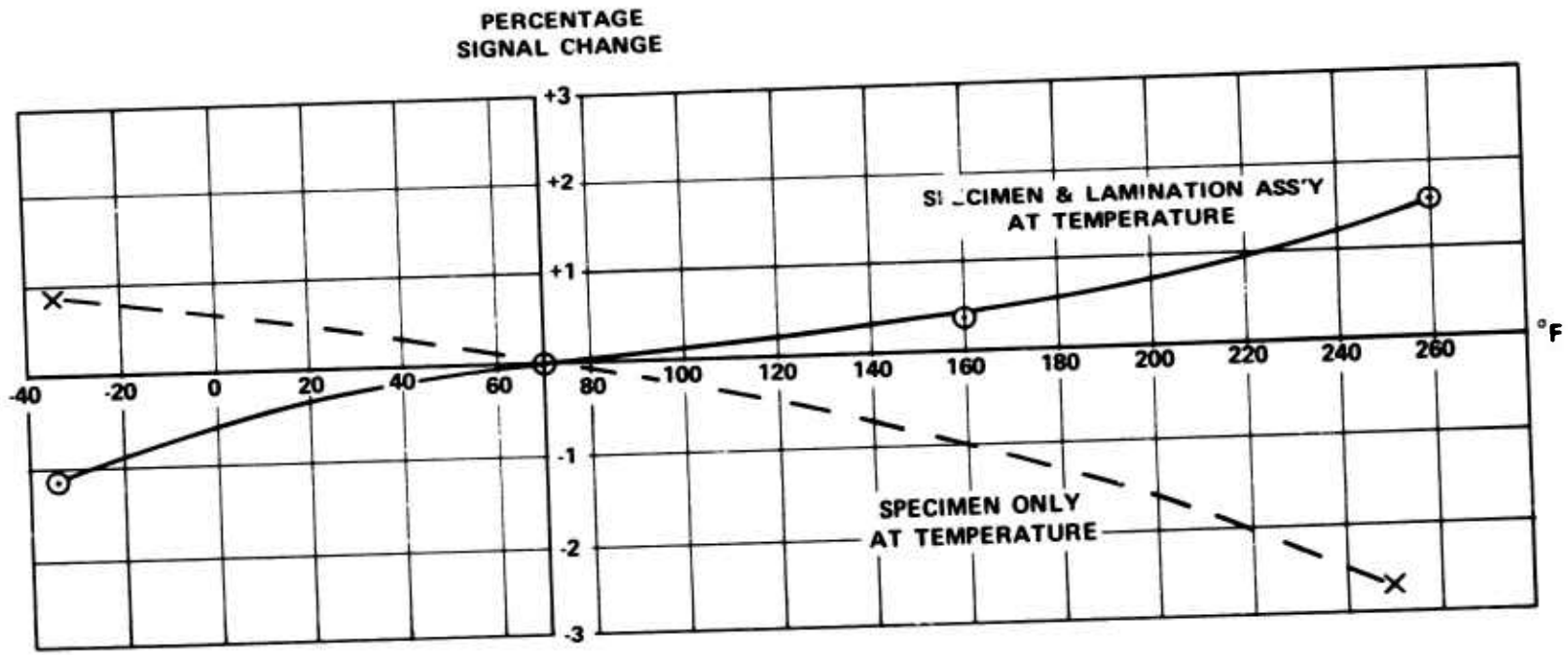

Figure 44. Comparison Data of Temperature Effects.

flux, is a contributing factor to the measurement inaccuracy and requires provisions for compensation.

A requisite to obtaining minimal measurement inaccuracies through changes in the core flux is the ability to maintain a constant value of magnetizing force throughout the operating temperature range of the torque sensor, from -35° to $+165^{\circ}$F. This function, derived from the ampere turn relationship of the primary coils, is temperature dependent. Since the resistance of copper is temperature dependent, the change with temperature affects the current input to the primary coils of the transformer, thereby altering the ampere turn relationship. In the designed system, the copper coil resistance change with temperature from -35° to $+165^{\circ}$F increases the coil impedance by .35 percent. Although the resistance change of the copper coils in the temperature range is significantly greater than this (approximately 50 percent), the high inductive reactance relative to resistance reduces the effect.

By evaluation of the empirically derived magnetostrictive transfer curves on the SAE 9310 carburizing steel, it has been determined that the output signal sensitivity is dependent on the current level used to establish the magnetizing force. Figure 27 shows the sensitivity versus excitation current for both the sleeved and nonsleeved specimens in the test program. If the worst-case condition from the curves of Figure 27 is used (the nonsleeved specimen), we can calculate that the percentage change in output signal is approximately equal to the percentage change of input current. However, by selective choice of the nominal operating value, the effect can be decreased. If we use the current value of .670 ampere as nominal, the change in signal is approximately .1 percent of the change in current for the nonsleeved specimen. For the sleeved specimen, the percentage change is .3 percent for the same current change.

For an operational system, the effect of copper change is not significant since a constant-current power supply is used to excite the torque sensor. The analysis is presented in order to firmly establish the regulation requirement. A consideration for design of the power supply would be the comparative trade-offs in complexity and the cost of the system in comparison with the regulation requirements actually needed.

Biasing Voltages Induced by Rotation of the Measurement Shaft

As with temperature, the shaft rotational speed has no influence on the value of shear stress used for the primary measurement parameter in the magnetostrictive torque sensing system. However,

secondary effects, such as biasing voltages generated as functions of the shaft rotation, provide a contribution to the measurement inaccuracy. Although the exact mechanism of the biasing voltage generation is not understood, a relationship between excitation frequency and surface velocity displacement of the shaft has been established. The following presentation of speed dependency on output signal sensitivity supports the analysis on the torque sensor predicted inaccuracy.

Data taken from a three-primary-pole lamination assembly and a shaft operating from 16,700 to 21,200 rpm show a signal error of .58 percent of reading. For this speed range, the corresponding shaft surface velocity was calculated as ranging from 1530 to 1970 inches per second. An empirically derived equation relating this error to the operating parameters is

$$\text{Percentage signal change} = \frac{K \times \text{surface velocity change}}{\text{No. of poles in structure}}$$

$$\therefore K = \frac{(\text{Percentage signal change}) \times \text{No. of poles in structure}}{\text{surface velocity change}}$$

By substituting the test parameters from above, K is calculated as

$$K = \frac{.58\% \times 3 \text{ poles}}{440 \text{ in./sec}}$$

$$K = \frac{.0039\% \text{ poles}}{\text{in./sec}}$$

$$\therefore \text{P.E.} = \frac{.0039\% \text{ poles}}{\text{in./sec}} \times \frac{\Delta \text{ surface velocity}}{\text{No. of poles}}$$

where P.E. = percentage error
Δ = change of surface velocity

This equation was tested on a second production system of a Lycoming torquemeter operating at shaft speeds from 7500 to 15,000 rpm. The corresponding surface velocity range was 695 to 1390 inches per second. From this information, the calculated error in signal is determined by

$$\text{P.E.} = \frac{.0039\% \text{ poles}}{\text{in./sec}} \times \frac{695 \text{ in./sec}}{3 \text{ poles}}$$

$$\therefore \text{P.E.} = .9\%$$

The actual change in signal measured for this test was .7 percent, which is in accord with the calculated value. No attempt was made to modify the derived K value since the calculated error represents a worst-case condition in comparison to the measured value.

By evaluating the system error as a function of rotational speed versus excitation frequency, the measured error at an input frequency of 6000 Hz was compared to error obtained from calculation. The derived K value was obtained on a system operating at 2000 Hz excitation frequency. The measured error for the same range of surface velocity change was .3 percent as compared to a calculated error of .58 percent. The derived equation was modified to incorporate the effect of excitation frequency and is now stated as

$$\text{P. E.} = \frac{.0039\% \text{ poles}}{\text{in./sec}} \times \frac{\text{surface velocity}}{\text{No. of Poles}} \times \frac{f}{f + \Delta f}$$

where f = excitation frequency

Δf = frequency of excitation minus the 2000-Hz initial frequency used to derive the value of K

If we substitute the excitation frequency of 6000 Hz into the equation, the multiplier dependent on frequency is calculated as

$$\frac{f}{f + \Delta f} = \frac{6000}{6000 + 4000} = \frac{6}{10}$$

Therefore, the calculated error is .35 percent, which is within measurement accuracy of the actual value (.3 percent).

The modified equation is used to predict the measurement error for each of the three parameter ranges in the system performance parameters. For each system, a 2-inch-diameter shaft is assumed for determining the surface velocity, and the range is determined from 50 to 100 percent of the maximum speed. A four-pole sensor operating at 3000 Hz is used for the calculations. The equation for calculation is

$$\text{P. E.} = \frac{.0039\% \text{ poles}}{\text{in./sec}} \times \frac{\Delta \text{ surface velocity}}{4 \text{ poles}} \times \frac{3000}{3000 + 1000}$$

$$= .00073\% \times \frac{\Delta \text{ surface velocity}}{\text{in./sec}}$$

System I

Speed Range
3000 to 6000 rpm [Change in surface velocity (Δ) = 314 in./sec]

Calculated P.E. = .235%

System II

Speed Range
3300 to 6000 rpm [Change in surface velocity (Δ) = 345 in./sec]

Calculated P.E. = .259%

System III

Speed Range
13,000 to 26,000 rpm [Change in surface velocity (Δ) = 1360 in./sec]

Calculated P.E. = .9945%

REPEATABILITY

Performance analysis is also dependent on the ability of the system to provide a repeatable signal in an operational environment. Separation of the factors which contribute to either measurement accuracy or measurement repeatability is based upon: (1) accuracy is a predictable effect due to the known magnitudes of the influencing conditions, and (2) repeatability is affected by unknown magnitudes or instability of the conditions and is considered as altering the system in a random manner. The factors that affect signal repeatability are:

1. Secondary coil voltages V_T and V_C as affected by variations of the input excitation parameters; i.e., excitation current and frequency

2. Sensing of torsional shear stress in a shaft subjected to additional stress components from thrust and bending loads

3. Variations in the core flux density by variations in the air gap induced through changes in relative alignment between the stationary lamination assembly and the shaft

Secondary Coil Voltages as Dependent Functions of the Input Parameters

Since the transformer-induced secondary voltages are proportional in magnitude to the excitation current and frequency, any variations of the input parameters will affect the signal repeatability. These variations are considered as drift in value from the nominal or by difference from nominal between similar units. The differences resulting from manufacturing and component tolerances are established by a comparative trade-off between unit cost and required operating capability.

The magnitude of induced secondary coil voltages is in direct proportion to the value of input excitation current. To eliminate the effect of change in input current from deriving a variable false information signal, the circuit concept of a bridge detector is used. Since the magnitudes of V_T and V_C are in equal proportion to the value of primary current (I_P), any change of I_P will alter the values by an equal amount and of the same sense. In the bridge detector, the null position is established independently of the magnitude in V_T and V_C voltages and therefore is not affected by equal change. However, the magnetostrictive sensitivity of the torque sensor alters the V_T and V_C voltages in opposite sense and of unequal magnitude. Therefore, a current regulation to obtain signal repeatability is required.

During the evaluation on transfer curve sensitivity of the SAE 9310 steel, the relationship of magnetostrictive sensitivity to input current was established. For the nonsleeved shaft specimen, a region of minimal sensitivity variation was noted in the range from .600 to .700 ampere of input current. Figure 27 shows the signal sensitivity to input current.

This data showed that a .1 percent change of signal could be maintained by 1 percent current regulation.

The frequency regulation obtained from data on Figure 28 would be 3.3 percent to limit the signal variation at .1 percent.

Stress Differentiation

For the magnetostrictive torque sensor, which uses a shaft subjected to stress components from other than torsional loads, a method for selective sensing of the measurement parameter, shear stress, is required. Since the magnitude of the unwanted stress components is not known, a method for compensation of the effect based upon a known relationship of stress orientation in the shaft is used.

In a shaft subjected to thrust loads, the resultant stresses would be oriented in the long direction of the shaft axis, i.e., axial stresses. Since the magnitude and direction of these stresses, either tension or compression, would alter the material permeability by a like amount around the shaft circumference, their effect would be to alter the secondary coil voltages V_T and V_C by a like amount. The effect of bridge detector null being an independent function of the voltage magnitude provides the compensation for thrust loads.

Bending forces applied to the shaft do not induce stresses of equal magnitude and sign in the axial planes of sensing as defined by the fore and aft positioning of secondary poles relative to the primary poles.

The magnitude of stress on the shaft circumference is dependent on the distance from the neutral axis, and the sense of stress is dependent on surface shape of measurement, i.e., tension on the convex surface and compression on the concave. Therefore, to be compensated by the measurement system, a diametrical position of the opposing secondary coils is used. On the convex surface, the two secondary coils, coupled to a primary coil and oriented to sense compressive shear stress, are connected by the series aiding wiring configuration with two of the coils on the concave surface. Therefore, an algebraic addition of the two voltages effects a cancellation to the sum. This same concept is applied to the secondary coils of tensile shear stress. The result is to effectively cancel bending stresses by symmetrical adding of voltages, equal in magnitude but opposite in sign, around the shaft.

To maintain symmetry, the manufacturing tolerances are imposed on the pole locations. In manufacture of the lamination assembly, an angular tolerance of 2° is considered acceptable without adding to manufacturing costs.

If the difference in stress of diametrically located secondary coils is used in the calculation,

$$\sigma_T - \sigma_C = \frac{Mr}{I} \quad (1 - \cos \theta)$$

it is derived that a $\pm$ 1 degree angular tolerance will result in cancelling of 99.5 percent of the voltages from bending. Since the bending stress magnitudes are not known and are considered as variable, an absolute value for percentage of repeatability is not established.

ADAPTABILITY

The features that make this system design readily adaptable to gas turbine engine installations are:

1. No contact of rotating parts is required. This provides an inherent increase of the torque sensor reliability and reduces the maintenance requirements.

2. A fixed geometry and size of sensor lamination assembly can be adapted to aircraft/engine installations of different torque ranges.

3. A split ring arrangement is used for the sensor lamination assembly. This facilitates the installation of the assembly around installed shafts.

4. A sleeved assembly provides for attachment of the selected magnetostrictive material to shafts fabricated of other than this material.

5. The axial length and the outside diameters of the lamination assembly are determined by the shaft outside diameter. The small envelope allows installation either internally of the engine or externally surrounding an extension of the power output shaft.

The estimated envelope dimension and weight of an operational system fabricated for an aircraft-engine installation are:

1. Torque Sensor (of four-pole geometry and including a housing for mounting of the sensor to an engine structure)

O. D.	4.00 inches
Length	2.25 inches
Weight	3.0 pounds

2. Indicator (including the packaging arrangement for mounting of the detector circuit and the power supply in the same unit)

O. D.	3.00 inches
Length	6.50 inches
Weight	8.00 pounds

Because of its small space requirements, the torque sensor is readily adaptable to an installation in an engine at a location in a suitable temperature environment. In an operational three-pole system for the Lycoming production engines, the torque sensor is mounted at the engine output around the power output shaft. At this location the operational temperature environment is limited to below 300°F. If the torque sensor had been mounted in the exhaust section of the engine, in a cooled bearing package, the temperature environment would have been between 400° and 450°F.

The advantages of locating the torque sensor in the cooler location are: increased reliability, lower costs, and accessibility.

A further advantage of the small space requirement is the feasibility of installing the torque sensor external of the engine rather than internally. This can be accomplished by mounting the torque sensor on an engine inlet cover plate and sensing the shaft torque from the shaft which couples the engine to the aircraft transmission or gearbox.

The following analysis is used to demonstrate a system design that standardizes the signal output of the system and permits adaptation of the system to shafts fabricated from materials which do not display suitable magnetostrictive properties.

For the program evaluation, a shaft of 2-inch OD was selected for the test specimen. With this diameter shaft and the design specifications of torque, a fixed-size lamination assembly can be fabricated to provide a standardized electrical output. Specifically, the design specifications of torque are:

1. 75 - 250 ft-lb
2. 250 - 725 ft-lb
3. 100 - 300 ft-lb

By using these torque ranges and establishing the shear stress maximum of 5,800 psi at 725 ft-lb, the shear stress to torque relation in the three ranges becomes:

Torque Range (ft-lb)	Surface Shear Stress (psi)
75-250	600-2000
250-725	2000-5800
100-300	800-2400

By equalizing the value of shear stress at 5,800 psi for the three torque ranges through adjustment of the shaft ID, the electrical signal output of the system can be standardized in units of percentage torque. This is possible with the linear magnetostrictive transfer curve of the SAE 9310 material. The shaft parameters that equalize the shear stress are as follows:

Torque Range (ft-lb)	Shaft OD (in.)	Shaft ID (in.)	Shaft Polar Moment of Inertia ($in.^4$)	Shaft Surface Shear Stress (psi)
75-250	2	1.810	.520	1,930-5,800
250-725	2	.894	1.510	2,000-5,800
100-300	2	1.740	.620	1,930-5,800

A limiting factor to this method of shear-stress adjustment may be the integrity of mechanical design for a shaft of a thin-wall section. To increase the shaft wall thickness and still maintain the limiting value for maximum shear stress with the OD fixed at 2 inches, a cylindrical sleeve can be attached to the shaft in the area of torque sensor measurement.

To demonstrate the feasibility of sleeve assembly, a design is presented for a shaft of 1-inch bore with a sleeve attached. The 5,800-psi shear stress is maintained on the sleeve OD, which remains fixed at 2 inches. The torque range from 75 to 250 ft-lb is used for the example since it adapts the worst-case condition in the three given torque ranges.

By consideration of two cylindrical shafts constrained to twist through the same angle, it can be equated that the shear stress (τ) on the surface of the outer cylinder is determined by

$$\tau = \frac{T_r}{J_T}$$

where T = applied torsional moment
r = radius to outer cylinder surface
J_T = sum of the two-cylinder polar moments of inertia

when the lengths and shear modulus of rigidity for the two cylinders are equal.

By using this relationship and substituting with the parameter values of

T = 250 ft-lb = 3000 in.-lb, the maximum value for applied torque;
τ = 5,800 psi, the desired shear stress at maximum torque;
r = 1 inch, the radial distance to the outer cylinder surface;

the equation for the polar moment of inertia of the shaft sleeve assembly is

$$J_{shaft} + J_{sleeve} = .517 \text{ in.}^4$$

If we use a value of sleeve thickness determined from prior experience with magnetostrictive torque sensors as providing a sufficient wall thickness for magnetic field penetration, the sleeve polar moment of inertia is calculated as

$$J_{sleeve} = \frac{\pi}{2} (r_o^4 - r_i^4) = .335 \text{ in.}^4$$

where r_o = 1 inch
$r_i \neq .945$ inch

By substituting this value in the equation and solving for the shaft radius dimensions, the equation is

$$r_{o\ shaft}^4 - r_{i\ shaft}^4 = .116 \text{ in.}^4$$

If the value for shaft inner radius of .500 inch is used, the outer radius is calculated as

$$r_o = .930 \text{ inch}$$

With these parameter values and the shaft-sleeve concept, the shaft wall thickness has been increased from .095 to .430 inch. Figure 45 depicts the design concepts for both methods of obtaining a desired shear stress at maximum torque range.

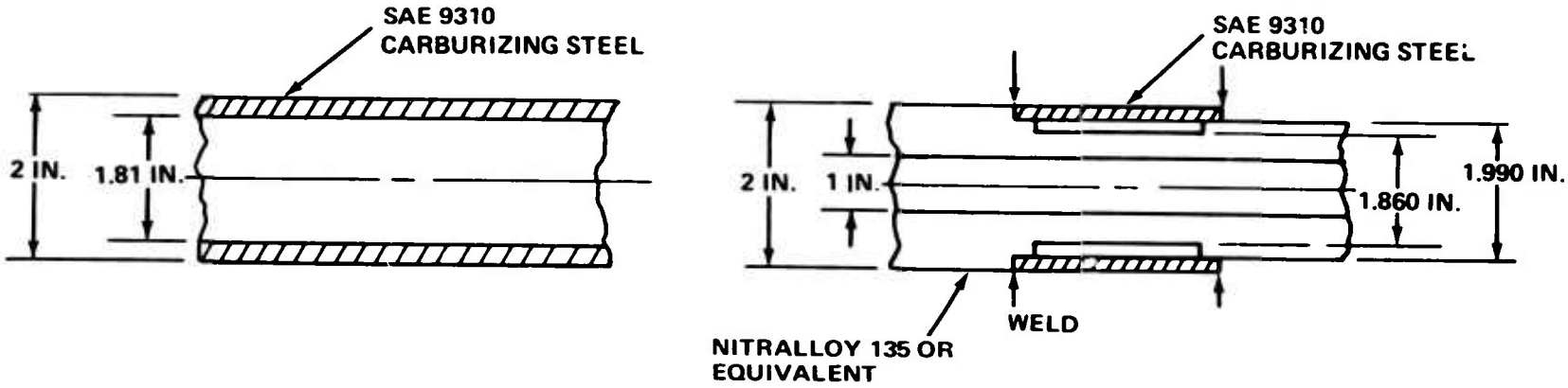

Figure 45. Sleeved and Nonsleeved Design With Adjusted Shear Stress.

Although the sleeve design presented is for adjustment of shaft shear stress, another concept of the sleeve attachment is of significant importance in the adaptability analysis. As stated earlier, the SAE 9310 steel after carburization is suited for engine shafting under limited temperature conditions. This limitation is imposed by a decarburizing effect which would occur at temperature above this limit (Reference 5). In practice this material when carburized is limited in operating environments to temperatures below 300°F. To utilize the SAE 9310 material after carburizing in the environment above 300°F, the sleeve concept can be utilized. To demonstrate this concept, a portion of the test program utilized a shaft sleeve assembly where the shaft was fabricated of a nitralloy 135 material with an attached sleeve of SAE 9310. Electron-beam welding is used to fasten the sleeve of SAE 9310 material to the nitralloy base material of the shaft. These steels are representative of the quality grades of steel used in aircraft gas turbine engines. The high quality steels used in gas turbine engine shafts are not among the materials listed in Reference 6 as not being adaptable to the electron-beam welding process. Figure 3 shows the shaft assembly. The nitralloy 135 material was selected for the base material of the shaft since it is suited to operating environmental temperatures in excess of the 500°F limit in the design specifications. In this assembly, the SAE 9310 carburizing steel is not used as a bearing or coupling member, and therefore need not be carburized as would be necessary to surface harden the material for use as a gear or spline.

By this approach, the torque sensor magnetostrictive material, i.e., SAE 9310 steel, can be adapted to shaft configurations which exceed the temperature limits for operation of a carburizing material.

The preceding analysis of shear stress adjustment and shaft modification for the attachment of the magnetostrictive material was used to demonstrate the ability of the system to provide standardization. This is a concept for logistics control whereby the torque measuring systems of different Army helicopters could be supplied from a common source. The lamination assembly design of pole orientation and dimensional requirements can, if required, be individualized for each installation. However, by standardizing the shaft OD, a fixed-size lamination assembly can be designed for the systems of the torque ranges of the design specifications.

MAINTAINABILITY

The minimum maintenance requirements for the new magnetostrictive torque measuring system developed under this program were established by concepts conceived during the design phase of the system.

These concepts are:

1. Assurance of long life for engine components of the system without routine maintenance or overhaul

2. Provisions for a self-check facility of the torque system to establish a confidence level for the complete operational system

3. Establishment of a standardization procedure to allow free interchange of the aircraft electronic components in the system without degradation of accuracy

To provide a torque measuring system capable of displaying the design specification accuracy, the complete system must be factory calibrated as a unit. Since the magnetostrictive torque measuring system is independent of shaft rotational speed for operation, this calibration can be performed during manufacture, in a static loading fixture, capable of establishing the desired reference torque accuracy. At the time of this calibration, the sensitivity of the torque measuring system can be adjusted by components of the associated electronics to standardize the measured torque with that of the reference calibration torque. After this calibration, the accuracy of the complete system is dependent on the stability of the electronic components and on variations in the system's sensitivity as functions of the operational environment. Unit calibration for the system is considered necessary since the manufacturing and process techniques used in the fabrication of the torque sensor would be cost prohibitive in establishing a torque sensor design of fixed sensitivity.

After completion of the factory calibration and standardization of the system's electrical output by amplifier gain adjustment in the associated electronics, the complete torque measuring system would be required to remain intact during service life. Although the engine components of the torque system are capable of providing an MTBF of 60,000 hours, the MTBF of the readout indicator is estimated at 2000 hours. Coupled to this limitation in MTBF of the readout indicator, the logistics of supply in maintaining the complete system limit this principle for maintaining the system measurement accuracy.

To provide a means for interchangeability of the electronic components and readout indicator between torque systems without degradation of measurement accuracy, a resistive voltage divider network for matching the gain of the calibrated amplifier to alternate system components was considered. By this procedure, a reference voltage source would be included as part of the electronic circuitry. This voltage would be

supplied to a resistive voltage divider network installed on the engine and electrically connected through a switch to the torque sensor only during field calibration of the torque system. During calibration of the torque system, the reference voltage and voltage network would be energized by a push-button switch, located on the torque indicator bezel. The resistance voltage divider would be adjusted to supply the corresponding reference voltage equal to the torque sensor output voltage at a corresponding reference torque. This value of reference torque would be established in the range of the maximum required accuracy for the engine torque system and would be the same for all engines of that series. The resistive voltage divider network would remain as an integral element of the engine components for the torque system and would be used to:

1. Establish a confidence check on the operational system

2. Allow free interchange of the aircraft torque system components

The procedure would require actuation of the reference network and setting of the amplifier gain on the replacement unit to indicate a known and standardized value of engine torque

In summary, the operational advantages of the system are:

1. No maintenance for the aircraft electronic components of the torque measuring system

2. A system concept providing for free interchangeability of aircraft system parts by addition of a reference network in the associated electronics and torque sensor

A three-piece calibrated kit applied to the engine components of the torque sensor would consist of:

a. The sensor lamination assembly

b. The engine shaft with which it is calibrated

c. A standard resistance network to provide a measurable indication for establishing the required amplifier gain of the indicator package

RELIABILITY

The torque measuring system developed and tested under this program is similar in operating principle to the system now operating in CH-47 helicopters utilizing T55-L-11/11A gas turbine engines. The basic component parts of power supply, sensor, and signal converter in the gas turbine application have accumulated approximately 12,000 flight hours under the environmental and hostile conditions of Southeast Asia. The sensor and signal converter alone have been in use for more than an additional 50,000 flight hours.

The limitations of the present Lycoming torque measuring system were analyzed by utilizing the field usage information stored in the Lycoming Torque Measuring System data bank. These limitations were given considerable attention in the design phase of the system developed for this program in order to achieve a higher mean time between failures (MTBF). The major differences in the new design are:

1. Use of a power supply to provide 3000 Hz square wave excitation rather than 2000 Hz with sinusoidal excitation

2. Combining the power supply and the indicator into a single unit

3. An increase in the wire size of the secondary coils attached to the pole structures of the sensor's lamination assembly

The inherent MTBFs of the various portions of the new torque measuring system, based on the differences in the design of the present and new systems, are tabulated and explained below:

		Inherent MTBF (hr)
1.	Torque sensor	60,000
2.	Electronic circuitry	10,000
3.	Mechanical and electrical/mechanical components of indicator	2,000

Torque Sensor

With no physical contact between the engine shaft and the torque sensor, the inherent operating life of the torque sensor is dependent only on the components of construction. The torque sensor is a static structure

comprised of primary and secondary coil windings, i.e., essentially a multiple transformer. In design of the coil windings, the wire size was selected to assure an adequate margin of safety in the operating environment and under the imposed load conditions. The magnet wire used for the coil windings will meet or exceed the specifications of MIL-W-583C Class 155.

In predicting an MTBF for the new torque sensor, field usage inputs from the present Lycoming operational sensor were used. During actual engine operation of the torque sensor, two failures of the lamination assembly have occurred during 60,000 hours of operational life. As a result, an MTBF of 30,000 hours was established for the operational sensor. A failure analysis of the two sensors revealed that both incidences of failure were caused by breakage in the No. 34 AWG magnet wire used for the secondary coils. To increase the MTBF of the new torque sensor, No. 28 AWG wire will be used for the secondary coils. This wire has a breaking strength four times greater than the No. 34 AWG size wire. However, the newly designed torque sensor contains more secondary coils; therefore, the possibility of failure is greater. The two conditions are used to modify the established MTBF for the operational sensor as follows:

$$\text{Predicted MTBF} = \frac{60,000 \text{ hours}}{2} \times 4 \times \frac{12}{16}$$

where $\frac{12}{16}$ is the ratio of secondary coils in the new torque sensor to the secondary coils in the operational sensor.

From this, a predicted MTBF of 90,000 hours is derived for the new sensor. A conservative estimate of 60,000 hours is used to allow for the possibility of failure in the primary coils, which have been increased in number from 3 to 4.

Electronic Circuitry

The electronic circuitry for the torque measuring system developed under this program consists of two major sections (power supply/amplifier and detector) housed within the indicator enclosure.

In deriving a prediction for the MTBF of the power supply/amplifier section, an analysis based upon the power supply used in the present operational torque measuring system was used. The existing power supply was selected for the analysis since it contains a significant proportion of the electronic components that would be used in the new sensor. The addition of a detector circuit is not considered to add significantly

to the derived prediction. However, for the production unit, which would be required for the new torque sensor, the added components would be included in a formal MTBF study.

The MTBF for the power supply used in the present operational system to excite the torque sensor with a .670 ampere of sinusoidal current at 2000 Hz is 1500 hours. This analysis was performed in accordance with MIL-HDBK-217A and is documented by Reference 7. The changes in design of the new unit, i. e., 3000 Hz square wave excitation rather than 2000 Hz sinusoidal, is expected to improve the MTBF because of increased efficiency. The resultant of reduced internal heat generation will add to the computed MTBF. By packaging the power amplifier within the indicator device, the ambient temperature is controlled by the aircraft cockpit temperature system.

The circuit design concepts are expected to reduce the internal operating temperature from 200°F above ambient to approximately 150°F. This reduction in temperature will improve the equipment reliability by a factor of two.

A further improvement in system reliability of the proposed unit will be derived from a reduced number of components needed to provide the square wave excitation and the reduced power dissipation in the driving transistors which are switched on and off.

For the present operational system, the MTBF of 1500 hours was computed for the unit as comprised of seven major elements. By eliminating the oscillator section and its corresponding failure rate, the MTBF can be increased to 2500 hours as calculated for the same temperature environment. By applying a 2 to 1 correction for lower internal operating temperature, an MTBF of 5000 hours is predicted for the power supply. Further improvements in MTBF can be effected by conservative application of components. For example, if a MIL-C-62 aluminum electrolytic capacitor is derated 20 percent, the failure rate will be three times better at 122°F. By this modification in design of the power amplifier, a further increase in MTBF by a factor of two is estimated for the proposed unit. Therefore, an MTBF estimate of 10,000 hours is predicted for the electronic circuitry designed by Lycoming for the new torque sensor.

Mechanical Components of Indicator

Information supplied to Lycoming by indicator manufacturers shows an MTBF of 2000 hours for the following listed mechanical and electrome-

chanical components of the indicator:

1. Drive motor
2. Gear train
3. Feedback potentiometer

This prediction is based upon actual field usage and is compatible with the MTBF of present-day torque indicators.

The gear train has the highest reliability of all the components. Wear characteristics of the resistive element within the feedback potentiometer place this component behind the gear train in regard to reliability. The drive motor, because of bearing failure, has the lowest reliability of all the mechanical components.

In discussions with indicator manufacturers, Lycoming has learned that the reliability of future indicators may be as high as 6,000 hours. It is, therefore, conceivable that the MTBF of the overall indicator-electronic unit for the new torque measuring system can be increased to or exceed an MTBF of 6,000 hours for present-day electronic circuitry.

CONCLUSIONS AND RECOMMENDATIONS

1. The SAE 9310 material when properly heat treated provides a linear (.1% linearity deviation) magnetostrictive transfer curve.

2. Sleeved and nonsleeved shaft configurations show no significant transfer curve differences when evaluated under the same conditions.

3. The air gap can be selected based on minimum requirements for signal sensitivity. The larger air gap is desired to preclude rub possibilities and for linearizing the signal output as affected by shaft eccentric rotation. A gap of .035 inch measured radially is optimum.

4. The speed dependence of the signal is minimal. Less than .2 percent change in signal sensitivity was noted at a constant value of torque for a speed change of from 7, 900 to 16, 300 rpm. The change in signal sensitivity is not a dependent function of shaft torque. Therefore, at all values of continuous torque through the speed range, the percentage change in signal will occur.

5. Metal temperature reduces the magnetostrictive sensitivity of the shaft material. A compensatory effect when the torque sensor is at the same temperature as the shaft increases the signal sensitivity. The mechanism of compensation is not fully understood. However, the effect is to provide a limited temperature range, $\pm 90^{\circ}F$ operating about a nominal temperature of $180^{\circ}F$, in which the required accuracy for the system of ± 1 percent can be obtained.

6. Based on static tests and substantiation by rotation tests, a current of .670 ampere at an excitation frequency of 3000 Hz is nominal. Regulation for each 1.0 percent will maintain a signal repeatability of .2 percent.

7. The system used for the study has certain advantages which allow its construction to be adapted to gas turbine engines in temperature areas more suited to its operation. These are small size and installation capabilities. Evaluation of the system should be continued to demonstrate this ability by specific design requirements.

8. Further evaluation of temperature is necessary to obtain a better understanding of its effect on the system. The program should continue with fabrication of at least three systems, which would include the torque sensor, the indicator electronics package, and the procedures for standardization of the system to allow free field interchange.

LITERATURE CITED

1. Beth, R., and Meeks, W., MAGNETIC MEASUREMENT OF TORQUE IN A ROTATING SHAFT, The Review of Scientific Instruments, Vol. 25, No. 6,June 1954, pp. 603-607.

2. Dahle, O., THE TORDUCTOR AND THE PRESSDUCTER--TWO MAGNETIC STRESS GAUGES OF NEW TYPE, IVA (periodical published by the Royal Academy of Engineering Sciences) 25, 1954:5, pp. 221-238.

3. Scoppe, F. E., MAGNETOSTRICTIVE TORQUE TRANSDUCER, Instrumentation Technology, Journal of the Instrument Society of America, Vol. 16, No. 10, October 1969, pp. 95-99.

4. Barton, T. H., and Ionides, R. J., A QUANTITATIVE THEORY OF MAGNETIC ANISOTROPY TORQUE TRANSDUCERS, IEEE Transactions on Instrumentation and Measurement, Vol. IM-14, No. 4, December 1965, pp. 247-254.

5. MIL-HDBK-5B, METALLIC MATERIALS AND ELEMENTS FOR AEROSPACE VEHICLE STRUCTURES, Vol. 1, September 1971, pp. 2-4.

6. Khol, R., ELECTRON-BEAM WELDING, Machine Design, Vol. 42, No. 25, October 15, 1970, pp 136-141.

7. RELIABILITY PREDICTION (MTBF) ANALYSIS FOR THE TORQUE METER POWER INVERTER (P/N 211900-2), Avco Lycoming Report No. 105.2.27.1, October 1969.